สารออกฤทธิ์ทางชีวภาพจากเชื้อราสายพันธุ์ CRI 247-01 ที่แยกจากฟองน้ำทะเล และสายพันธุ์ CRIF1 ที่แยกจากปะการังอ่อน

นายชัยรัตน์ เกษตระทัต

วิทยานิพนธ์นี้เป็นส่วนหนึ่งของการศึกษาตามหลักสูตรปริญญาวิทยาศาสตรมหาบัณฑิต
สาขาวิชาเคมี ภาควิชาเคมี
คณะวิทยาศาสตร์ จุฬาลงกรณ์มหาวิทยาลัย
ปีการศึกษา 2550

BIOACTIVE COMPOUNDS FROM SPONGE-DERIVED FUNGUS STRAIN CRI 247-01 AND SOFT CORAL-DERIVED FUNGUS STRAIN CRIF1

Mr. Chairut Kasettrathat

A Thesis Submitted in Partial Fulfillment of the Requirements
for the Degree of Master of Science Program in Chemistry
Department of Chemistry
Faculty of Science
Chulalongkorn University
Academic Year 2007

Thesis Title	BIOACTIVE COMPOUNDS FROM SPONGE-DERIVED FUNGUS STRAIN CRI 247-01 AND SOFT CORAL-DERIVED FUNGUS STRAIN CRIF1
By	Mr. Chairut Kasettrathat
Field of Study	Chemistry
Thesis Advisor	Associate Professor Nattaya Ngamrojnavanich, Ph.D.
Thesis Co-advisor	Assistant Professor Khanitha Pudhom, Ph.D.

Accepted by the Faculty of Science, Chulalongkorn University in Partial Fulfillment of the Requirements for the Master's Degree

..... Dean of the Faculty of Science

(Professor Piamsak Menasveta, Ph.D.)

THESIS COMMITTEE

Sirirat Kokpol
.....Chairman

(Associate Professor Sirirat Kokpol, Ph.D.)

Nattaya Ngamrojnavanich
.....Thesis Advisor

(Associate Professor Nattaya Ngamrojnavanich, Ph.D.)

Khanitha Pudhom
..... Thesis Co-advisor

(Assistant Professor Khanitha Pudhom, Ph.D.)

Orawon Chailapakul
.....Member

(Associate Professor Orawon Chailapakul, Ph.D.)

.....Member

(Prasat Kittakoop, Ph.D.)

นายชัยรัตน์ เกษตระทัต : สารออกฤทธิ์ทางชีวภาพจากเชื้อราสายพันธุ์ CRI 247-01 ที่แยกจากฟองน้ำทะเล และสายพันธุ์ CRIF1 ที่แยกจากปะการังอ่อน. (BIOACTIVE COMPOUNDS FROM SPONGE-DERIVED FUNGUS STRAIN CRI 247-01 AND SOFT CORAL-DERIVED FUNGUS STRAIN CRIF1) อ. ที่ปรึกษา : รศ.ดร. นาตยา งามโรจนวณิชย์, อ. ที่ปรึกษาร่วม : ผศ.ดร. ขนิษฐา พุดหอม, 129 หน้า.

ได้ทำการศึกษาองค์ประกอบทางเคมีของเชื้อราจากทะเล 2 สายพันธุ์ คือ CRI 247-01 และ CRIF1 จากการศึกษาพบว่า เชื้อรา สายพันธุ์ CRI 247-01 ที่แยกจากฟองน้ำทะเล ผลิตสารใหม่ 1 ชนิด คือ **สาร 2** และผลิตสารที่มีรายงานแล้วได้แก่ 6-methoxymellein (**สาร 1**) และ vermillhotin (**สาร 3**) ในขณะที่ สารใหม่คือ **สาร 4** ผลิตโดยเชื้อราสายพันธุ์ CRIF1 ที่แยกมาจากปะการังอ่อน นอกจากนี้ ได้ทำการสังเคราะห์สารอนุพันธ์ เมททิลเอสเทอร์ (**สาร 5**), เบนซิลเอสเทอร์ (**สาร 6**) และ ไฮโดรจีเนต (**สาร 7**) จากสารเริ่มต้น **สาร 4** โดยทำการพิสูจน์โครงสร้างทางเคมีของสารเหล่านี้ด้วยเทคนิคทางสเปคโตรโคปี

จากการศึกษาพบว่า**สาร 3, 5** และ **6** สามารถยับยั้งการเจริญเติบโตของเซลล์มะเร็งได้ในระดับดีมาก นอกจากนี้ **สาร 6** ยังมีฤทธิ์ต้านสารอนุมูลอิสระที่เกิดจากเซลล์มะเร็งเม็ดเลือดขาวในคน (HL-60 Antioxidation) อีกด้วย

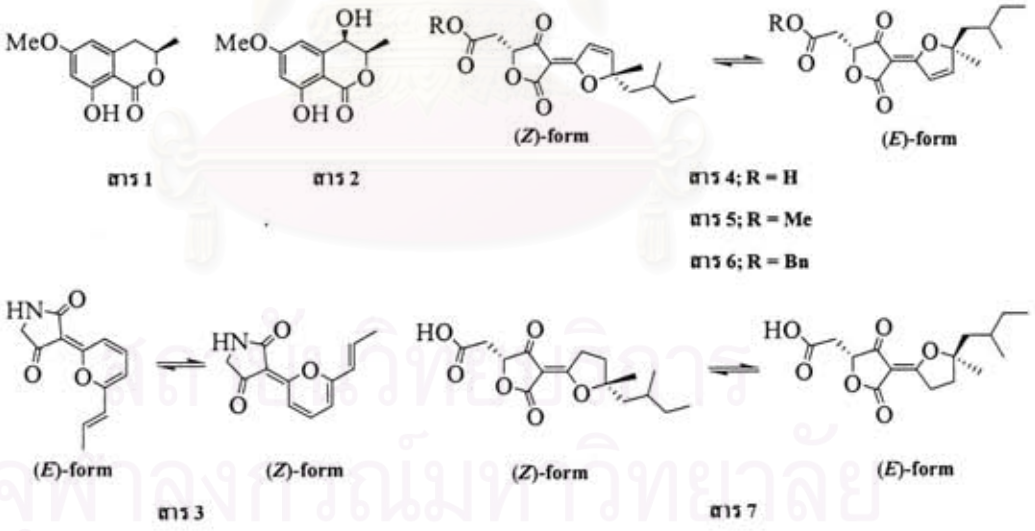

ภาควิชา เคมี
สาขาวิชา เคมี
ปีการศึกษา 2550

ลายมือชื่อนิสิต.....
ลายมือชื่ออาจารย์ที่ปรึกษา.....
ลายมือชื่ออาจารย์ที่ปรึกษาร่วม.....

4772269123 : MAJOR CHEMISTRY

KEY WORD: Marine fungi / *Hypoxylon monticulosum* / Cytotoxicity

CHAIRUT KASETTRATHAT : BIOACTIVE COMPOUNDS FROM SPONGE-DERIVED FUNGUS STRAIN CRI 247-01 AND SOFT CORAL-DERIVED FUNGUS STRAIN CRIF1. (สารออกฤทธิ์ทางชีวภาพจากเชื้อราสายพันธุ์ CRI 247-01 ที่แยกจากฟองน้ำทะเล และสายพันธุ์ CRIF1 ที่แยกจากปะการังอ่อน) THESIS ADVISOR : ASSOC. PROF. NATTAYA NGAMROJANAVANICH, Ph.D. THESIS CO-ADVISOR : ASST. PROF. KHANITHA PUDHOM, Ph.D. : 129 pp.

Chemical constituents of two marine-derived fungi, strains CRI 247-01 and CRIF1, were investigated. The sponge-derived fungus strain CRI 247-01 gave a new **compound 2**, along with two known compounds, 6-methoxymellein (**compound 1**) and vermillhotin (**compound 3**). While, a new **compound 4** was isolated from the strain CRIF1 which was isolated from a soft coral. Moreover, derivatives of **compound 4**, methylester (**compound 5**), benz ylester (**compound 6**), and hydrogenated product (**compound 7**) were prepared. Chemical structures of these compounds were elucidated on the basis of their spectroscopic data.

In this study, **compounds 3**, **5**, and **6** exhibited potent cytotoxic activity against cancer cell lines. Moreover, **compound 6** also inhibited antioxidant activity (HL-60 Antioxidation).

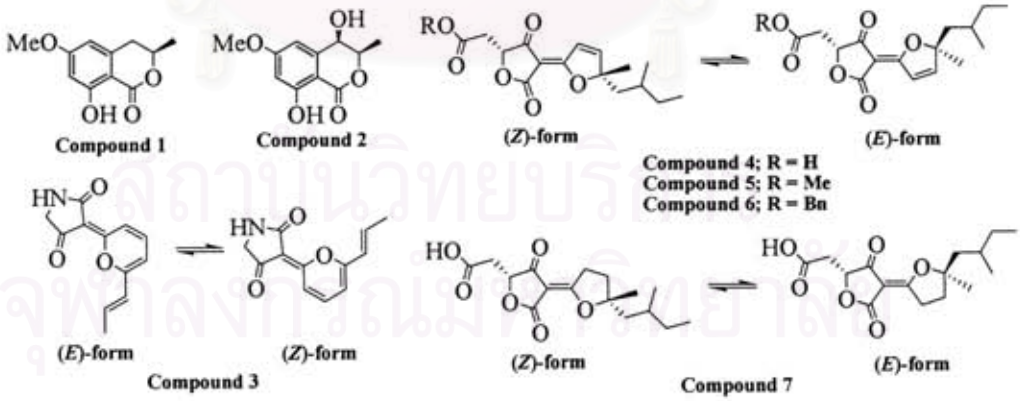

Department Chemistry — Student's signature Chairut Kasettrathat

Field of study Chemistry — Advisor's signature N. Nattaya

Academic year 2007 — Co-advisor's signature Khanitha Pudhom

ACKNOWLEDGEMENTS

I would like to express my heartfelt respect and gratitude to Assoc. Prof. Dr. Nattaya Ngamrojnavanich, my supervisor, for her invaluable guidance, kind supervision, and encouragement throughout this research. I would also like to thank my co-adviser, Asst. Prof. Dr. Khanitha Pudhom, for her kindness, valuable advice, and help.

I would like to thank Dr. Prasat Kittakoop as well for his invaluable guidance, excellent and kind supervision, encouragement, and also his kindness throughout this research, that enable me to pass through this course successfully.

I would like to express my deepest and sincere gratitude to Prof. Dr. Somsak Ruchirawat for his invaluable guidance, supervision, and encouragement.

I would like to thank the Chulabhorn Research Institute (CRI) for providing all facilities and also all the staffs of Natural Products, Biochemistry, Chemical Carcinogenesis, Immunology, and Pharmacology laboratory at CRI. Special thanks are given to the CRI staffs, especially, Mr. Sanya Sureram for his assistance on the isolation of fungi, and fermentation of the fungi; Mr. Somchai Pisutjaroenpong and Ms. Siriporn Wongbundit for NMR spectroscopic service; Ms. Kittiporn Trisupphakant for EI-MS analysis, UV, and IR spectral data; Mr. Nitirat Chimnoi for HRMS analysis; Ms. Jaratluck Akanimamee for antimalarial activity tests; Ms. Pakamas Intachote, Ms. Khajeelak Chiablaem, and Ms. Busakorn Saimanee for anticancer activity; and Ms. Somkid Sitthimonchai for chemoprevention activity. I would like to extend my appreciation to all the staffs of the chemistry research group at CRI for providing additional their invaluable guidance.

I would like to thank Assoc. Prof. Dr. Nongluksna Sriubolmas for the identification of fungi.

I would like to thank all my friends (Chulalongkorn University) for their truly help, encouragement, and friendship especially my colleagues in R503 (CRI) and during the course of my study.

Finally, for my family, I am deeply grateful to my parents for their care, love, and understanding.

CONTENTS

Page

LIST OF TABLES

Table **Page**

LIST OF FIGURES

Figure **Page**

Figure **Page**

Figure **Page**

LIST OF SCHEMES

Schemes **Page**

LIST OF ABBREVIATIONS

APCI-TOF	atmospheric pressure chemical ionisation-time of flight
actone-d_6	deuterated acetone
Bn	benzyl
br	broad
°C	degree Celsius
$CDCl_3$	deuterated chloroform
$CHCl_3$	chloroform
CH_2Cl_2	methylene chloride
COSY	correlation spectroscopy
c	concentration
calcd.	calculated
cm^{-1}	wave number unit
cm	centimetre
conc.	concentrated
2D	two dimensions
DEPT	distortionless enhancement by polarization transfer
DMSO	dimethylsulphoxide
DMSO-d_6	deuterated dimethylsulphoxide
d	doublet
dd	doublet of doublets
dq	doublet of quartets
dt	doublet of triplets
EI	electron impact
EtOAc	ethyl acetate
EtOH	ethanol
g	gram
H_2	hydrogen gas
H_2O	water
HCl	hydrochloric acid
HMBC	heteronuclear multiple bond correlation

HMQC	heteronuclear multiple quantum coherence
HRMS	high resolution mass spectroscopy
Hz	Hertz
h	hour
IC_{50}	50% inhibitory concentration
IR	infra-red radiation
J	coupling constant
L	liter
M	molar (mole/liter)
MHz	megahertz
MPLC	medium pressure liquid chromatography
MS	mass spectroscopy
Me	methyl group
MeOH	methanol
m	multiplet
m/z	a value of mass divided by charge
mL	milliliter
mg	milligram
min	minute
m.p.	melting point
mult	multiplicity
NMR	nuclear magnetic resonance
NOESY	nuclear overhauser effect spectroscopy
$NaHCO_3$	sodium hydrogen carbonate
nm	nanometer
ppm	part per million
q	quartet
s	singlet
sp.	species
t	triplet
U	unit
UV	ultraviolet radiation
v/v	volume by volume

μL	microliter
μM	micromolar
μg	microgram
ν_{max}	maximum wave number
λ_{max}	maximum absorption wavelength
δ	chemical shift (ppm)
ε	the reciprocating wavelength
$[\alpha]_D$	specific rotation
$\rightleftharpoons$	equilibrium

CHAPTER I

INTRODUCTION

The kingdom of fungi is the second largest group after insects, and widely distributed in nature. They are a kingdom of eukaryotic organisms, heterotrophic, and the majorities of fungi are saprophytes playing a major role in decomposition of complex organic materials in the environment. Fungi are generally regarded as being primarily terrestrial organisms and have been relatively little studied in marine habitats. Of nearly 100,000 described species of fungi, only about 500-1,500 are marine fungi. There appear to be some obligately marine organisms; for example the *Halosphaerialed*, an order of the fungal division *Ascomycetes*, is composed almost entirely of marine types (43 genera and 133 species). Many other fungi associated with freshwater and terrestrial habitats can grow in seawater, for example, when decomposing detritus finds its way into the sea (Munn, 2004).

Some fungi are pathogens of marine animals (such as crustaceans, corals mollusc and fish) or plants (such as seaweeds, intertidal grasses and mangrove roots) (Munn, 2004).

Thailand location consist of two sea areas, the Gulf of Thailand and Andaman Sea, possessing a variety of marine animals and plants that may support marine microorganisms which have become an important source of pharmacologically active metabolites. Many published reviews show the importance of these microorganisms as potential sources of pharmaceutical leads. More specifically, fungi from the marine environments have shown great potential as suggested by the diversity of secondary metabolites (Bugni and Ireland, 2004).

In the course the investigation on bioactive compounds from marine-derived fungi, the sponge-derived fungus strains CRI 247-01 and the fungus from soft coral CRIF1 were isolated from an orange sponge (Axinellidae family) CRI 247 and unidentified dark brown soft coral CRI 258, respectively. These samples were collected from Surin Island, Pang-nga Province, Thailand. Crude extracts from those

fungi showed interesting ^{1}H-NMR profiles with antimalarial and anticancer activity. The main objectives of this investigation are as follows:

1. To isolate the marine-derived fungi strains CRI 247-01 and CRIF1.
2. To isolate and purify secondary metabolites from strains CRI 247-01 and CRIF1.
3. To elucidate chemical structure of the isolated compounds.
4. To evaluate antimalarial, cancer chemoprevention and cytotoxic activities of the isolated compounds.

CHAPTER II

LITERATURE REVIEWS

Kohlmeyer and Volkmann- Kohlmeyer (1991) listed 321 species of filamentous higher marine fungi, including 255 Ascomycetes, 60 mitosporic fungi, and only six Basidiomycetes. Marine fungi do not represent specific taxa, but are a group defined by their ecology and physiology. They can be divided into obligate and facultative marine fungi. Kohlmeyer (1974 cited in Osterhage, 2001) defined obligate marine fungi as those "that grow and sporulate exclusively in a marine or estuarine (brackish water) habitat; facultative marine are fungi from freshwater or terrestrial areas also able to grow in the natural marine environment." This implicates that always the ability to germinate in the natural marine environment has to be assessed before defining a marine-derived fungal isolate as obligate or facultative marine. The isolation of a fungal strain from a marine sample does not prove that this fungus is active in the marine environment. It is always possible to isolate a terrestrial fungus being a contaminant. Possibly such a fungal isolate was dormant in the form of spores or hyphal fragments until the surrounding conditions in the laboratory became favorable for germination and growth. Most fungi isolated from marine samples are not proven to be obligate or facultative marine. Thus, the more general expression marine-derived fungi are therefore used (Osterhage, 2001).

2.1 Historical perspective

Historically, fungi have influenced many aspects of human culture and development. One of the most notable effects of fungi on human culture is St. Anthony's fire which was caused by ergot alkaloids found in *Claviceps purpurea*-infected rye. During the middle ages, ergotism outbreaks were severe and resulted in mania, hallucinations, swollen flesh, and loss of limbs. Although ergot alkaloids cause detrimental effects at high doses, they have medicinally useful properties, such as inducing labor, at low doses. Further studies on the use of ergotamine, a major active constituent of *C. purpurea*, demonstrated ergotamine to be an effective migraine

treatment and increased our understanding of migraine headaches while aiding the design of effective treatments (Hart, 1999).

Although the ergot alkaloids have interesting medicinal properties, antibiotic production by fungi provided the stimulus for an entire era of drug discovery research. The earliest report indicating the antibacterial potential of fungi occurred in 1876 when Tyndall described the antagonistic effect of a *Penicillium* sp. on bacteria (Florey et al., 1949 Cited in Bugni and Ireland, 2004). In 1896, Gosio reported that he had isolated small amounts of a crystalline substance that had antibacterial properties. The compound was later confirmed to be mycophenolic acid (Florey et al., 1949 Cited in Bugni and Ireland, 2004). Although there were numerous reports describing antibiotic properties of fungi in the late 1800s and early 1900s, the landmark discovery came in 1929 when Sir Alexander Fleming described the effects of *Penicillium notatum* and penicillin on bacteria. Unfortunately, the importance of his work was not fully realized until the early 1940s when a group at Oxford began investigating penicillin for use as an antibiotic in humans. After the potential of penicillin was elaborated, Giuseppe Brotzu, in 1945, began investigating seawater samples near a sewage outlet in Sardinia for antibiotic producing microbes (Abraham and Loder, 1972 Cited in Bugni and Ireland, 2004)**.** Brotzu hypothesized that self-purification of water might be due in part to bacterial antagonism. He obtained a fungus from a seawater sample that exhibited antibacterial activity and noted that it was similar to *Cephalosporium acremonium* (now named *Acremonium chrysogenum*). This observation led to the discovery of cephalosporin C. In the intervening years, the actinomycetes became the primary focus of drug discovery work, but interest in fungi resurged when cyclosporin A was isolated from *Tolypocladium inflatum* in 1976 and was approved for clinical use as an immunosuppressant in 1983. However, the rediscovery of high numbers of previously described metabolites has to some extent precluded the study of traditional terrestrial sources of fungi and led researchers to explore unique habitats, such as the marine environment, for fungi with potentially new biosynthetic diversity (Bugni and Ireland, 2004).

Although cephalosporin C was isolated from a marine-derived fungus, studies reporting chemistry from marine-derived fungi were rare until the 1990s. A few studies were performed between 1970 and 1990 followed by a nearly exponential growth through the 1990s. Although siccayne (**1**) was most likely the first antibiotic isolated from an obligate marine fungus, the compound had been previously isolated from a terrestrial species (Kupka et al., 1981). Overall, research on marine-derived fungi has led to the discovery of 272 new natural products including many that have novel carbon skeletons, thus, providing evidence that marine-derived fungi have the potential to be a rich source of pharmaceutical leads.

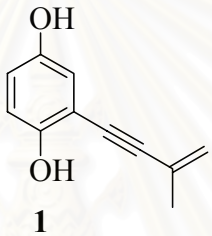

1

Marine-derived fungi are a source of significant chemical diversity and this fact is supported by the 272 new compounds that have been isolated and described, thus far. As illustrated, research on marine-derived fungi blossomed in the 1990s, and notably since 1998. Although the annual number of reported new compounds was highest in 1998 and 2000, the general trend indicates that the number of new metabolites is still on the rise. Biological activities are mainly focused in the areas of antibiotic and anticancer properties, but other selective activities include cell cycle inhibition, antagonism of platelet activating factor, antiviral activity, neuritogenic activity, phosphatase inhibition and kinase inhibition, and radical scavenging activities (Bugni and Ireland, 2004).

2.2 Chemistry and biological activities from marine-derived fungi

2.2.1 Metabolites from sponge-derived fungi

Three new quinazoline alkaloids, aurantiomides A (**2**), B (**3**), and C (**4**), along with the known metabolite anacine (**5**) were isolated from the sponge-derived fungus, strain SP0-19 identified as *Penicillium aurantiogriseum* (Trichomaceae) which was isolated from the sponge *Mycale plumose* (Mycalidae) collected in Jiaozhou Bay, Qingdao, China. Compounds **3** showed moderate cytotoxicity against HL-60 and P388. Compound **4** selectively inhibited BEL-7402 and P388 cell lines (Xin et al., 2007).

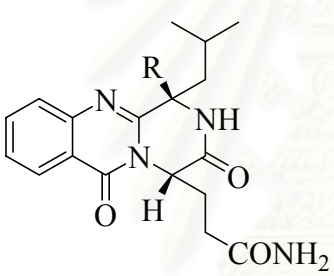

2: R = OCH_3
3: R = OH
5: R = H

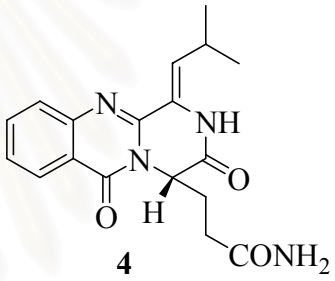

4

Investigation of the secondary metabolites of the marine-derived fungus *Spicellum roseum* isolated from the sponge *Ectyplasia perox* (from the Caribbean Island of Dominica) led to the isolation of two new cyclohexadepsipeptides, spicellanide A (**6**) and spicellamide B (**7**) (Kralj et al., 2007).

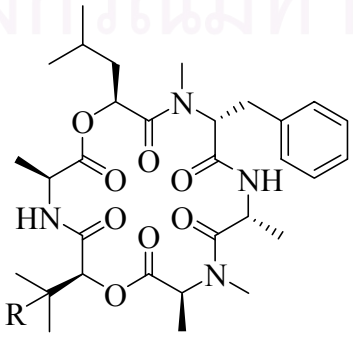

6: R = H
7: R = OH

Four cytotoxic meroterpenoids, tropolactones A–D (**8-11**), were isolated from the whole broth extract of a marine-derived fungus of the genus *Aspergillus* sp. which was obtained from an unidentified sponge collected at 40 feet from Manele Bay, Lanai, Hawaii. Tropolactones A-C (**8-10**) showed in vitro cytotoxicity against human colon carcinoma (HCT-116) with respective IC_{50} values of 13.2, 10.9 and 13.9 μg/mL (Cueto et al., 2006).

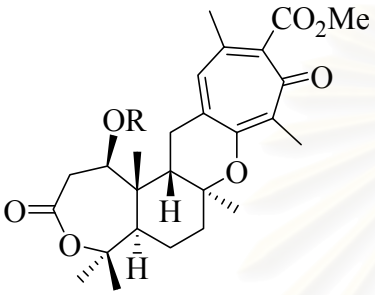

8: R = H
9: R = $COCH_3$

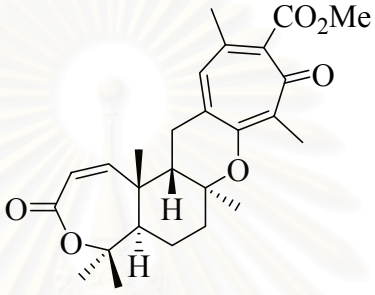

10

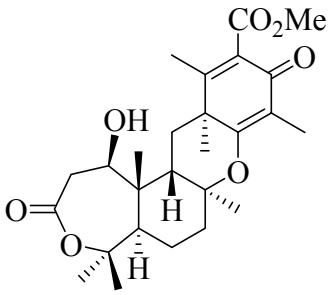

11

Gymnastatins F-H (**12-14**) and gymnamide (**15**) have been isolated from the mycelial MeOH extract of the *Halichondria* sponge-derived fungus *Gymnascella dankaliensis*. Among these compounds, gymnastatins F (**12**) and G (**13**) possess a unique bicyclo[3.3.1]nonane ring as natural products, and they were found to exhibit potent growth inhibition against the P388 cancer cell line (ED_{50} 0.13 and 0.030 μg/mL, respectively) (Amagata, Minoura, and Numata, 2006).

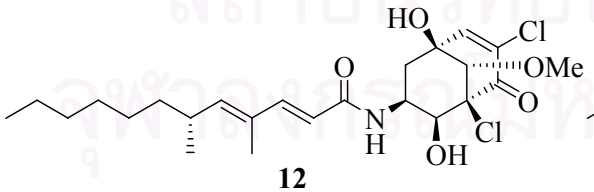

12

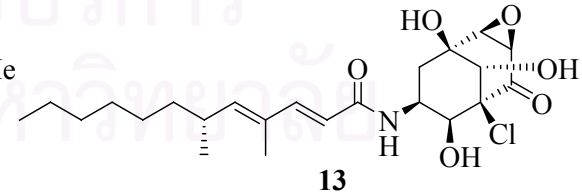

13

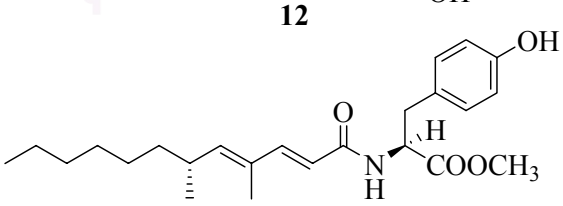

14

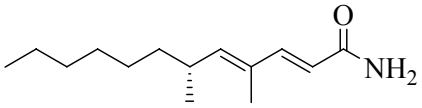

15

2.2.2 Metabolites from algicolous fungi

Investigation of the fungal strain *Monodictys putredinis* isolated from the inner tissue of a marine green alga collected in Tenerife, Spain, led to the isolation of compounds (**16-18**) were examined for their cancer chemopreventive potential. Xanthone **17** was shown to inhibit cytochrome P450 1A activity with an IC_{50} value of 3.0 μM. Compounds **17** and **18** displayed moderate activity as inducers of NAD(P)H:quinone reductase (QR) in cultured mouse Hepa 1c1c7 cells, with CD values (concentration required to double the specific activity of QR) of 12.0 and 12.8 μM, respectively. Compound **18** showed weak inhibition of aromatase activity (Krick et al., 2007).

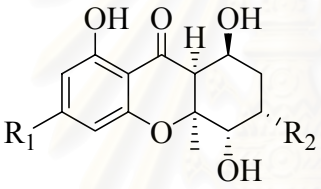

16: $R_1 = CH_3$, $R_2 = OH$
17: $R_1 = H$, $R_2 = CH_3$
18: $R_1 = OCH_3$, $R_2 = CH_3$

Induction of the production of emericellamides A and B (**19-20**) by the marine-derived fungus *Emericella* sp. (isolated from the surface of a green alga of the genus *Halimeda*, which was collected at Madang Bay in Papua New Guinea) was observed during co-culture with the marine actinomycete *Salinispora arenicola*. Emericellamides A and B showed modest antibacterial activities against methicillin-resistant *Staphylococcus aureus* with MIC values of 3.8 and 6.0 μM, respectively (Oh et al., 2007).

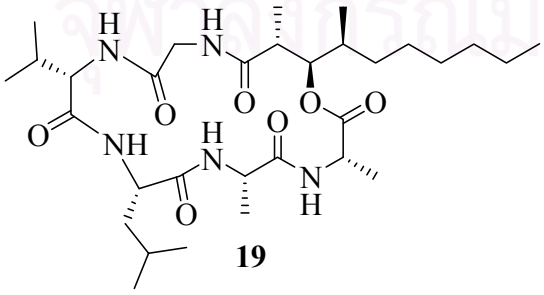

19

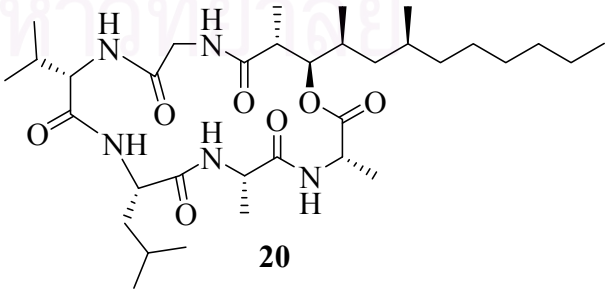

20

New cyclopentenones, bromomyrothenone B (**21**) and botrytinone (**22**), and the known cyclonerodiol (**23**) were isolated from the marine algicolous fungus of the genus *Botrytis*. The fungus was isolated from the surface of the marine green alga *Enteromorpha compressa* collected at Baegunpo, Busan, Korea (Li, Zhang, Lee et al., 2007).

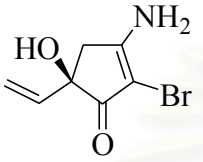

21

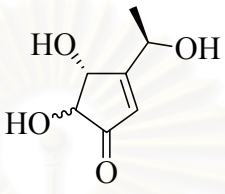

22

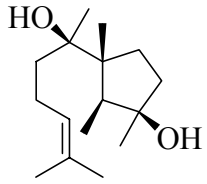

23

A new antibacterial dioxopiperazine, dehydroxy*bis*dethio*bis*(methylthio) gliotoxin (**24**), and the previously described *bis*dethio*bis*(methylthio)gliotoxin (**25**) and gliotoxin (**26**), have been isolated from the broth of a marine-derived fungus of the genus *Pseudallescheria*. The fungal strain was isolated from the surface of the marine brown alga *Agarum cribrosum* collected in the Uljin, Gyeongbuk Province, Korea. Compounds **24-26** exhibit potent antibacterial activity against the methicillin-resistant and multidrugresistant *Staphylococcus aureus* with MIC values of 31.2, 31.2, and 1.0 mg/ml, respectively. Compound **26** also exhibited a significant radical scavenging activity against 1,1-diphenyl-2-picrylhydrazyl (DPPH) with IC_{50} value of 5.2 mM (Li, Kim et al., 2006).

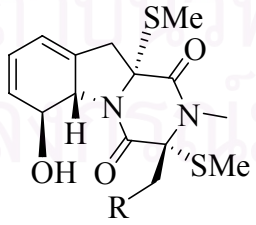

24: R = H
25: R = OH

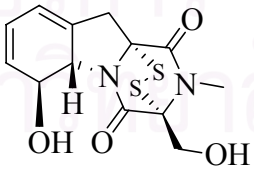

26

2.2.3 Metabolites from fungi obtained from woody substrates

A novel quinone derivative, griseusin C (**27**), along with a known quinone, naphthoquinone C (**28**), was isolated from the lyophilized culture broth of the marine-derived fungus *Penicillium* sp. which was collected from mangrove plant, *Kandelia candel*, collected from Hainan Island, South China (Li, Zheng, Sattler et al., 2006).

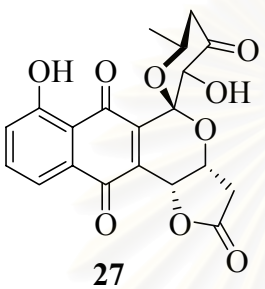

27

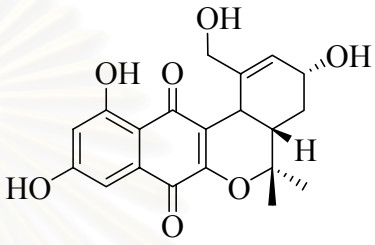

28

A novel 1-isoquinolone analog designated as marinamide (**29**) and its methyl ester (**30**) were produced by the application of mixed fermentation technique to two mangrove endophytic fungi (strains Nos. 1924 and 3893) from the South China Sea. Marinamide (**29**) and its methyl ester (**30**) exhibited significant antibacterial activities against *Escherichia coli* (diameter of bacteriostatics ring/cm: 1.4 (**29**); 2.0 (**30**)), *Pseudomonas pyocyanea* (0.9 (**29**); 1.7 (**30**)) and *Staphylococcus auereu* (1.0 (**29**); 1.3 (**30**)) at the concentration of 1 mg/mL (Feng, and Yongcheng, 2006)..

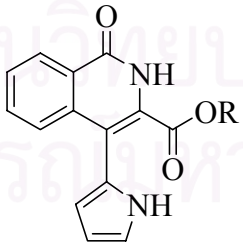

29: R = H
30: R = CH_3

A new isochroman, 6-hydroxy-3-methylisochroman-5-carboxylic acid (**31**), and six known compounds (**32-37**) were isolated from the culture of marine-derived mangrove fungus 1893# (Chen et al., 2006).

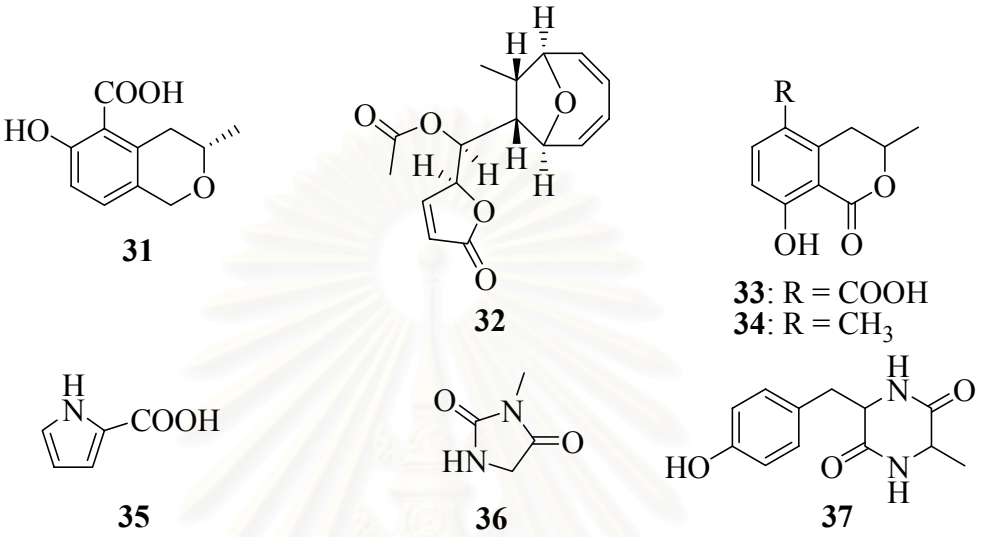

Xyloketal F (**38**), an unusual metabolite with strong L-calcium channel blocking activity, was isolated from the mangrove endophytic fungus *Xylaria* sp. (#2508) collected at the South China Sea coast. The L-calcium channel blocking activities of **38** were determined, and at the same concentration (0.03 μmol/L), the inhibiting rates were 50.33% (Wu et al., 2005).

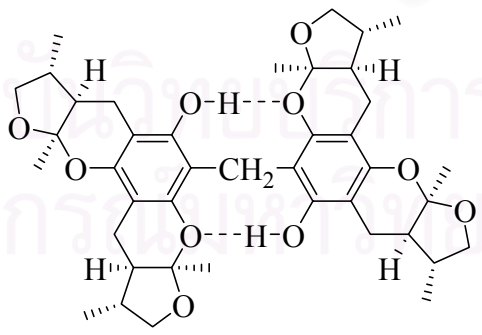

38

2.2.4 Metabolites from tunicate-derived fungi

Trichodermamides A (**39**) and B (**40**), two modified dipeptides, have been isolated from cultures of the marine-derived fungus *Trichoderma virens* which was obtained from a sample of the marine ascidian *Didemnum molle.* The trichodermamides possess a rare cyclic *O*-alkyl-oxime functionality incorporated into a six-membered ring. Trichodermamide B displayed significant in vitro cytotoxicity against HCT-116 human colon carcinoma with an IC_{50} of 0.32 μg/mL (Garo et al., 2003).

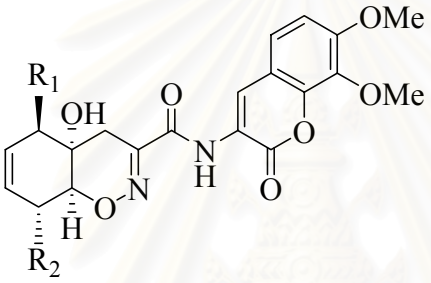

39: $R_1 = R_2 = OH$
40: $R_1 = Cl$, $R_2 = OH$

Two new carboxylic acids, tanzawaic acids E (**41**) and F (**42**) in addition to the unknown benzopyran 3,7-dimethyl-1,8-dihydroxy-6-methoxy-isochroman (**43**), and the known mycotoxin 3,7-dimethyl-8-hydroxy-6-methoxyisochroman (**44**) were produced by a marine-derived strain of *Penicillium steckii* isolated from an unidentified tunicate (Malmstrøma, Christophersena, and Frisvadb, 2000).

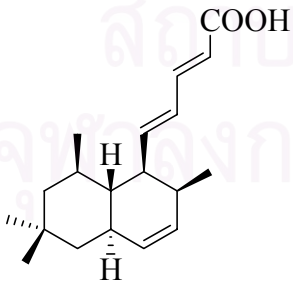

41

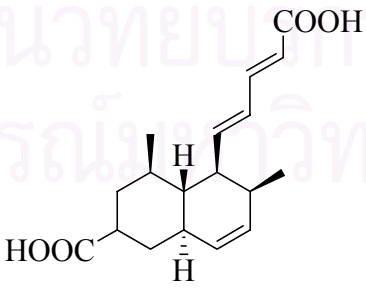

42

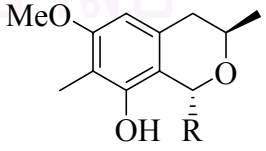

43: R = OH
44: R = H

2.2.5 Metabolites from sediment-derived fungi

Aspergiolide A (**45**), an anthraquinone derivative with naphtho[1,2,3-de]chromene-2,7-dione skeleton, has been isolated from culture of a marine-derived fungus *Aspergillus glaucus*was which was obtained from the marine sediment around the mangrove roots collected in Fujian province of China. Compound **45** showed selective cytotoxicity against A-549, HL-60, BEL-7402, and P388 cell lines (Du, 2007).

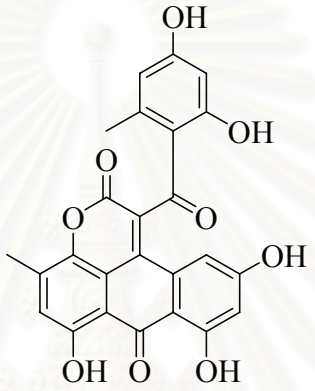

45

The three new 10-phenyl-[12]-cytochalasins Z7, Z8, and Z9 (**46-48**), together with two known analogues, cytochalasins E (**49**) and K (**50**), were isolated from the marine-derived fungus *Spicaria elegans* which was isolated from the marine sediments collected in Jiaozhou Bay, China. Compound **49** was evaluated for their cytotoxic effects on P388 and A-549 cell lines with an IC_{50} value of 0.093 μM and 0.0062 μM. (Liu et al., 2006).

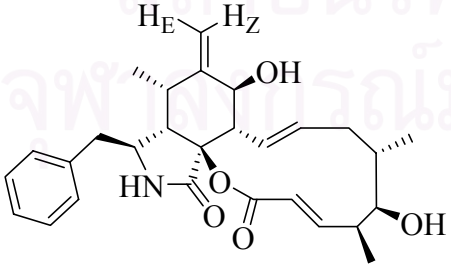

46

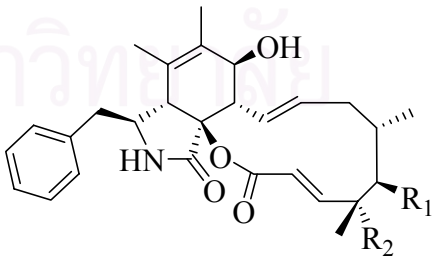

47: R_1 = OH, R_2 = H
48: R_1 = H, R_2 = OH

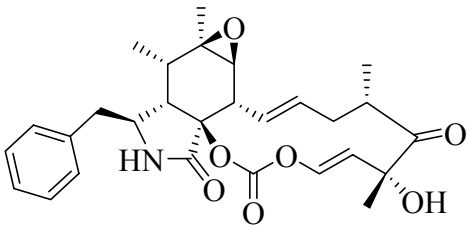

49

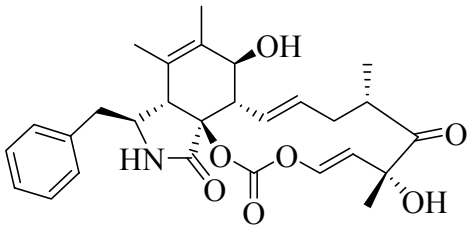

50

2.2.6 Metabolites from mollusc-derived fungi

The isolation of four new doubly prenylated indole alkaloids, the notoamides A–D (**51-54**). These alkaloids were obtained from a culture of marine-derived fungus, *Aspergillus* sp., which was isolated from the common mussel, *Mytilus edulis* (Kato et al., 2007).

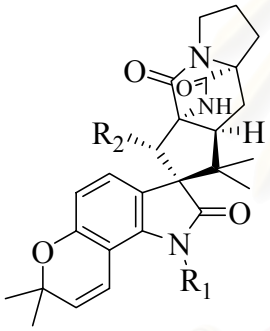

51: R_1 = OH, R_2 = H
52: R_1 = R_2 = H

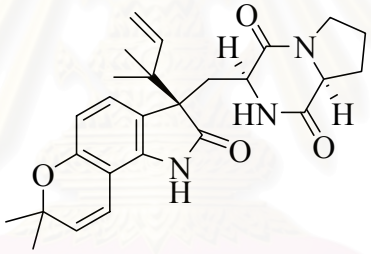

53

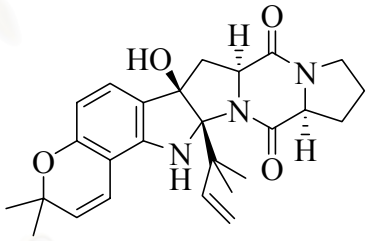

54

A new polyketide, aspermytin A (**55**), was isolated from a cultured marine fungus, *Aspergillus* sp., which was separated from the mussel, *Mytilus edulis*. Aspermytin A induced neurite outgrowth in rat pheochromocytoma (PC-12) cells (Tsukamoto et al., 2004).

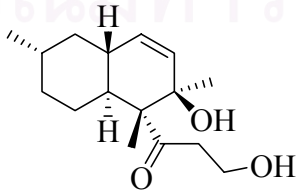

55

2.2.7 Metabolites from fungi isolated from coral

The spiroxins (**56-60**) were purified from the culture extract of a marine-derived fungus strain LL-37H248 which was isolated from a soft orange coral collected from the waters of Dixon Bay, Vancouver Island, Canada. In addition to cytotoxicity, these compounds showed antibiotic activity and were active in a mouse xenograft model against human ovarian carcinoma. The mechanism of action of these compounds was shown to be due, in part, to their effect on DNA (McDonald et al., 1999).

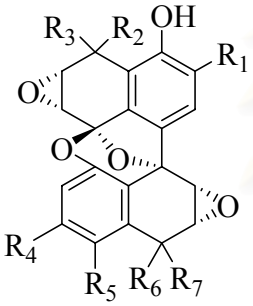

56: R_1 = Cl, R_2,R_3 = O, R_4 = H, R_5 = OH, R_6,R_7 = O
57: R_1 = Cl, R_2,R_3 = O, R_4 = Cl, R_5 = OH, R_6,R_7 = O
58: R_1 = H, R_2,R_3 = O, R_4 = H, R_5 = H, R_6,R_7 = O
59: R_1 = H, R_2 = OH, R_3 = H, R_4 = H, R_5 = H, R_6,R_7 = O
60: R_1 = Cl, R_2,R_3 = O, R_4 = Cl, R_5 = OH, R_6 = OH, R_7 = H

2.2.8 Metabolites from fungi obtained from non-algal plants and grasses

A new polyketide glycoside, cladionol A (**61**), was isolated from the culture broth of a fungus *Gliocladium* sp., which was separated from sea grass *Syringodium isoetifolium*. Cladionol A (**61**) exhibited exhibited cytotoxicity against murine leukemia L1210 and human epidermoid carcinoma KB cells with IC_{50} values of 5 and 7 μg/mL, respectively (Kasai et al., 2005).

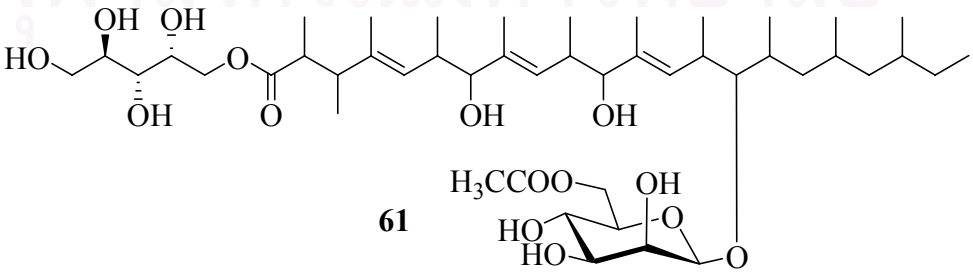

61

A new cyclic pentadepsipeptide, sansalvamide (**62**), has been isolated from organic extracts of the mycelium of a fungus of the genus *Fusarium* collected from the surface of the seagrass *Halodule wrightii*. Sansalvamide exhibited selective *in vitro* cytotoxicity toward COLO 205 colon and SK-MEL-2 melanoma cancer cell lines (Belofsky, Jensen, and Fenical, 1999).

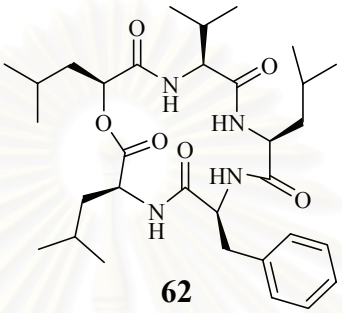

62

2.2.9 Metabolites from fungi isolated from fish

Three new pyrrolidine alkaloids, scalusamides A-C (**63-65**), were isolated from the culture broth of the fungus *Penicillium citrinum*, which was separated from the the gastrointestine of a marine fish. Scalusamide A (**63**) exhibited antifungal and antibacterial activities (Tsuda et al., 2005).

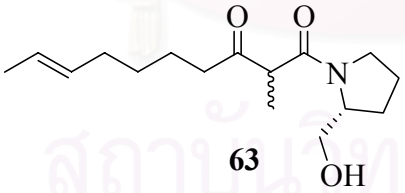

63

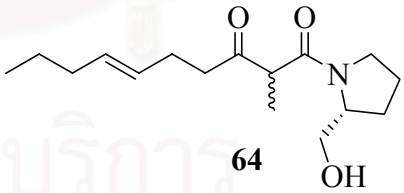

64

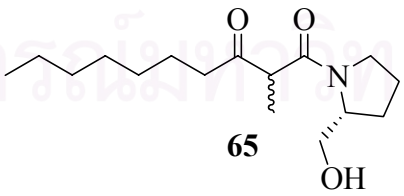

65

And a novel tetracyclic alkaloid, perinadine A (**66**), was isolated from the culture broth of the same fungus *Penicillium citrinum*, which was separated from the gastrointestine of a marine fish (Sasaki et al., 2005).

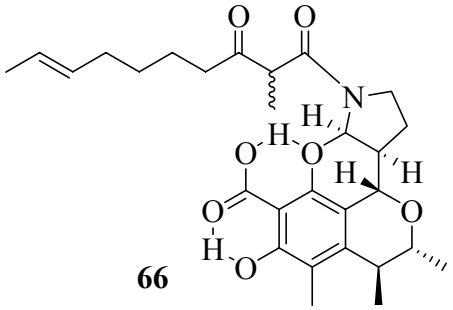

66

2.2.10 Metabolites from miscellaneous substrates

The sesquiterpene lactone, 8-hydroxy-9-oxo-7(11)-eremophilien-12,8-olide (**67**) was isolated from the marine fungus *H. oceanicum* from the South China Sea (Li, Lin et al., 2001).

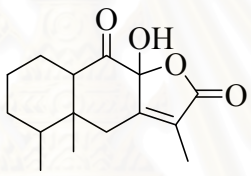

67

And cultures of the marine fungus *H. oceanicum* (LL-15G256) were found to have potent antifungal activity in assays designed to detect inhibitors of fungal cell wall biosynthesis. Bio-activity guided isolation provided the macrocyclic polyesters 15G256a (**68**), 15G256α -1 (**69** and 15G256β (**70**) that were partially responsible for the antifungal activity. In addition, fermentation beers contained a series of related, but unreported metabolites designated 15G256ι (**71**), 15G256ε (**72**), 15G256ο (**73**), 15G256α-2 (**74**), 15G256β-2 (**75**), 15G256ν (**76**), and 15G256π (**77**) (Schlingmann, Milne, and Carter, 2002).

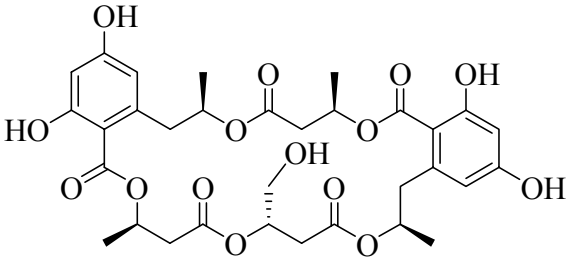

68

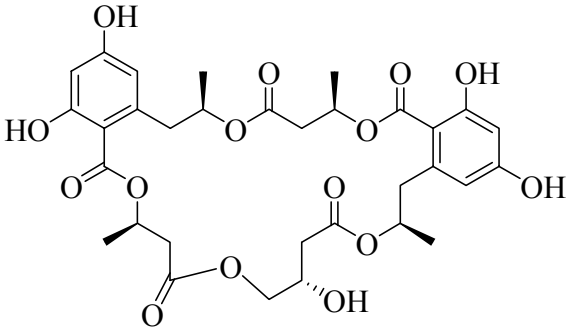

69

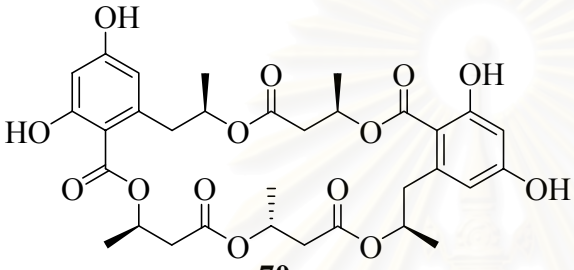

70

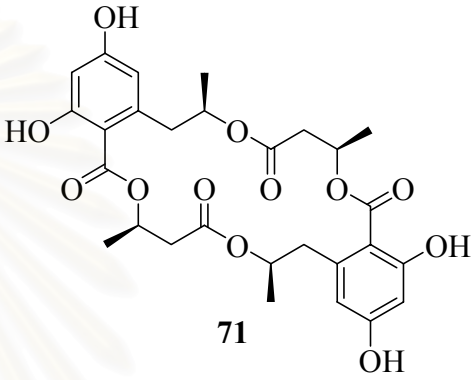

71

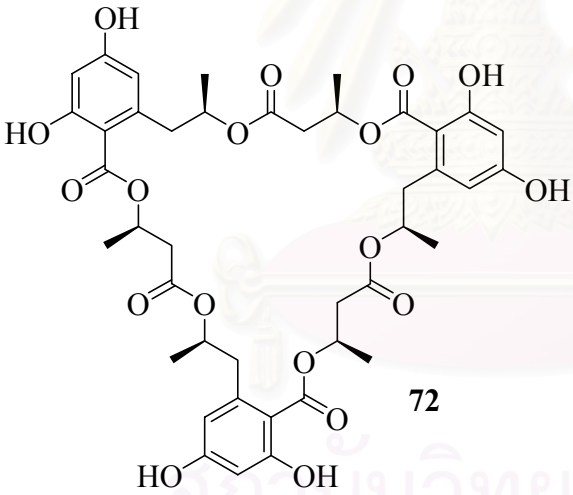

72

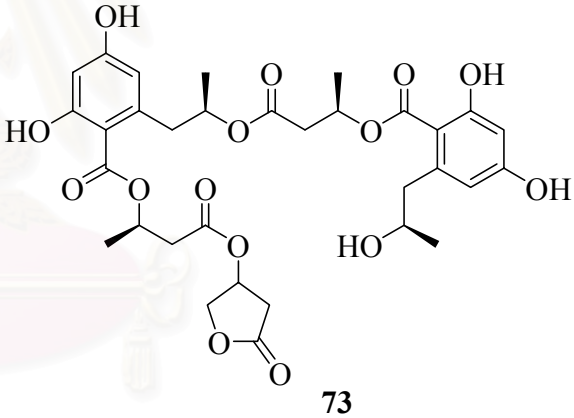

73

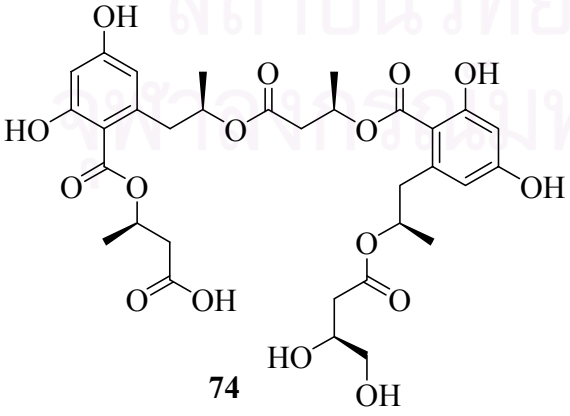

74

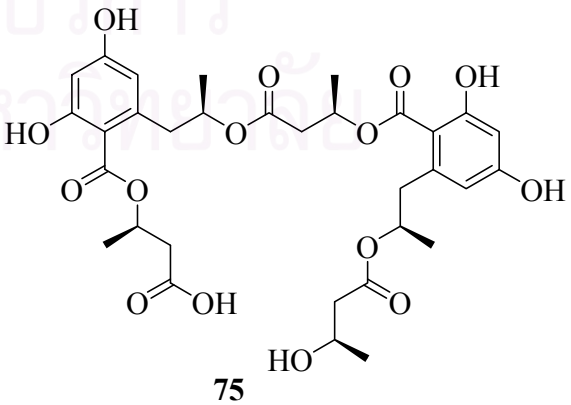

75

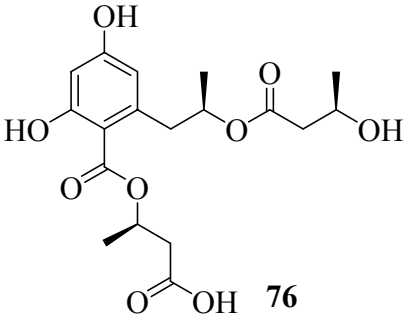

76

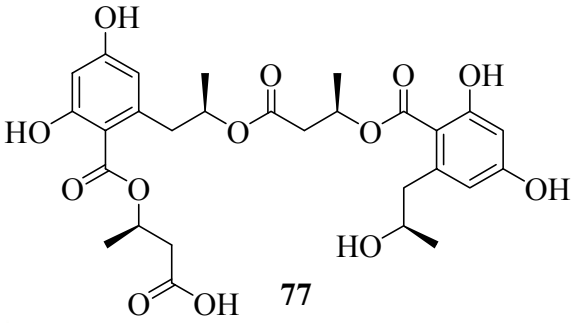

77

In addition, fermentations of the marine fungus *H. oceanicum* (LL-15G256) were found to have potent antifungal activity. Isolation and purification of the antifungal agents provided two classes of compounds, macrocyclic polylactones and the lipodepsipeptides 15G256*γ* (**78**), 15G256*δ* (**79**) and 15G256*ε* (**80**). The isolation and structure elucidation of the lipodepsipeptides, all containing D-glutamate, L-serine, and the rare amino acid *β*-ketotryptohan (Schlingmann, Milne, Williams et al., 1998).

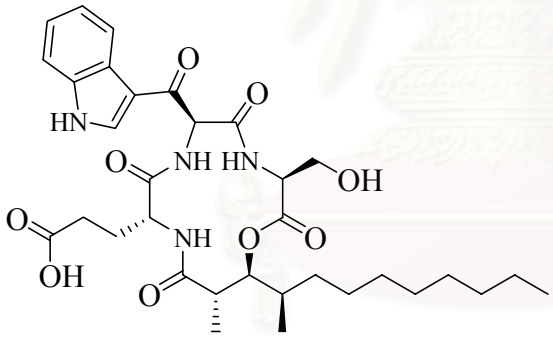

78

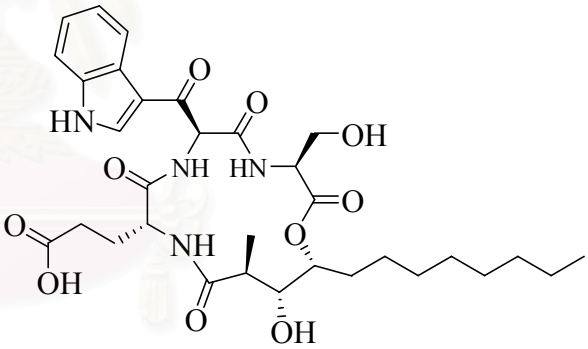

79

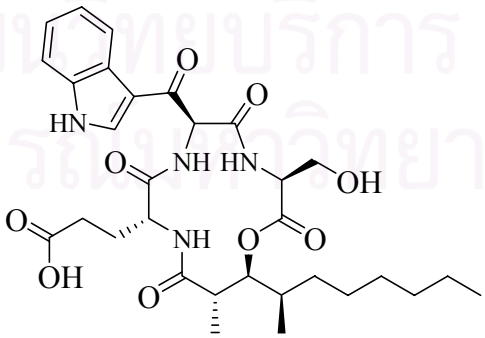

80

CHAPTER III

EXPERIMENTS

3.1 Chromatography

3.1.1 Analytical thin-layer chromatography (TLC)

Thin layer chromatography (TLC) was carried out on a silica gel 60 PF_{254} pre-coated plate. Detection was visualized under ultraviolet light at wavelengths 254 and 366 nm.

3.1.2 Column chromatography

Column chromatography (CC) was performed using Sephadex LH-20 (Pharmacia Code No. 17-0090-01) and Silica gel 60H (Merck Code No. 7734) as packing materials.

3.1.3 Medium pressure liquid chromatography (MPLC)

MPLC was performed with a BÜCHI 681 chromatographic Pump, connected to a BÜCHI UV/VIS FILTER-PHOTOMETER detector set at a wavelength 220 nm. Sorbents for the MPLC column was C-18 reversed-phase, with a column size of 2 × 20.5 cm.

3.2 Structure elucidation

Structures were elucidated by the interpretation of one and two dimensional NMR spectra. Additional spectroscopic techniques such as MS, UV-vis, FT-IR and optical rotation properties were also employed for the structural elucidation.

3.2.1 Nuclear magnetic resonance spectroscopy (NMR).

^{1}H NMR spectra were recorded on a Varian Gemini 2000 spectrometer operating at 200 MHz spectrometer (with $CDCl_3$, acetone-d_6 and DMSO-d_6 as solvents). ^{1}H NMR spectra of pure compounds and all other NMR measurements were performed on a Bruker AM-400 (400 MHz) or a Bruker AVANCE 600. NMR spectrometer was operated at 400 or 600 MHz (^{1}H), and 100 or 150 MHz (^{13}C), respectively. NMR spectra of pure compounds were processed using Bruker software. They were calibrated using solvent signals (^{13}C: $CDCl_3$ 77.00 ppm, acetone-d_6

(CD_3COCD_3) 29.8, 206.0 ppm and DMSO-d_6 (CD_3SOCD_3) 39.5 ppm) or a signal of the portion of the partly or not deuterated solvent (^1H: $CHCl_3$ in $CDCl_3$ δ 7.26 ppm, acetone in acetone-d_6 δ 2.05 ppm, water (H_2O) in acetone-d_6 δ 2.8 ppm, DMSO in DMSO-d_6 δ 2.50 ppm, and water (H_2O) in DMSO-d_6 δ 3.31 ppm). Structural assignments were based on the interpretation of the following NMR experiments: ^1H, ^{13}C, DEPT, ^1H-^1H COSY, ^1H-^{13}C direct correlation (HMQC), and ^1H-^{13}C long-range correlation (HMBC).

3.2.2 Mass spectrometer (MS).

EI-MS spectra were obtained from a Finnigan Mat GCQ mass spectrometer.

Accurate mass was obtained from the time of flight (TOF) mass spectrometric technique, using a Micro TOF, Bruker daltoincs by APCI ionization mode or ESI mode.

3.2.3 Ultraviolet-visible measurements (UV-vis).

UV-vis spectra were recorded on a Shimadzu UV-vis 2001s spectrophotometer.

3.2.4 Fourier transform infrared spectroscopy (FT-IR).

FT-IR spectra were recorded on a Perkin Elmer Spectrum One spectrophotometer. Samples for IR were examined using a Universal Attenuted Total Reflectance, solid or liquid (UATR-solid, UATR-liquid).

3.2.5 Optical rotation

Optical rotations were measured with using a sodium D line (589 nm) JASCO DPI-370 digital polarimeter in MeOH equipped with a 1 mL cell (cell length 1.00 cm).

3.2.6 Melting point

Melting points were recorded on a Büchi 535 and uncorrected.

3.3 Chemicals

3.3.1 Solvents.

All solvents used in this research such as methanol, dichloromethane, ethyl acetate, and hexane were commercial grade and purified prior to use by distillation.

3.4 Culture media

Culture media used for cultivation of marine-derived fungi were potato dextrose agar (PDA, Britania, 24 g PDA in sea water 1 L) and potato dextrose broth (PDB, potato 200 g and sucrose 15 g in sea water 1 L). All culture media were sterilized by autoclaving at 121 °C for 15 minutes.

3.5 Sample collection and isolation of marine-derived fungi

Two marine-derived fungi, strains CRI 247-01 and CRIF1, were isolated from an orangish marine sponge CRI 247 (Axinellidae family) and unidentified soft coral CRI 258, respectively. The two marine samples were collected from Surin Island, Pang-nga Province, Thailand, in November 2005. In order to isolate the marine-derived fungi, each marine sample was suspended in sea water. Each organism was cut into small pieces and put on the surface of PDA agar plates, and then incubated at room temperature for 3-7 days until colonies appeared. The colonies of fungi were individually picked up and was transferred to a new PDA agar plate and incubated at room temperature for 3-7 days.

3.6 Identification of fungal strains

Isolated fungal strains CRI 247-01 and CRIF1 were taxonomically identified by Assoc. Dr. Nongluksna Sriubolmas, Department of Microbiology, Faculty of Pharmaceutical Sciences, Chulalongkorn University, Bangkok, Thailand.

3.7 Evaluation of biological activities

Antimalarial activity, anticancer activity and cancer chemoprevention were evaluated at the Chulabhorn Research Institute (CRI), Bangkok, Thailand.

3.7.1 Antimalarial activity

3.7.1.1 Parasite culture

Human erythrocytes (type O) infected with *Plasmodium falciparum* strain 94, (Chloroquine resistant) was maintained in continuous culture, according to the method described by Trager and Jensen (1976). RPMI 1640 culture medium (Gibco, USA) supplemented with 25 mM of HEPES (Sigma, USA), 40 mg/L gentamicin sulfate (Government Pharmaceutical Organization, Thailand) and 10 mL of human serum was used in continuous culture.

Before starting the experiment, *P. falciparum* culture was synchronized by using sorbitol induced hemolysis according to the method of Lambros and Vanderberg (1979) to obtain only ring-infected cells and then incubated for 48 h prior to the drug testing to avoid effect of sorbitol.

The experiments were started with synchronized suspension of 0.5% - 1% infected red blood cell during ring stage. Parasites were suspended with culture medium supplemented with 15% human serum to obtain 10% cell suspension. The parasite suspension was put into 96-well microculture plate; 50 μL in each well and then added 50 μL of various test drug concentrations. These parasite suspensions were incubated for 48 h in the atmosphere of 5% CO_2 at 37 ^{o}C.

After 48 h incubation, parasite culture was fixed by adding 0.25% (v/v) glutaraldehyde (Sigma) in phosphate buffer saline (PBS) and these were kept for DNA staining.

3.7.1.2 Parasite DNA staining and flow cytometric analysis

Before parasite DNA staining, 5×10^{6} red blood cells from each glutaraldehyde-fixed sample were washed once with PBS and resuspended in PBS containing propidium iodide (PI) (Molecular Probe) at a final concentration at 10 μg/mL, and held for at least 1 h in dark. The PI stained cells were excited with 488 nm. Red fluorescence was detected at 585 nm. Red blood cells were gated on the basis of their forward scatter and side scatter. For each sample, 30,000 cells were required, stored and analyzed. Percent parasitemia, fluorescence intensity, and any

abnormal fluorescence pattern were obtained from an integrated fluorescence histogram between the test and the control sample (chloroquine hydrochloride, IC_{50} = 2.98×10^{-7} M).

3.7.2 Anticancer activity

Anticancer activity was assessed against 11 cancer cell lines *in vitro*, including S102 (human hepatocellular carcinoma), HepG2 (human hepatoblastoma carcinoma), A549 (human lung adenocarcinoma, non-small cell ATCC No. CCL-185), HuCCA-1 (human cholangiocarcinoma), KB (human epidermoid carcinoma in mouth), HeLa (human cervical carcinoma), MDA-MB-231 (hormone-independent breast cancer), H69AR (lung cancer, small cell, multidrug resistance), T47D (hormone-dependent breast cancer), HL-60 (human promyelocytic leukemia cell), and P388 (mouse lymphoid neoplasm). Cytotoxicity assay was performed by crystal violet (Kriengsak Lirdprapamongkol et al., 2003), MTT assay (Mosmann, 1983), and XTT assay (Scudiero et al., 1988).

3.7.3 Cancer chemoprevention

Activity of cancer chemoprevention was evaluated based upon 7 independent models, including DPPH (scavenging of diphenyl picrylhydrazyl radicals), XXO (scavenging of $O_2^{\cdot-}$ generating by xanthine/xanthine oxidase), IXO (inhibition of xanthine oxidase), HL-60 Antioxidation (inhibition of TPA-induced $O_2^{\cdot-}$ generation in differentiated HL-60 cell), ORAC (oxygen radical absorbance capacity-against $ROO^{\cdot}$), and LOX (inhibition of lipoxygenase activity).

3.7.3.1 Diphenyl-picryl-hydrazyl (DPPH) assay

The DPPH assay was performed according to van Amsterdam et al. (1992) with some modifications. Samples were reacted with 1,1-diphenyl-2-picrylhydrazyl (DPPH) stable free radical generating formazan form which was measured photometrically. For the reaction, 195 μL of 100 μM DPPH solution was pipetted in 96-well plate. 5 μL of sample or DMSO as blank or 10 mM Vitamin C as positive control was mixed. After 37 ^{o}C incubation for 30 min the optical density (OD) at 515 nm wavelength was measured by a microplate reader. Percentage of scavenging of

DPPH radical (% scavenging) was calculated using below equation. The samples which contain scavenging activity higher than 50% were further analyzed the value of 50% inhibitory concentration (IC_{50}) which was calculated using the Microsoft Excel.

$$\%\,\text{Scavenging} = 100 - \frac{(\text{ODsample})}{(\text{ODcontrol})} \times 100$$

3.7.3.2 HL-60 antioxidant by reduction of Cytochrome C

Differentiation of HL-60

The differentiation of human promyelocytic leukemic cells (HL-60) to granulocyte was performed following the method established by Takeuchi, Nakajima, and Morimoto (1994) with minor modifications. $2.5x10^5$ cells/mL of HL-60 were differentiated with culture medium containing 1.3% DMSO and incubated in 37 ^oC CO_2 incubator for 4 days. The differentiated cells were harvested by centrifugation and washed twice with Hank's balanced salt solution, pH 7.8 containing 30 mM Hepes and resuspended at concentration $1x10^6$ cells/mL.

HL-60 antioxidant assay

Inhibition of TPA-induced superoxide radical formation in differentiated HL60 by determination of cytochrome c reduction (Pick and Mizel, 1981). For this assay, 25 μL of a 10-fold diluted sample in H_2O or 10% DMSO as negative control was mixed with 100 μL of $1x10^6$ cells/mL cell suspension in 96-well plate. After 37 ^oC incubation for 5 min, 25 μL of HBSS was added to sample and negative control while added 25 μL of 600 U/mL of SOD for positive control and then 75 μL of 4.17 mg/mL cytochrome c were added. To start the reaction, 25 μL of 0.55 mg/mL TPA was added. The mixture was incubated at 37 ^oC for 30 min. The reaction was stopped by keeping on ice for 15 min. After centrifugation at 2000 rpm for 10 min, 200 μL of the supernatant was aspirated and the optical density (OD) was measured at 550 nm wavelength with a microplate reader. Percentage of inhibition of TPA-induced superoxide radical formation (% inhibition) was calculated using the equation shown below. The samples which provide inhibition of TPA-induced superoxide radical formation activity more than 50% were further investigated, and IC_{50} value was computed using the Microsoft Excel.

$$\% \text{ Inhibition} = 100 - \frac{(\text{ODsample})}{(\text{OD}_{\text{DMSO}})} \times 100$$

Cell viability assay

Since some samples exert high toxicity, cell viability was examined in parallel to avoid false positive results. Cell viability was measured fluorimetrically by enzymatic hydrolysis of the fluorogenic esterase substrate calcein AM. For this assay, the cell pellet after HL-60 Antioxidant assay was collected by centrifugation, washed twice with PBS and then added 50 μL of warm 0.25 μM calcein AM. The fluorescence was continuously measured every 1 min for 10 min using an excitation wavelength of 485 nm and an emission wavelength of 520 nm with cutoff 515 nm using a microplate fluorescence reader. Percentage of cell viability (% cell viability) was calculated from V_{max} by following equation.

$$\% \text{ Cell viability} = 100 - \frac{(V_{max} \text{ of sample})}{(V_{max} \text{ of DMSO})} \times 100$$

3.7.3.3 Scavenging of superoxide anion by reduction of XTT

Superoxide anion radical was generated by the xanthine/xanthine oxidase system. Superoxide anion could reduce XTT to form a water soluble formazan. The amount of superoxide anion can be determined indirectly by measuring the formazan product of XTT.

Measuring of the XTT-reduction for XXO model

The activity to scavenge superoxide anion was performed by following the formazan product of XTT. The procedure was done as described by Ukeda et al. (1997) with some modifications. The premix containing 110 μL of 50 mM $NaHCO_3$ buffer, pH 9.4, 20 μL of 0.5 mM hypoxanthine, 20 μL of EDTA, 20 μL of 0.25 mM XTT and 10 μL of sample or 10 μL of pure DMSO as negative control or 2 mM allopurinol as positive control was pipetted in a 96-well plate. The reaction was initiated with 20 μL of 150 mU/mL xanthine oxidase or buffer as background. The kinetic measurement was immediately performed by microplate reader at 480 nm for

5 min, every 20 seconds. Percentage of scavenging of superoxide anion (% scavenging) was calculated from the following equation.

$$\%\,\text{Scavenging} = 100 - \frac{(V_{max}\,\text{of sample})}{(V_{max}\,\text{of DMSO})} \times 100$$

Measuring of uric acid formation for IXO model

Xanthine oxidase activity was determined by quantifying the amount of uric acid produced from xanthine. The method was followed as described by Nagao, Seki, and Kobayashi (1999) with some modifications. The premix containing 130 μL of 50 mM $NaHCO_3$ buffer, pH 9.4, 20 μL of 0.5 mM xanthine, 20 μL of EDTA and 10 μL of sample or 10 μL of pure DMSO as negative control or 2 mM allopurinol as positive control was pipetted in 96-well plate. The reaction was initiated with 20 μL of 150 mU/mL xanthine oxidase and then immediately measured in a kinetic at 295 nm for 5 min, every 30 seconds. Percentage of inhibition of uric acid formation (% inhibition) was quantitated and calculated from the following equation.

$$\%\,\text{Inhibition} = 100 - \frac{(V_{max}\,\text{of sample})}{(V_{max}\,\text{of DMSO})} \times 100$$

7.3.3.4 Microplate-oxygen radical absorbance capacity assay (MORAC)

The oxygen radical absorbance capacity assay (ORAC) was developed by Cao and Prior (1999). The mixture containing 175 μL of 75 mM phosphate buffer, pH 7.0, 10 μL of 7×10^{-5} mM fluorescein and 10 μL of 1/80 dilution sample or DMSO as negative control or 20 μM Trolox as positive control was preincubated at 37 °C for 10 min. The reaction was initiated by addition of 15 μL of 255 mM AAPH as $ROO^{\bullet}$ generator. The plate was subjected immediately to the fluorescence microplate reader at 37 °C measuring at excitation 485 nm and emission 530 nm with cutoff 530 nm. The signal was read every 2 min for 45 min, and the area under curve (AUC) was calculated autometrically.

The final results were expressed as ORAC units, where 1 ORAC unit equals the net protection of fluorescein produced by 1 μM trolox, a water soluble vitamin E analog. Scavenging capacities >1 ORAC unit were considered as positive. The ORAC values were calculated using the equation as shown below.

$$\text{ORAC} = \frac{(\text{AUCsample} - \text{AUCblank})}{(\text{AUCtrolox} - \text{AUCblank})}$$

7.3.3.5 Lipoxygenase inhibition assay

Lipoxygenase is a dioxygenase that catalyzes conversion of linoleic acid and other polyunsaturated lipids that contain a *cis*,*cis*-1,4-pentadiene moiety. The reaction can be followed by observing the absorption at 234 nm wavelength. The assay was performed as described by Gleason et al. (1995) with some modications. For the assay, 120 μL of 10 mM PBS, pH 7.4, 20 μL of 2500 U/mL LOX and 20 μL of 1/10 dilution sample or NDGA for positive control or 10% DMSO as negative control were pipetted in 96-well plate for UV measurement. The plate was preincubated at room temperature for 10 min with shaking. The reaction was started with 40 μL of 0.5 mM arachidonic acid (diluted in PBS buffer), further incubated at room temperature for 10 min with shaking. The optical density was measured at the wavelength 234 nm. The LOX inhibition was calculated by the following equation.

$$\% \text{ Inhibition} = 100 - \frac{(\Delta\text{ODsample})}{(\Delta\text{OD}_{\text{DMSO}})} \times 100$$

ΔODsample = OD (Sample with enzyme) – OD (Sample without enzyme)

$\Delta\text{OD}_{\text{DMSO}}$ = OD (DMSO with enzyme) – OD (DMSO without enzyme)

3.8 Extraction and isolation of the marine-derived fungus strain CRI 247-01

3.8.1 Fermentation, extraction and isolation

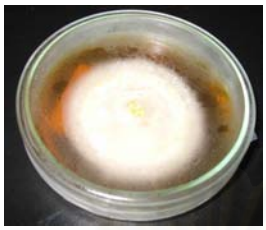

Colony of the marine-derived fungus stain CRI 247-01 on PDA medium

The fungus strain CRI 247-01 was grown on PDA at room temperature for 7 days, after which was transferred into 20×1 L Erlenmeyer flasks each containing 250 mL of PDB. Fermentation was conducted under static conditions (without shaking) at room temperature for 24 days. The fungal culture was filtered to obtain the fermentation broth (3.75 L) and mycelia.

Fermentation broth was extracted with an equal volume of EtOAc to obtain a dark brown solid (213.9 mg), while mycelia were extracted sequentially with MeOH (500 mL×2) and CH_2Cl_2 (500 mL×2). The MeOH and CH_2Cl_2 extracts were combined and extracted with EtOAc (500 mL×3) to obtain a dark brown solid (2.55 g). The extraction procedure is summarized in **Scheme 3.1**.

Scheme 3.1: Extraction of fermentation broth and mycelia of the marine-derived fungus strain CRI 247-01

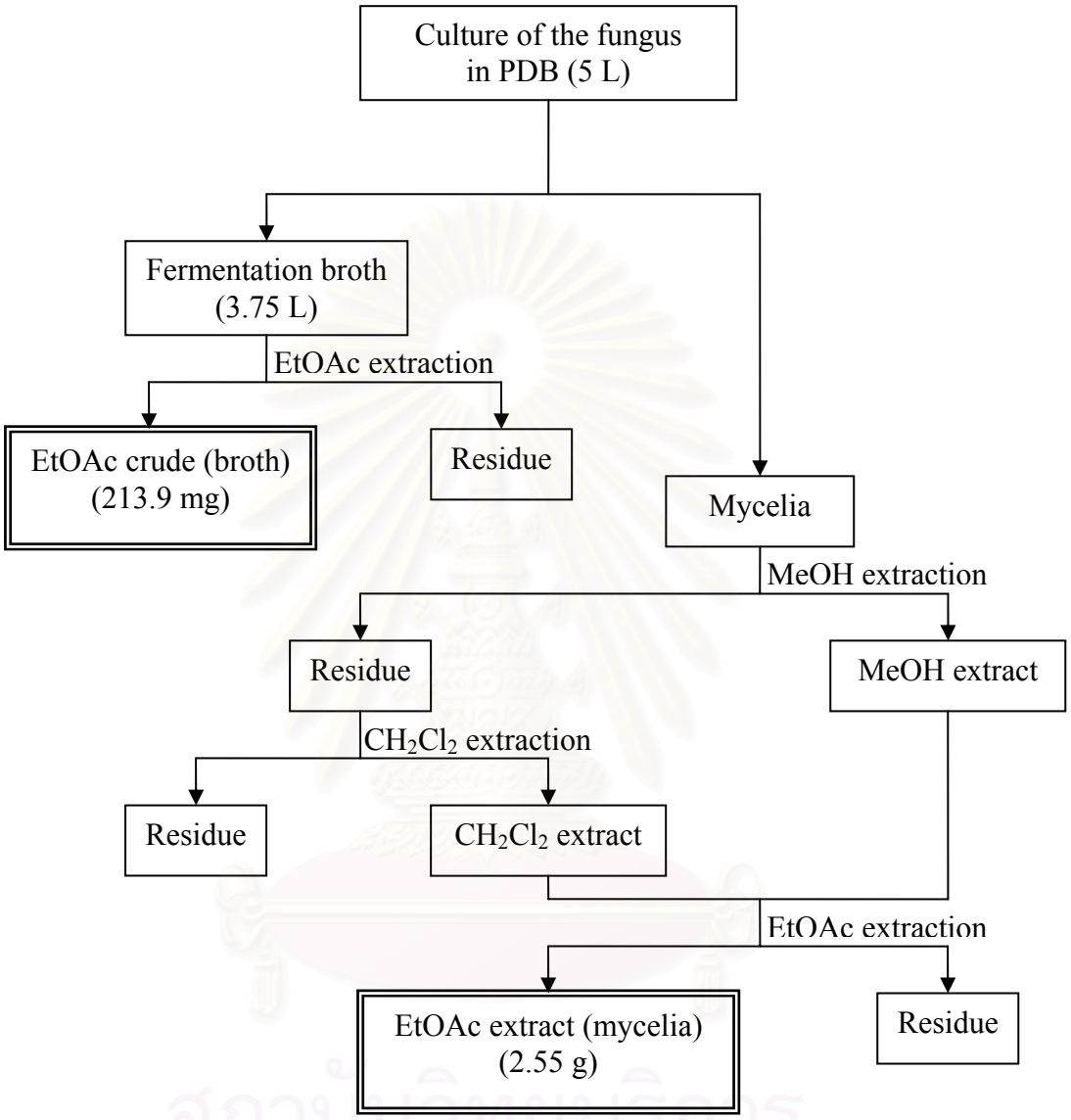

The crude broth extract was chromatographed on a Saphadex LH-20 column (2×125 cm) and eluted with MeOH to obtain ten fractions (A1 to A10). Fractions A8, A9, and A10 (64 mg) were combined, and further purified by column chromatography on silica gel (2×23 cm), eluted with a gradient elution each 50 mL of Haxane : EtOAc = 80 : 20 (50 mL), CH_2Cl_2 : EtOAc = 80 : 20 (50 mL), and CH_2Cl_2 : MeOH = 95 : 5 (50 mL), to obtain **Compound 1** (6-methoxymellein, 20.8 mg), **Compound 2** (5.6 mg) and **Compound 3** (vermilhotin, 23.2 mg) (**Scheme 3.2**) .

Scheme 3.2: Isolation of a broth extract of the marine-derived fungus strain CRI 247-01

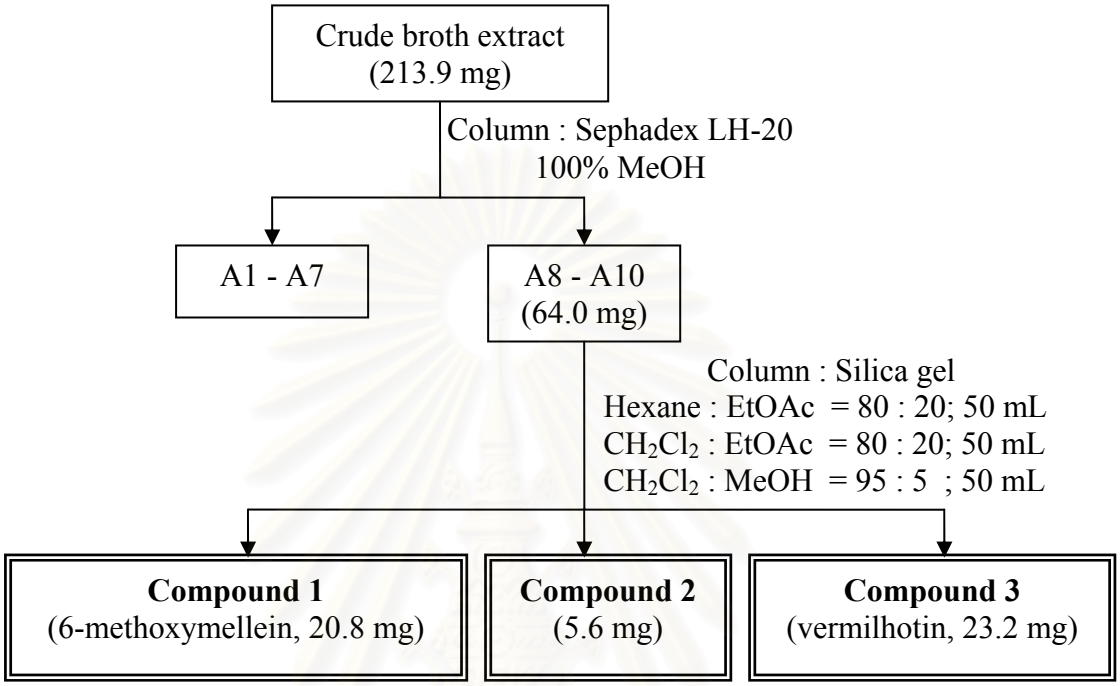

The crude extract of mycelia was separated with a Saphadex LH-20 column (3×85 cm) and eluted with MeOH to obtain three major fractions (B4, B7-B9, and B10-B12). A fraction B4 (191.2 mg) was dissolved in MeOH, however, it was not completely dissolved. The residue from fraction B4 (18.1 mg) was subjected to column chromatography on silica gel (1.5×20 cm), using the solvent mixture of hexane and EtOAc (80:20) as an eluent, yielding 7.2 mg of ergosterol as a colorless solid. Fractions B7, B8, and B9 were combined (29.3 mg) and purified with column chromatography on silica gel (1.5×20 cm), eluted with a mixture of EtOAc and MeOH (90:10), to obtain adenosine (8.4 mg). **Compound 1** (6-methoxymellein, 45.5 mg), **Compound 2** (6.0 mg), and **Compound 3** (vermilhotin, 21.3 mg) were obtained from the combined fraction B10 – B12 (81.9 mg) after purification with column chromatography on silica gel (2×23.5 cm) using 3 steps of elution with the following solvent mixtures (50 mL each); Haxane : EtOAc = 80 : 20, CH_2Cl_2 : EtOAc = 80 : 20 and CH_2Cl_2 : MeOH = 95 : 5 (**Scheme 3.3**).

Scheme 3.3: Isolation of a cell extract of the marine-derived fungus strain CRI 247-01

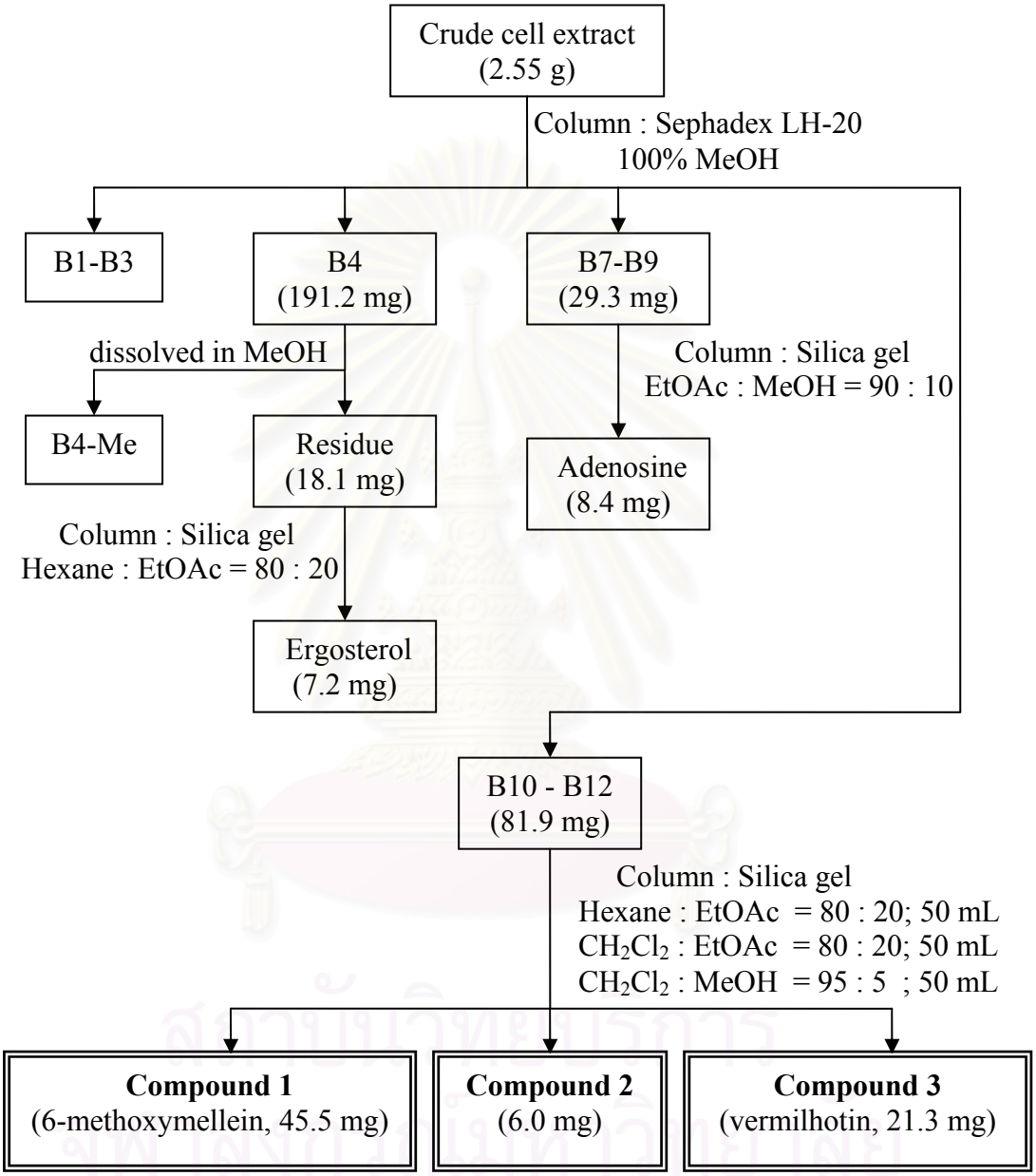

3.9 Extraction and isolation of chemical constituents of *Hypoxylon monticulosum* CRIF1

3.9.1 Fermentation, extraction and isolation

Colony of the marine-derived fungus *H. monticulosum* CRIF1 on PDA

The fungus *H. monticulosum* CRIF1 was maintained on PDA medium at room temperature for 7 days, and then inoculated into 10 × 1 L Erlenmeyer flasks, each containing 250 mL of PDB, and further incubated under static condition.

The fermentation broth (2.5 L) of *H. monticulosum* was filtered through a filter paper. The broth filtrate was partitioned with EtOAc 3 times. The EtOAc layers were combined, and evaporated under reduced pressure at temperature not exceeding 40 ºC to yield a dark brown solid (4.95 g).

Fungal mycelia were extracted twice with MeOH (each with 500 mL) and the fungal residue was subsequently extracted twice with CH_2Cl_2 (each with 500 mL). The MeOH and CH_2Cl_2 extracts were combined and extracted with EtOAc (3×500 mL) to give a mycelial crude extract (dark brown solid, 1.93 g) (**Scheme 3.4**).

Scheme 3.4: Extraction of fermentation broth and mycelia of the marine-derived fungus *H. monticulosum* CRIF1

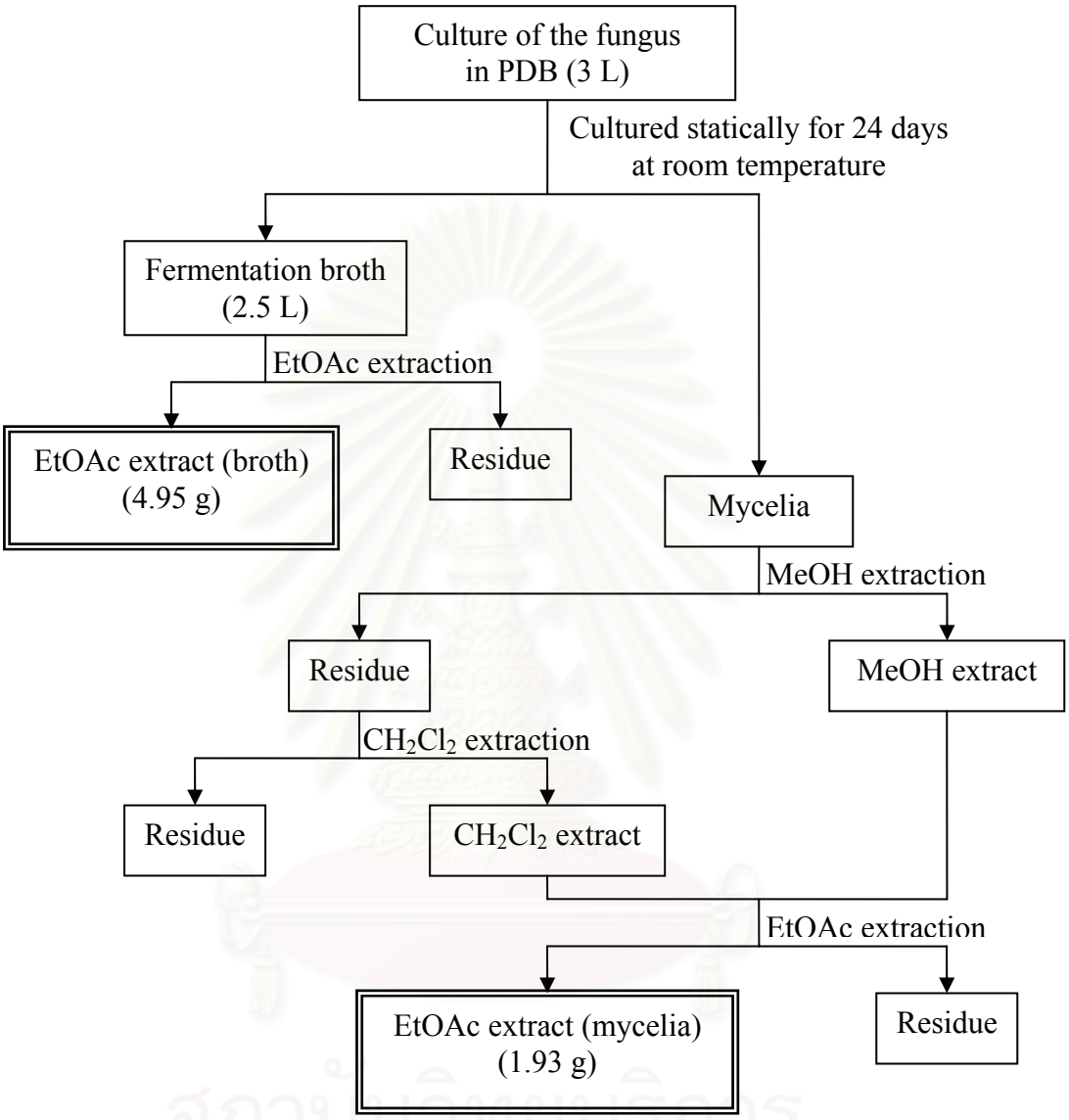

A broth extract (4.95 g) was fractionated on Sephadex LH-20 column (3.5×53 cm). The column was eluted with 100% MeOH, and fractions (50 mL each) were collected. Fraction HM-A5 (3.53 g) was separated on a Sephadex LH-20 column (3×85 cm) using 100% MeOH as an eluting solvent. Fraction HM-B5 (80.8 mg from 2.99 g) was further purified by MPLC eluted with a mixture of MeOH:H_2O (50:50) to give **compound 4** (19.4 mg) as shown in **Scheme 3.5**.

Scheme 3.5: Isolation of a broth extract of *H. monticulosum* CRIF1

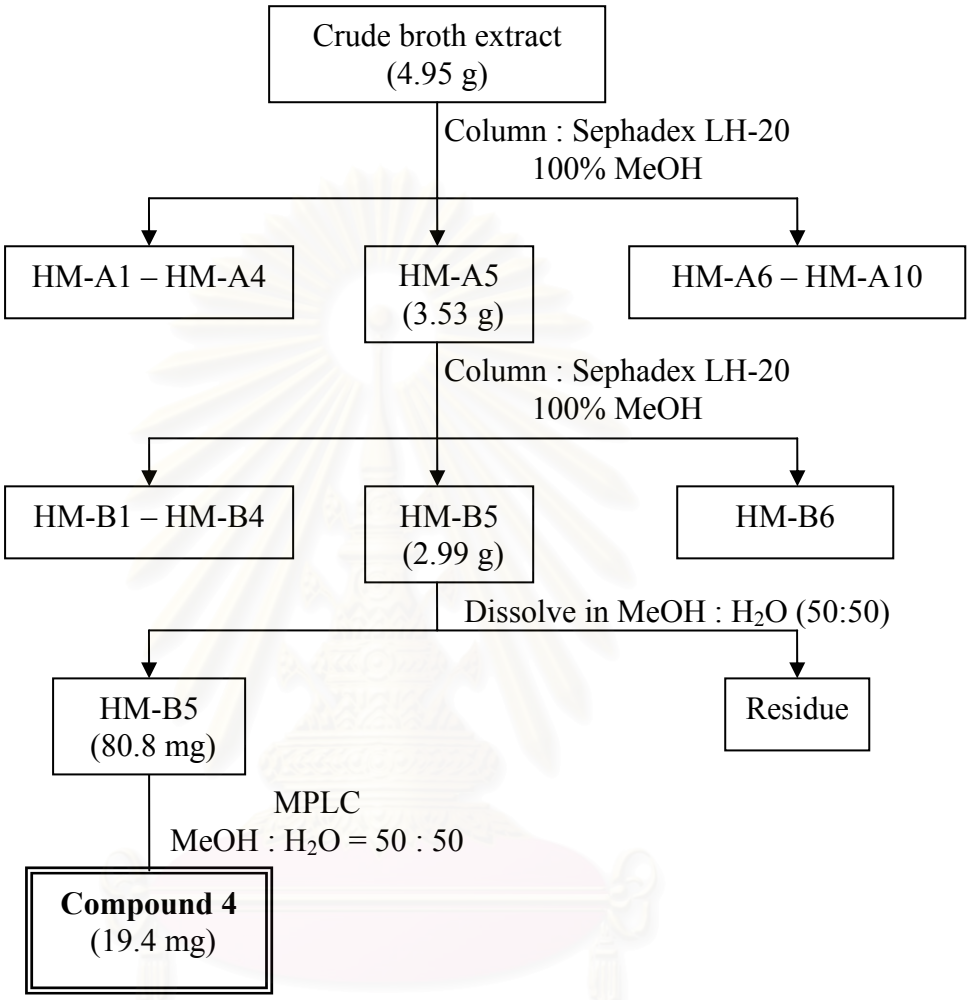

The crude extract of mycelia was chromatographed on a Sephadex LH-20 column (3×85 cm) using 100 % MeOH as a mobile phase to give 18 fractions. The fraction HM-D9 (378.8 mg) was further purified on a Sephadex LH-20 column (2×125 cm, 100 % MeOH) to afford **compound 4** (173.1 mg) as shown in **Scheme 3.6**.

Scheme 3.6: Isolation of mycelial extract of *H. monticulosum* CRIF1

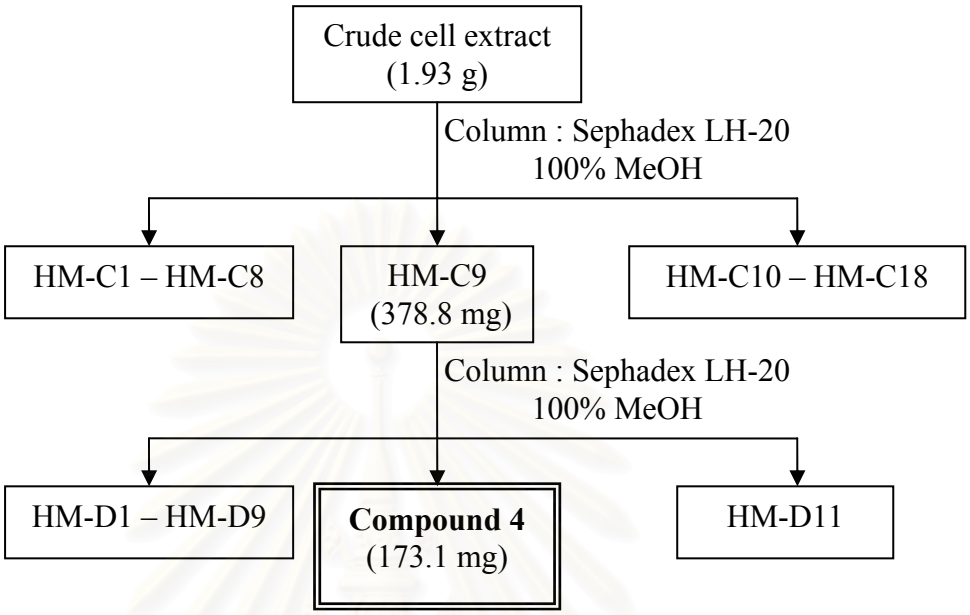

3.9.2 Derivatization of **compound 4**

3.9.2.1 Esterification

*Methyl ester of **compound 4***

Compound 4 (97.9 mg) is dissolved in 25 mL of anhydrous MeOH, 2-3 drop of conc. HCl is added and the mixture is refluxed for 5h.

The solution is cooled and evaporated in vacuum and the residue is purified by silica gel (2.5×21 cm) to give a yellow viscous oil of **compound 5** (52.9 mg) as shown in **Scheme 3.7**.

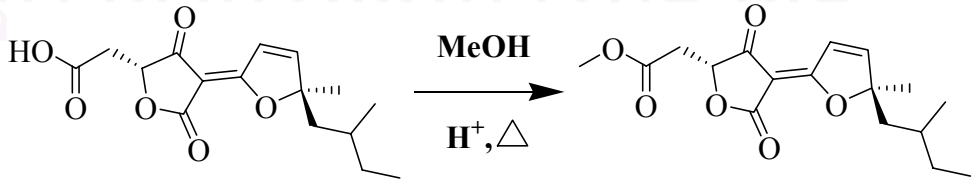

Compound 4 **Compound 5**

Scheme 3.7: Methyl esterification of **compound 4**

Benzyl ester of ***compound 4***

A mixture (30 mL) containing **compound 4** (125.3 mg), benzyl alcohol (5 mL), and a catalytic amount of *p*-toluenesulfonic acid monohydrate (TsOH) was refluxed in toluene (25 mL) using a Dean-Stark apparatus (approximately 3 h).

When the reaction mixture was cooled and evaporated in vacuum, the residue was purified by a Sephadex LH-20 column (2×43 cm) to give a yellow viscous oil of **compound 6** (100.4 mg) (**Scheme 3.8**).

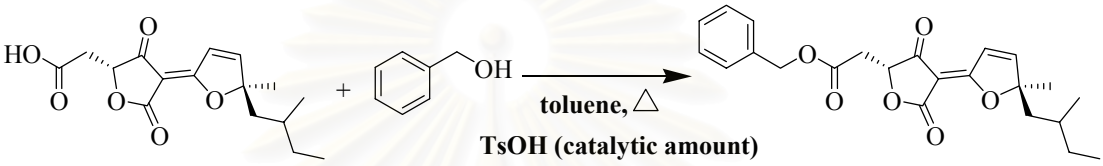

Compound 4 **Benzyl alcohol** **Compound 6**

Scheme 3.8: Benzyl esterification of **compound 4**

3.9.2.2 Hydrogenation

A 50 mL two-necked flask was sealed with a septum, and connected to a gas inlet tube. **Compound 4** (54.6 mg) was dissolved in 15 mL of anhydrous EtOH, and 6.0 mg of 10% palladium on charcoal was added to a mixture. The system was flown with H_2 three times, and the reaction mixture was kept under H_2 and vigorously stirred at room temperature for 8 h.

The catalyst was removed by filtration through celite on a sintered glass funnel, and washed with EtOH. The filtrate was evaporated under vacuum, and the residue was purified by a Sephadex LH-20 column (2×42 cm), followed by another Sephadex LH-20 column (1.5×31 cm) to give yellow viscous oil of **compound 7** (29.0 mg) as shown in **Scheme 3.9**.

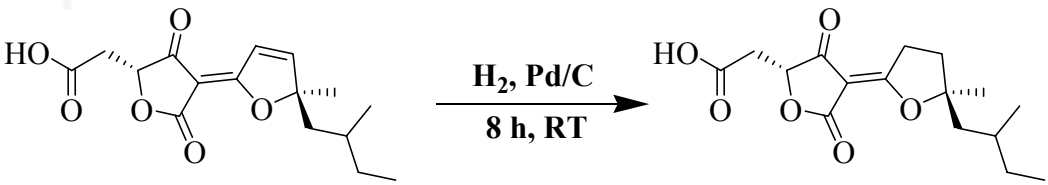

Compound 4 **Compound 7**

Scheme 3.9: Hydrogenation of **compound 4**

Compound 1 (6-methoxymellein)

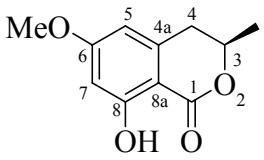

Compound 1

$C_{11}H_{12}O_4$

White needle

m.p.	74-76 °C
$[\alpha]_D^{28}$	–41.2 (*c* 0.87 in MeOH)

[Lit. (Sondheimer, 1957); m.p. 75-76°C; $[\alpha]_D^{24}$: –56 (*c* 1 in MeOH)]

R_f	0.25 (20% EtOAc in Hexane)
UV (MeOH) λ_{max} (log ε)	221.5 (3.81), 267.5 (3.69), 301.5 (3.30) nm
HRMS (APCI-TOF) *m/z*	209.0813 $[M+H]^+$
	(calcd. for $[C_{11}H_{12}O_4+H]^+$ 209.0814)
IR (UATR -Solid) ν_{max}	3080, 2979, 2939, 2846, 1658, 1625, 1581, 1507, 1438, 1369, 1310, 1246, 1221, 1203, 1156, 1116, 1098, 1068, 1033, 963, 937, 910, 897, 839, 799, 756, 702, 679 cm^{-1}

^1H NMR and ^{13}C NMR data in $CDCl_3$: see **Table 4.1/ Page 51**

Compound 2

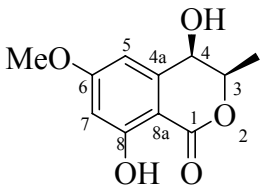

Compound 2

$C_{11}H_{12}O_5$

White amorphous solid

$[\alpha]_D^{29}$	–2.5 (*c* 0.96 in MeOH)
R_f	0.20 (5% EtOAc in CH_2Cl_2)
UV (MeOH) λ_{max} (log ε)	222.8 (4.04), 266.2 (3.95), 302.6 (3.65) nm
HRMS (APCI-TOF) *m/z*	225.0752 $[M+H]^+$
	(calcd. for $[C_{11}H_{12}O_5+H]^+$ 225.0763)
IR (UATR-Solid) ν_{max}	3399, 2973, 2925, 2852, 1651, 1625, 1582, 1500, 1439, 1373, 1307, 1242, 1202, 1157, 1115, 1031, 987, 963, 933, 886, 850, 806, 751, 706, 664 cm^{-1}

^1H NMR and ^{13}C NMR data in acetone-d_6: see **Table 4.2/ Page 55**

Compound 3 (vermilhotin)

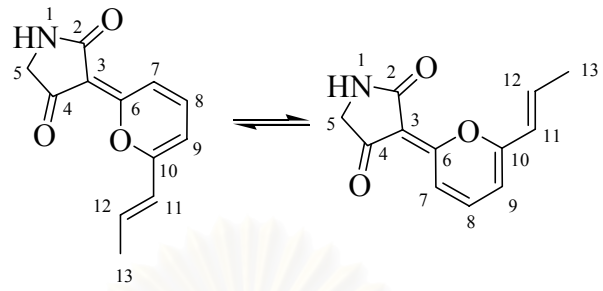

(*E*)-form **(*Z*)-form**

Compound 3

$C_{12}H_{11}NO_3$

Red micro-needles

m.p.	213.0–214.5 °C (decomposed)
[Lit. (Hosoe et al., 2006); m.p. 212-214 °C]	
R_f	0.20 (5% MeOH in CH_2Cl_2)
UV (MeOH) λ_{max} (log ε)	222.5 (4.16), 276.0 (4.34), 319.0 (3.78), 438.5 (4.19) nm
HRMS (APCI-TOF) *m/z*	218.0811 $[M+H]^+$ (calcd. for $[C_{12}H_{11}NO_3+H]^+$ 218.0817)
IR (UATR-Solid) ν_{max}	3173, 3042, 2919, 2853, 2706, 2353, 2120, 1870, 1698, 1650, 1610, 1552, 1489, 1460, 1430, 1376, 1349, 1310, 1258, 1233, 1213, 1193, 1151, 1076, 979, 961, 930, 873, 815, 780, 730, 719, 676 cm^{-1}

^1H NMR and ^{13}C NMR data in DMSO-d_6 (600 MHz): see **Table 4.4/ Page 63**

Compound 4

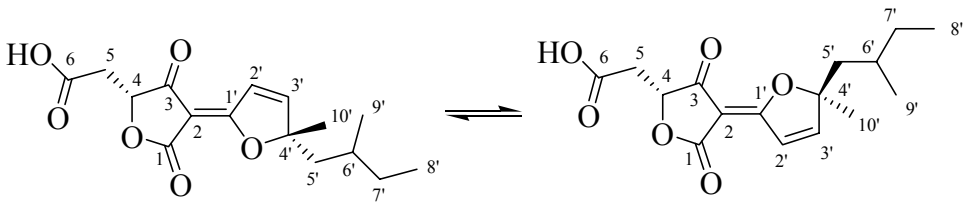

(*Z*)-form **(*E*)-form**

Compound 4

$C_{16}H_{20}O_6$

Off white amorphous solid

$[\alpha]_D^{27}$	–20.6 (*c* 1.10 in MeOH)
	–28.8 (*c* 1.05 in $CHCl_3$)
R_f	0.33 [5%(10%CH_3COOH/MeOH) in CH_2Cl_2]
UV (MeOH) λ_{max} (log ε)	317.0 (4.28) nm
HRMS (APCI-TOF) *m/z*	309.1331 $[M+H]^+$
	(calcd. for $[C_{16}H_{20}O_6+H]^+$ 309.1338)
IR (UATR-Liquid) ν_{max}	3433, 3113, 3079, 2962, 2931, 2873, 1755, 1696, 1583, 1563, 1427, 1353, 1267, 1236, 1200, 1142, 1047, 1021, 992, 913, 821, 784, 736, 703, 680 cm^{-1}

^1H NMR and ^{13}C NMR data in DMSO-d_6: see **Table 4.5-4.7/ Page 73-75**

Compound 5

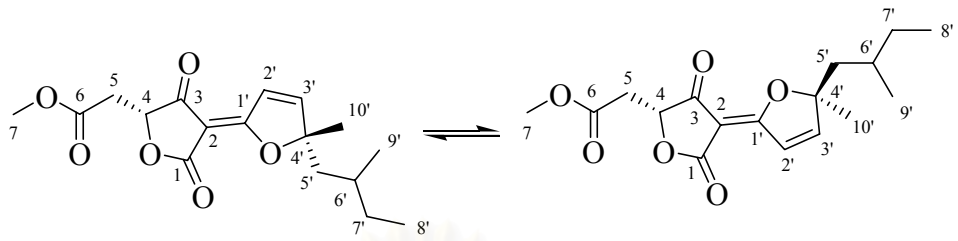

(*Z*)-form **(*E*)-form**

Compound 5

$C_{17}H_{22}O_6$

Yellow viscous oil

$[\alpha]_D^{27}$	–2.3 (*c* 1.02 in MeOH)
$[\alpha]_D^{25}$	–11.4 (*c* 1.00 in $CHCl_3$)
R_f	0.30 (50% EtOAc in hexane)
UV (MeOH) λ_{max} (log ε)	259.8 (3.83) nm
HRMS (APCI-TOF) *m/z*	323.1490 $[M+H]^+$
	(calcd. for $[C_{17}H_{22}O_6+H]^+$ 323.1495)
IR (UATR-Solid) ν_{max}	3080, 2959, 2926, 2873, 1740, 1698, 1583, 1564, 1456, 1437, 1375, 1354, 1327, 1266, 1198, 1165, 1141, 1080, 1047, 1019, 986, 946, 896, 856, 819, 704, 674 cm^{-1}

^{1}H NMR and ^{13}C NMR data in DMSO-d_6:

(Assignments are based on data correlation with those of **compound 4**.)

(*E*)-form

^{1}H NMR data (DMSO-d_6, 400 MHz):

δ 8.01 (1H, d, *J* = 5.8 Hz, H-3′), 7.28 (1H, d, *J* = 5.8 Hz, H-2′), 4.84 (1H, dd, *J* = 4.2, 6.4 Hz, H-4), 3.59 (3H, s, H-7)[a], 2.91 (1H, d, *J* = 4.2 Hz, H-5a), 2.82 (1H, dd, *J* = 4.3, 6.4 Hz, H-5b), 1.99 (1H, dd, *J* = 3.7, 8.9 Hz, H-5′a), 1.62 (1H, dd, *J* = 7.5, 9.1 Hz, H-5′b), 1.52 (3H, s, H-10′), 1.21 (1H, m, H-6′), 1.21 (1H, m, H-7′a), 1.10 (1H, m, H-7′b), 0.84 (3H, d, *J* = 6.4 Hz, H-9′), 0.77 (3H, t, *J* = 7.2 Hz, H-8′).

^{13}C NMR data (DMSO-d_6, 400 MHz):

δ 194.0 (C, C-3), 178.6 (C, C-1′), 170.2 (C, C-6), 170.1 (C, C-1), 163.6 (CH, C-3′), 121.7 (CH, C-2′), 102.5 (C, C-4′), 93.3 (C, C-2), 78.3 (CH, C-4), 52.1 (CH_3, C-7)[b], 43.7 (CH_2, C-5′), 35.6 (CH_2, C-5), 30.2 (CH, C-6′), 30.1 (CH_2, C-7′)[c], 23.5 (CH_3, C-10′), 21.0 (CH_3, C-9′), 11.3 (CH_3, C-8′).

(*Z*)-form

^{1}H NMR data (DMSO-d_6, 400 MHz):

δ 8.01 (1H, d, *J* = 5.8 Hz, H-3′), 7.38 (1H, d, *J* = 5.8 Hz, H-2′), 4.90 (1H, dd, *J* = 4.2, 6.5 Hz, H-4), 3.57 (3H, s, H-7)[a], 2.95 (1H, d, *J* = 3.9 Hz, H-5a), 2.86 (1H, dd, *J* = 4.3, 6.4 Hz, H-5b), 2.03 (1H, dd, *J* = 3.7, 9.0 Hz, H-5′a), 1.66 (1H, dd, *J* = 7.4, 8.8 Hz, H-5′b), 1.52 (3H, s, H-10′), 1.21 (1H, m, H-6′), 1.21 (1H, m, H-7′a), 1.10 (1H, m, H-7′b), 0.84 (3H, d, *J* = 6.4 Hz, H-9′), 0.78 (3H, t, *J* = 7.2 Hz, H-8′).

^{13}C NMR data (DMSO-d_6, 400 MHz):

δ 196.5 (C, C-3), 179.6 (C, C-1′), 170.1 (C, C-1), 167.4 (C, C-6), 163.6 (CH, C-3′), 121.7 (CH, C-2′), 102.0 (C, C-4′), 93.3 (C, C-2), 78.5 (CH, C-4), 52.2 (CH_3, C-7)[b], 43.6 (CH_2, C-5′), 35.5 (CH_2, C-5), 30.2 (CH, C-6′), 30.0 (CH_2, C-7′)[c], 23.4 (CH_3, C-10′), 21.0 (CH_3, C-9′), 11.3 (CH_3, C-8′).

[a,b,c] interchangeable between (*E*)-form and (*Z*)-form

Compound 6

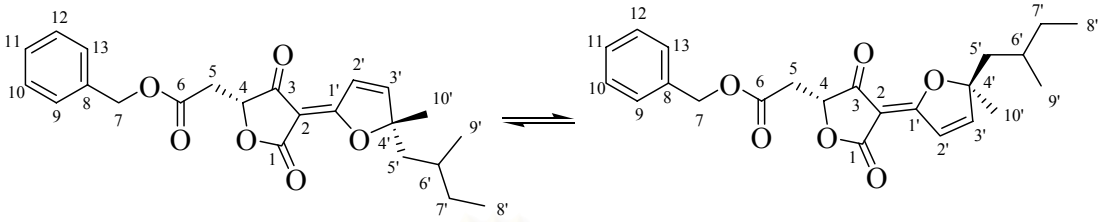

(*Z*)-form **(*E*)-form**

Compound 6

$C_{23}H_{26}O_6$

Yellow viscous oil

$[\alpha]_D^{26}$	–8.0 (*c* 1.27 in MeOH)
$[\alpha]_D^{25}$	–17.3 (*c* 1.16 in $CHCl_3$)
R_f	0.33 (20% EtOAc in hexane)
UV (MeOH) λ_{max} (log ε)	318.0 (4.28) nm
HRMS (APCI-TOF) *m/z*	399.1808 $[M + H]^+$
	(calcd. for $[C_{23}H_{26}O_6+H]^+$ 399.1808)
IR (UATR-solid) ν_{max}	3073, 2961, 2931, 2873, 1737, 1697, 1583, 1563, 1498, 1456, 1384, 1356, 1327, 1265, 1235, 1162, 1140, 1079, 1047, 1017, 987, 907, 818, 783, 748, 698, 673 cm^{-1}

^{1}H NMR and ^{13}C NMR data in DMSO-d_6:

(Assignments are based on data correlation with those of **compound 4**.)

(*E*)-form

^{1}H NMR data (DMSO-d_6, 400 MHz):

δ 8.01 (1H, d, *J* = 5.8 Hz, H-3′), 7.34 (5H, m, H8-H13), 7.29 (1H, d, *J* = 5.8 Hz, H-2′), 5.10 (1H, d, *J* = 2.4 Hz, H-7a), 5.09 (1H, d, *J* = 2.2 Hz, H-7b), 4.88 (1H, dd, *J* = 4.3, 6.0 Hz, H-4), 3.04 (1H, dd, *J* = 1.3, 4.3 Hz, H-5a), 2.96 (1H, t, *J* = 6.5 Hz, H-5b), 2.01 (1H, dd, *J* = 3.4, 14.7 Hz, H-5′a), 1.61 (1H, dd, *J* = 4.7, 7.3 Hz, H-5′b), 1.52 (3H, s, H-10′), 1.23 (1H, m, H-6′), 1.23 (1H, m, H-7′a), 1.11 (1H, m, H-7′b), 0.85 (3H, d, *J* = 6.3 Hz, H-9′), 0.78 (3H, t, *J* = 7.6 Hz, H-8′).

^{13}C NMR data (DMSO-d_6, 400 MHz):

δ 193.9 (C, C-3), 178.6 (C, C-1′), 170.2 (C, C-6), 169.6 (C, C-1), 163.6 (CH, C-3′), 136.1 (C, C-8), 128.8-128.3 (CH, C-9 – C-13)[d], 121.7 (CH, C-2′), 102.5 (C, C-4′), 93.7 (C, C-2), 78.3 (CH, C-4), 66.4 (CH_2, C-7), 43.7 (CH_2, C-5′), 35.6 (CH_2, C-5), 30.2 (CH_2, C-7′), 30.1 (CH, C-6′)[e], 23.4 (CH_3, C-10′), 20.9 (CH_3, C-9′), 11.3 (CH_3, C-8′).

(*Z*)-form

^{1}H NMR data (DMSO-d_6, 400 MHz):

δ 8.01 (1H, d, *J* = 5.8 Hz, H-3′), 7.39 (1H, d, *J* = 5.8 Hz, H-2′), 7.34 (5H, m, H8-H13), 5.10 (1H, d, *J* = 2.4 Hz, H-7a), 5.09 (1H, d, *J* = 2.2 Hz, H-7b), 4.94 (1H, dd, *J* = 4.4, 6.0 Hz, H-4), 2.99 (1H, dd, *J* = 1.2, 4.3 Hz, H-5a), 2.92 (1H, t, *J* = 6.5 Hz, H-5b), 2.01 (1H, dd, *J* = 3.7, 14.7 Hz, H-5′a), 1.65 (1H, dd, *J* = 4.8, 7.2 Hz, H-5′b), 1.52 (3H, s, H-10′), 1.23 (1H, m, H-6′), 1.23 (1H, m, H-7′a), 1.11 (1H, m, H-7′b), 0.85 (3H, d, *J* = 6.3 Hz, H-9′), 0.78 (3H, t, *J* = 7.6 Hz, H-8′).

^{13}C NMR data (DMSO-d_6, 400 MHz):

δ 196.4 (C, C-3), 179.6 (C, C-1′), 169.5 (C, C-1),167.4 (C, C-6), 163.6 (CH, C-3′), 136.1 (C, C-8), 128.8-128.3 (CH, C-9 – C-13)[d], 121.7 (CH, C-2′), 102.0 (C, C-4′), 93.3 (C, C-2), 78.5 (CH, C-4), 66.4 (CH_2, C-7), 43.6 (CH_2, C-5′), 35.8 (CH_2, C-5), 30.2 (CH_2, C-7′), 30.0 (CH, C-6′)[e], 23.4 (CH_3, C-10′), 20.9 (CH_3, C-9′), 11.3 (CH_3, C-8′).

[d,e] interchangeable between (*E*)-form and (*Z*)-form

Compound 7

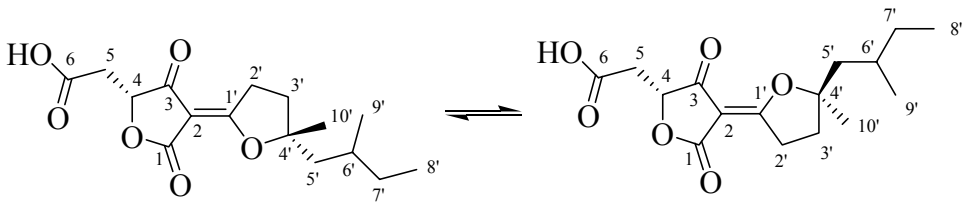

(*Z*)-form **(*E*)-form**

Compound 7

$C_{16}H_{20}O_6$

Yellow viscous oil

R_f	0.70 [5%(10% CH_3COOH/MeOH) in CH_2Cl_2)
UV (MeOH) λ_{max} (log ε)	276.5 (4.06) nm
HRMS (APCI-TOF) *m/z*	309.1343 $[M - H]^-$
	(calcd. for $[C_{16}H_{20}O_6\text{-}H]^-$ 309.1338)
IR (UATR-solid) ν_{max}	3466, 2960, 2926, 2873, 1733, 1698, 1582, 1461, 1410, 1386, 1326, 1293, 1200, 1182, 1131, 1082, 1047, 1018, 955, 900, 816, 778, 734, 669 cm^{-1}:

^1H NMR and ^{13}C NMR data in $CDCl_3$:

(Assignments are based on data correlation with those of **compound 4**.)

(*E*)-form

^1H NMR data ($CDCl_3$, 400 MHz):

δ 6.47 (1H, bs, OH-6, carboxylic), 4.81 (1H, dd, *J* = 4.0, 7.7 Hz, H-4), 3.55 (1H, m, H-2′a), 3.44 (1H, m, H-2′b), 3.01 (1H, dd, *J* = 4.0, 9.2 Hz, H-5a), 2.81 (1H, dd, *J* = 6.9, 10.8 Hz, H-5b), 2.09 (2H, m, H-3′), 1.79 (1H, t, *J* = 4.0 Hz, H-5′a), 1.66 (1H, m, H-5′b), 1.60 (1H, m, H-6′), 1.53 (3H, s, H-10′), 1.34 (1H, m, H-7′a), 1.25 (1H, m, H-7′b), 1.02 (3H, d, *J* = 6.4 Hz, H-9′), 0.89 (3H, t, *J* = 7.4 Hz, H-8′).

^{13}C NMR data ($CDCl_3$, 400 MHz):

δ 193.2 (C, C-3), 185.8 (C, C-1′), 173.7 (C, C-1), 170.8 (C, C-6), 100.7 (C, C-4′), 95.1 (C, C-2), 78.2 (CH, C-4), 46.5 (CH_2, C-5′), 35.7 (CH_2, C-5), 34.1 (CH_2, C-2′), 33.4 (CH_2, C-3′), 30.9 (CH, C-6′), 30.6 (CH_2, C-7′), 24.8 (CH_3, C-10′), 20.5 (CH_3, C-9′), 11.2 (CH_3, C-8′).

(*Z*)-form

^{1}H NMR data ($CDCl_3$, 400 MHz):

δ 6.47 (1H, bs, OH-6, carboxylic), 4.84 (1H, dd, *J* = 4.2, 7.1 Hz, H-4), 3.55 (1H, m, H-2′a), 3.44 (1H, m, H-2′b), 3.01 (1H, dd, *J* = 4.0, 9.2 Hz, H-5a), 2.81 (1H, dd, *J* = 6.9, 10.8 Hz, H-5b), 2.09 (2H, m, H-3′), 1.81 (1H, t, *J* = 4.0 Hz, H-5′a), 1.70 (1H, dd, *J* = 5.8, 7.7 Hz, H-5′b), 1.60 (1H, m, H-6′), 1.55 (3H, s, H-10′), 1.34 (1H, m, H-7′a), 1.25 (1H, m, H-7′b), 1.02 (3H, d, *J* = 6.4 Hz, H-9′), 0.89 (3H, t, *J* = 7.4 Hz, H-8′).

^{13}C NMR data ($CDCl_3$, 400 MHz):

δ 197.4 (C, C-3), 186.6 (C, C-1′), 173.5 (C, C-1), 166.9 (C, C-6), 100.3 (C, C-4′), 94.7 (C, C-2), 78.3 (CH, C-4), 46.4 (CH_2, C-5′), 35.7 (CH_2, C-5), 33.7 (CH_2, C-2′), 33.4 (CH_2, C-3′), 30.9 (CH, C-6′), 30.6 (CH_2, C-7′), 24.8 (CH_3, C-10′), 20.4 (CH_3, C-9′), 11.2 (CH_3, C-8′).

CHAPTER IV

RESULTS AND DISCUSSION

4.1 Chemical constituents of the marine-derived fungus strain CRI 247-01 metabolites

Anticancer assay revealed that a crude extract of the sponge-derived fungus CRI 247-01 possessed interesting activity. The fungal extract also exhibited cytotoxicity against cell lines with IC_{50} ranges from 10.0 to 35.0 μg/mL; this interesting bioactivity initiated the investigation of bioactive compounds of this fungus. Isolation of the EtOAc extract of culture broth of the sponge-derived fungus CRI 247-01 (culture incubation period, 24 days) by chromatographic techniques led to the identification of a new dihydro-isocoumarin (**compound 2**), together with two known compounds, dihydro-isocoumarin named 6-methoxymellein (**compound 1**) (Sondheimer, 1957) and a tetramic acid derivative named vermilhotin (**compound 3**) (Hosoe et al., 2006). The crude extract from the mycelia of CRI 247-01 was subjected to a multi-step chromatographic fractionation, and **compounds 1-3** were isolated from the cell extract, along with two known compounds, ergosteol and adenosine. Chemical structures of these compounds were elucidated by analyses of spectroscopic data, including IR, UV, NMR and MS spectra, as well as by comparison of their spectral data with those of published values.

Compound 1
(6-methoxymellein)

Compound 2

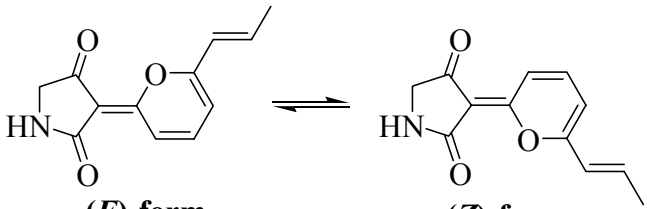

(*E*)-form **(*Z*)-form**

Compound 3
(vermilhotin)

Structure elucidation of compound 1

(*6-Methoxymellein; (R)-8-hydroxy-6-methoxy-3-methylisochroman-1-one*)

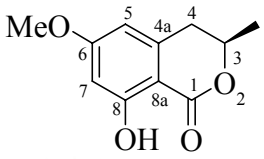

Compound 1 was obtained as white needle. The APCI-TOF mass spectrum of **compound 1** provided the $[M+H]^+$ ion peak at *m/z* 209.0813 (calcd. for $[C_{11}H_{12}O_4+H]^+$ 209.0814), which indicated the molecular formula of this compound as $C_{11}H_{12}O_4$. UV spectrum of **compound 1** in MeOH showed maximum absorptions at λ_{max} 221.5, 267.5, and 301.5 nm (**Fig. A1, Page 91**). Its IR spectrum showed sharp and strong of carbonyl of hydrogen-bonded lactones stretching vibration at λ_{max} 1658 cm^{-1} (**Fig. A2, Page 91**). The degree of unsaturation counted from this molecular formula was six.

The ^1H NMR of **compound 1** ($CDCl_3$, 400 MHz) (**Fig. A3, Page 92**) exhibited a methyl doublet at δ_H 1.51 (*J* = 6.4 Hz, 3-Me) attributable to the methyl group on the carbon bearing an oxygenated proton at δ_H 4.67 (*J* = 6.4, 7.2 Hz, H-3). A doublet at δ_H 2.86 (*J* = 7.2 Hz, H-4) was assigned to the virtually equivalent methylene protons coupling to H-3. A sharp three-proton singlet (6-OMe) at δ_H 3.83 was of the methoxy group, and the one-proton doublet of quintet at δ_H 4.67 (*J* = 6.4, 7.2 Hz, H-3) arised from the coupling of the methyl and methylene group. The aromatic region contained two signals (*J* = 2.4 Hz, typical for *meta*-coupled protons) at δ_H 6.36 (*J* = 2.4 Hz, H-7) and δ_H 6.25 (*J* = 2.4, 1.2 Hz, H-5), while the exchangeable proton (8-OH) of the intramolecularly bonded hydroxyl group was observed at δ_H 11.25. The connectivity from H-3 through H-4 and 3-Me was confirmed by COSY spectrum (**Fig. A8, Page 95**). The ^1H, ^1H COSY spectrum of **compound 1** revealed the correlations of the following protons: H-3 (δ_H 4.67, *J* = 6.4, 7.2 Hz); H-4 (δ_H 2.86, *J* = 7.2 Hz); and 3-Me (δ_H 1.51, *J* = 6.4 Hz).

^{13}C NMR spectrum ($CDCl_3$) of **compound 1** (**Fig. A5, Page 93**) revealed the presence of eleven carbons, which could be classified by DEPTs (**Fig. A6, Page 93**) as two methyl (δ_C 20.7 and 55.5), one methylene (δ_C 34.8), three methine (δ_C 75.5, 99.4 and 106.1) and five quaternary carbons (δ_C 101.5, 140.9, 164.5, 165.7 and 169.8). Taken together with an analysis of HMQC spectrum (**Fig. A7, Page 94**), each existing proton can be assigned to its carbon atom. Particularly COSY and HMBC techniques could be explained into the structure of **compound 1**.

The complete structure of **compound 1** was established by analysis of the HMBC spectrum (**Fig. A9, Page 96**) which showed the correlations from H-3 (δ_H 4.67) to C-1 and aromatic C-4a; and H-4 (δ_H 2.87) to aromatic C-4a, C-5, and C-8a. The HMBC correlations were also observed from H-5 to C-4, C-6, C-7, and C-8a; H-7 to C-8 and C-8a; and 6-OMe protons to C-6. A low field exchangeable proton (8-OH) was a characteristic of hydrogen-bonded hydroxyl group on C-8 by HMBC correlation 8-OH to C-7, C-8, and C-8a (**Fig 4.1**).

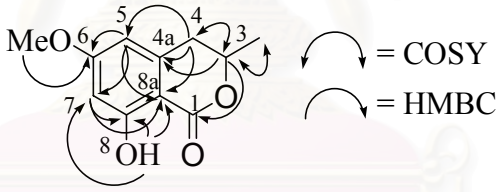

Figure 4.1: The gross structure of **compound 1**

Based on these spectral data, **compound 1** was identified as (-)-6-methoxymellein. Since **compound 1** showed negative specific rotation ($[\alpha]_D^{28}$ = –41.2, *c* 0.87 in MeOH) similar to that of (-)-6-methoxymellein ($[\alpha]_D^{24}$ = –56, *c* 1 in MeOH, Sondheimer (1957)), therefore the absolute configuration at C-3 was more likely to be *R*. Specific rotation value of (+)-6-Methoxymellein or angelicin B was $[\alpha]_D^{20}$ = +31.5, *c* 0.5 in MeOH, its was reported by Shibano et al., (2006).

Table 4.1: NMR spectral data for **compound 1** and 6-methoxymellein

position	**Compound 1** ($CDCl_3$)		6-Methoxymellein ($CDCl_3$)		
	δ_C	δ_H (mult., *J* in Hz)	δ_C[a]	δ_C[b]	δ_H (mult., *J* in Hz)[a]
1	169.8 (C)	-	169.8 (C)	169.9 (C)	-
2	-	-	-	-	-
3	75.5 (CH)	4.67 (dq, 6.4, 7.2)	75.4 (CH)	75.5 (CH)	4.67 (m)
4	34.8 (CH_2)	2.86 (d, 7.2)	34.8 (CH_2)	34.8 (CH_2)	2.87 (d, 6.6)
4a	140.9 (C)	-	140.8 (C)	141.0 (C)	-
5	106.1 (CH)	6.25 (dt, 1.2, 2.4)	99.4 (CH)	106.1 (CH)	6.25 (d, 2.2)
6	165.7 (C)	-	165.7 (C)	165.8 (C)	-
7	99.4 (CH)	6.36 (d, 2.4)	101.5 (CH)	99.5 (CH)	6.37 (d, 2.7)
8	164.5 (C)	-	164.5 (C)	164.6 (C)	-
8a	101.5 (C)	-	106.1 (C)	101.6 (C)	-
3-Me	20.7 (CH_3)	1.51 (3H, d, 6.4)	20.6 (CH_3)	20.7 (CH_3)	1.51 (3H, d, 6.6)
6-OMe	55.5 (CH_3)	3.83 (3H, s)	55.5 (CH_3)	55.6 (CH_3)	3.85 (3H, s)
8-OH	-	11.25 (s)	-	-	11.25 (s)

[a,b] Assignment was by Czepa and Hofmann (2003); Stoessl and Stothers (1978), respectively.

Structure elucidation of compound 2

(*(3R,4R)-4,8-dihydroxy-6-methoxy-3-methylisochroman-1-one*)

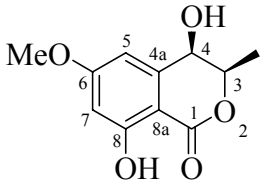

Compound 2 was obtained as a pale red solid. The UV spectrum of **compound 2** (**Fig. A13, Page 98**) in MeOH showed absorptions at λ_{max} 222.8, 266.2, and 302.6 nm similar to those of **compound 1**. The IR spectrum (**Fig. A14, Page 98**) of this compound showed carbonyl absorption (C=O stretching vibration) at 1651 cm^{-1} (typical for chelation between the ortho position of carbonyl and hydroxyl group, and benzenoid absorptions (1625, 1582, 1500 cm^{-1}). Medium broad of OH stretching vibration absorption at 3399 cm^{-1} indicated one hydroxyl group (non-chelated). The APCI-TOF mass spectrum of the **compound 2** showed the $[M+H]^+$ ion peak at *m/z* 225.0752 (calcd. for $[C_{11}H_{12}O_5+H]^+$ 225.0763) indicating its molecular formula as $C_{11}H_{12}O_5$. The mass of **compound 2** accounted for an additional oxygen atom in **compound 1** indicated that the remaining oxygen was present as an OH. The degree of unsaturation counted from this molecular formula was six.

The ^1H NMR spectrum (acetone-d_6, 400MHz) of **compound 2** (**Fig. A15, Page 99**) were similar to that of **compound 1**, showing signals of methine proton (H-4) at δ_H 4.61; mehtine proton (H-3) at δ_H 4.71; and hydroxyl group (4-OH) at δ_H 4.81. The methine proton (H-3) showed a complex signal of a doublet of quintet (J = 2.3, 6.6 Hz), which was coupled with H-4 (J = 2.2, 5.9 Hz) and a methyl group (3-Me) at δ_H 1.47 (J = 6.6 Hz). An additional hydroxyl proton (4-OH) was a doublet with J = 6.1 Hz. The two aromatic protons appeared as doublet at δ_H 6.46 (J = 2.4 Hz, H-7) and doublet of doublet at δ_H 6.56 (J = 0.4, 2.4 Hz, H-5), suggesting the presence of *meta*-coupling aromatic protons. A sharp three-proton singlet (6-OMe) at δ_H 3.88 was of the methoxy group and the hydroxyl proton (8-OH) appeared as a singlet at δ_H 11.33 (downfield shift due to H-bonding).

^{13}C NMR (acetone-d_6) and DEPT analysis (**Fig. A18, Page 100**) led to the classification of the 10 carbons, consisting of two methyl (δ_C 15.2 and 55.2), four methine (δ_C 66.4, 77.9, 100.4, and 106.1), and four quaternary carbons (δ_C 143.9, 164.0, 166.0, and 169.2).

The connectivity of C-3, 3-Me, C-4 and 4-OH was successfully established by analysis of the ^{1}H NMR and COSY (**Fig. A20, Page 102**) spectra. Analysis of the HMBC (**Fig. A21, Page 103**) spectra revealed the correlations from H-3 and 4-OH to C-4a; H-4 to C-4a, C-5 and C-8a; H-5 to C-6 C-7, and C-8a; 6-OMe to C-6; H-7 to C-5, C-6, C-8 and C-8a; 8-OH to C-7, C-8, and C-8a; long length 3-Me, H-5, and H-7 to C-1. And he downfield shift of 8-OH was a characteristic of a chelated hydroxyl group. On the basis of these data, **compound 2** was identified as 4-hydroxy-6-methoxymellein.

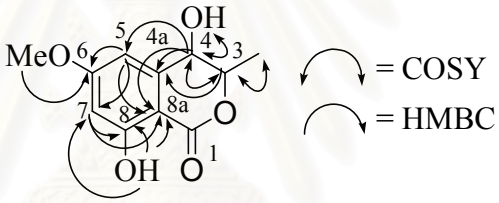

Figure 4.2: The gross structure of **compound 2**

The coupling constant value of 2.3 Hz for H-3 and H-4 suggested *cis* orientation H-3 and H-4. Previously, 4-hydroxymellein with a *cis* orientation possessed $J_{H\text{-}3,H\text{-}4}$ = 2 Hz (Venkatasubbalah and Chilton, 1990), while the *trans* isomer had $J_{H\text{-}3,H\text{-}4}$ = 8 Hz (Ayer, Lu, and Orszanska, 1993). Thus, the absolute configuration of **compound 2** should be either (3*R*, 4*R*) or (3*S*, 4*S*) (**Fig 4.3**).

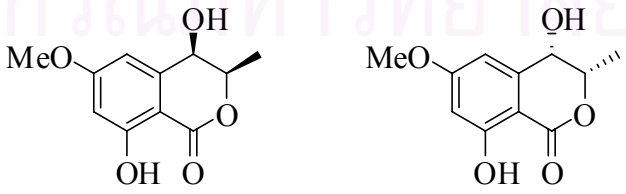

II.I **II.II**

(3*R*,4*R*)–Configuration (3*S*,4*S*)-Configuration

Figure 4.3: Possible configurations of **compound 2**

Compound 2 exhibited negative specific rotation $[\alpha]_D^{29}$ = –2.5 (*c* 0.96 in MeOH). Previously, (3*S*,4*S*)-(+)-4-hydroxymellein was reported to possess positive specific rotation (**II.III**, $[\alpha]_D^{20}$ = +37.4, *c* 0.33 in MeOH), (Camarda, Merlini and Nasini, 1976), while (3*R*,4*R*)-(-)-4-hydroxymellein exhibited negative specific rotation (**II.IV**, $[\alpha]_D^{25}$ = –36.0, *c* 0.87 in MeOH), (Cabras et al., 2006) (**Fig 4.4**). With this analogy of specific rotation, the absolute configuration at C-3 and C-4 in **compound 2** should be 3*R* and 4*R*.

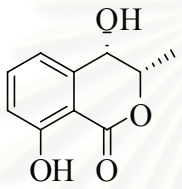

II.III

(3*S*,4*S*)-(+)-4-hydroxymellein

($[\alpha]_D^{20}$ = +37.4, *c* 0.33 in MeOH)

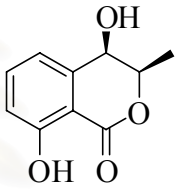

II.IV

(3*R*,4*R*)-(-)-4-hydroxymellein

($[\alpha]_D^{25}$ = –36.0, *c* 0.87 in MeOH)

Figure 4.4: Specific rotation of (3*S*,4*S*)-(+)-4-hydroxymellein and (3*R*,4*R*)-(-)-4-hydroxymellein

Compound 2 was therefore identified as (3*R*,4*R*)-(-)-4-hydroxy-6-methoxymellin or (3*R*,4*R*)-4,8-dihydroxy-6-methoxy-3-methylisochroman-1-one (**II.V**) (**Fig 4.5**).

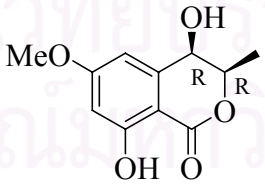

II.V

(3*R*,4*R*)-(-)-4-hydroxy-6-methoxymellein

$[\alpha]_D^{29}$ = –2.5 (*c* 0.955 in MeOH)

Figure 4.5: Stereochemistry of **compound 2**

Table 4.2: NMR spectral data for **compound 2**

Compound 2 (acetone-d_6)				
position	δ_C	δ_H (mult., *J* in Hz)	COSY (H to H)	HMBC (H to C)
1	169.2 (C)	-	-	-
2	-	-	-	-
3	77.9 (CH)	4.71 (dq, 2.3, 6.6)	4, 3-Me	3-Me, 4, 4a
4	66.4 (CH)	4.61 (dq, 2.2, 5.9)	3, 4-OH	4a, 5, 8a
4a	143.9 (C)	-	-	-
5	106.1 (CH)	6.56 (dd, 0.4, 2.4)	7	6, 7, 8a
6	166.0 (C)	-	-	-
7	100.4 (CH)	6.46 (d, 2.4)	5	5, 6, 8, 8a
8	164.0 (C)	-	-	-
8a	100.4 (C)	-	-	-
3-Me	15.2 (CH_3)	1.47 (3H, d, 6.6)	3	3, 4
6-OMe	55.2 (CH_3)	3.88 (3H, s)	-	6
4-OH	-	4.81 (d, 6.1)	4	3, 4, 4a
8-OH	-	11.33 (s)	-	7, 8, 8a

Possible biosynthetic pathway of **compound 1** (6-methoxymellein) and **compound 2** is shown below. Pentaketide chain **II.VI** from the condensation of acetyl-CoA and malonyl-CoA is cyclized to form isocoumarin **II.VII**. Reduction and *O*-methylation of **II.VII** leads to the formation of **compound 1** (6-methoxymellein), while the cyclization of **II.VII** gives to **II.VIII** and when epoxidation, cyclization, and *O*-methylation of **II.VIII** via intermediate **II.IX** give rise to the formation of **compound 2**. Biosynthesis of isocoumarin was previously reported by Kurosaki and Nishi (1988) and Abell, Sutkowski, and Staumton (1987) (**Fig 4.6**).

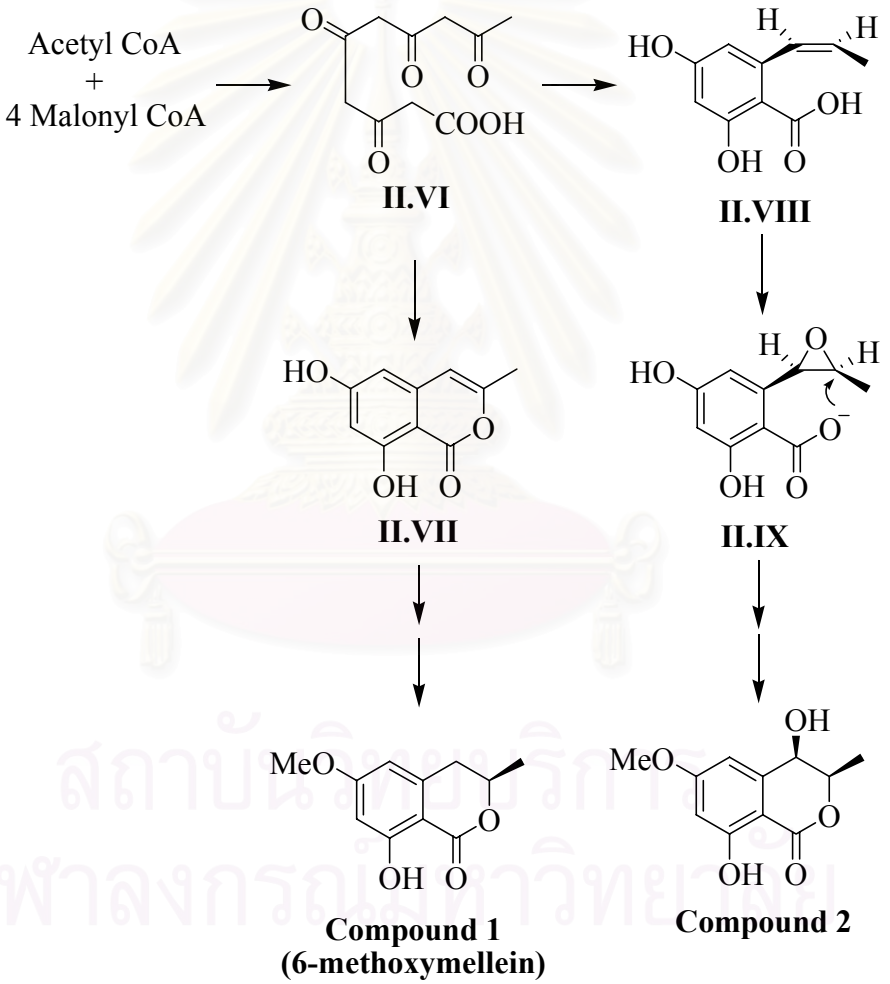

Figure 4.6: Possible biosynthetic pathway of **compound 1** (6-methoxymellein) and **compound 2**

Structure elucidation of compound 3

(*Vermilhotin; 3-(6-((E)-prop-1-enyl)-2H-pyran-2-ylidene)pyrrolidine-2,4-dione*)

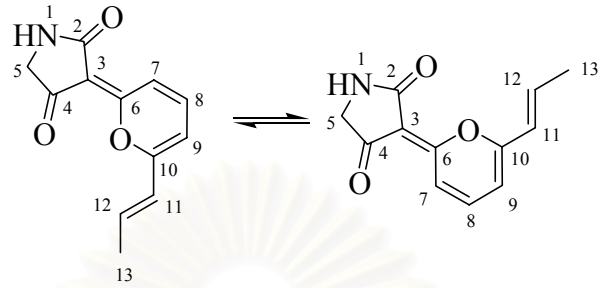

(*E*)-form **(*Z*)-form**

Compound III.I **Compound III.II**

Compound 3 (Vermihotin) was obtained as red needles. It possessed a molecular formula of $C_{12}H_{11}NO_3$ from APCI MS measurements, indicating an unsaturation degree of eight. The UV spectrum (**Fig. A26, Page 106**) of **compound 3** showed a major UV maximal absorption at 438.5 and absence of benzenoid UV bands (250-290 nm) indicated an extensively conjugation but not through an aromatic system. The IR spectrum of **compound 3** (**Fig. A27, Page 106**) showed the characteristic bands of a γ-lactam (1698 cm^{-1}), a conjugated cyclic ketone (1650 cm^{-1}), and secondary amide (3173, 1650, 1610 cm^{-1}).

The ^{13}C NMR spectrum (DMSO-d_6) of **compound 3** (**Fig. A30, Page 108**) showed twenty-three carbons. However the molecular formula was $C_{12}H_{11}NO_3$ (twelve carbons) suggested that it was a mixture of two compounds. Signals of ^{1}H and ^{13}C spectra indicated that there were two compounds with the ratio about 1:2 (**compound III.I**/**compound III.II**), as shown in **Table 4.3**.

Table 4.3: ^{1}H and ^{13}C NMR data of **compound III.I** and **compound III.II** (ratio 1:2) in DMSO-d_6 (600 MHz)

Compound III.I		**Compound III.II**	
δ_C	δ_H (mult., *J* in Hz)	δ_C	δ_H (mult., *J* in Hz)
195.3	-	192.9	-
170.1	-	171.4	-
165.8	-	164.4	-
158.0	-	157.8	-
143.3	7.64 (dd, 7.1, 9.3)	142.6	7.62 (dd, 7.1, 9.3)
137.4	7.13 (dq, 7.1, 15.3)	136.6	7.16 (dq, 7.1, 15.3)
123.2	6.37 (dq, 1.7, 15.4)	123.2	6.37 (dq, 1.7, 15.4)
116.0	7.98 (d, 9.3)	115.5	8.01 (d, 9.2)
108.7	6.62 (d, 7.0)	108.6	6.62 (d, 7.0)
98.3	-	98.4	-
50.9	3.61 (d, 0.7)	50.4	3.57 (d, 0.6)
18.8	1.94 (dd, 1.6, 7.1)	18.8	1.95 (dd, 1.6, 7.1)
-	7.48 (N*H*, brs)	-	7.66 (N*H*, brs)

Structure elucidation of compound III.I

The segment III.III was established by the ^{1}H-^{1}H COSY (**Fig. A34, Page 110**) and HMBC spectra (**Fig. A35, Page 111**). The ^{1}H-^{1}H COSY showed a cross peak between an exchangeable NH and H-5 methylene. The HMBC spectrum revealed the correlations from NH proton to C-2, C-3, and C-4; and H-5 to C-2. And The COSY spectrum enabled the assembly of a major Segment III.IV consisting of (C-11)–(C-12)–(C-13) and (C-7)–(C-8)–(C-9). The segments were connected by the HMBC spectrum showing the correlations from H-9 to C-10 and C-11; and both H-7 and H-8 to C-6 (**Fig. A35-A37, Page 111-112**) (**Fig. 4.7**).

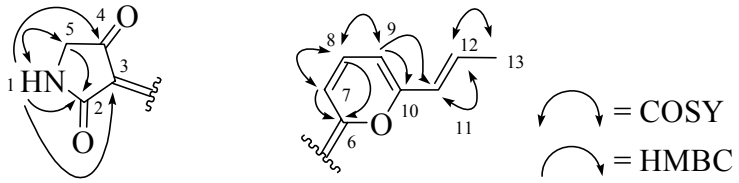

Segment III.III Segment III.IV

Figure 4.7: Two partial structures of Segments III.III and III.IV

The connection of segments III.III and III.IV can only be made via the (C-3)-(C-6) double bond leading to the gross structure of **compound III.I** (8 USD), as confirmed by the HMBC correlation of H-7 to C-3. The stereochemistry at C-11 and C-12 was *trans*-configuration because the coupling constant of H-11 and H-12 was about 15 Hz, however the stereochemistry at C-3 and C-6 could be either (*E*)- or (*Z*)-form. The difference between the two isomers was the chemical shift of H-7, δ_H 7.98 for **compound III.I** and δ_H 8.01 for **compound III.II**. In view of the deshielding effect caused by the C-4 ketone, the H-7 of the **compound III.II** should have more deshielding effect than that of the **compound III.I**; the **compound III.II** was therefore assigned as the (*Z*)-form, while the **compound III.I** was (*E*)-form (**Fig 4.8**).

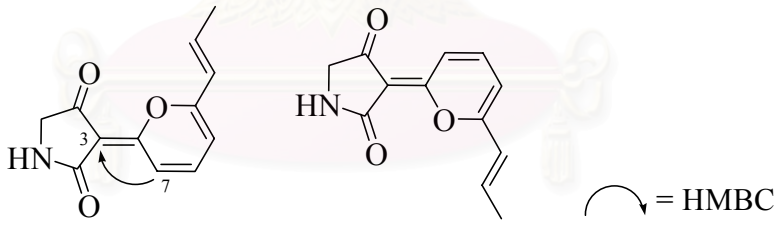

(*E*)-form (*Z*)-form

Compound III.I **Compound III.II**

Figure 4.8: The structure of **compound III.I** (*E*) and **compound III.II** (*Z*)

Compounds III.I and **III.II** were known compounds and named vermelhotin which were isolated from an unidentified fungus IFM 52672 (Hosoe et al., 2006). The structure of the *E* isomer was confirmed by X-Ray crystallography. The NMR spectrum in $CDCl_3$ showed that (*E*)-form was a stable form. However NMR spectral evidence for apiodionen obtained from the acid-treated fermentation broth of *Apiosordaria effuse* SANK 15803 revealed an equilibrium mixture of *α*- and *β*-forms

(Takahashi et al., 1992). Bripiodionen isolated from *Streptomyces* sp. WC76599 existed as a 1:1 mixture of (*E*:*Z*) in DMSO-d_6 (Shu et al., 1997) (**Fig 4.9**).

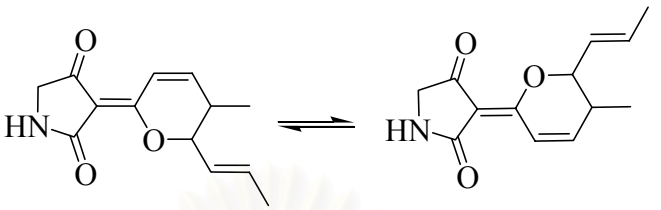

α-apiodionen *β*-apiodionen

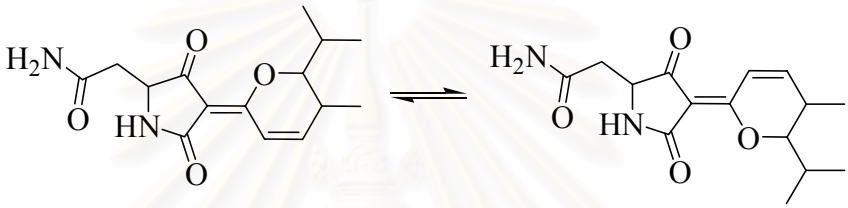

(*E*)- bripiodionen (*Z*)- bripiodionen

Figure 4.9: Structure equilibrium of apiodionen and bripiodionen

Compound 3 was in the equilibrium ratio 1:2 of (*E*)-form:(*Z*)-form in polar organic solvent (DMSO-d_6), and it was more likely that the (*Z*)-form was stable than the (*E*)-form in polar organic solvent (**Fig**. **4.10**).

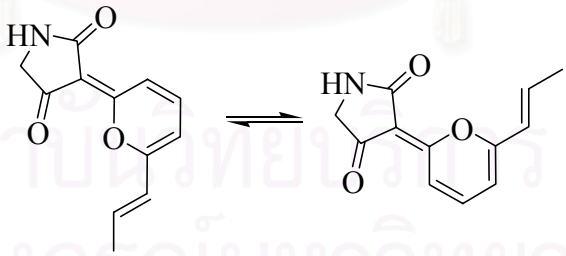

(*E*)-form **(*Z*)-form**

Figure 4.10: Structure equilibrium of **compound 3**

The isomeric behavior of **compound 3** may involve two sets of rapidly interchanging internal isomers [(*E*)-form ⇌ III.V] and [III.VI ⇌ (*Z*)-form], where each set arises through an electron transfer along the intramolecular electron shift. The slowly interconverting external isomers [(*E*)-form ⇌ III.V] ⇌

[III.VI ⇌ (*Z*)-form] may arise from the rotation of the pyrane ring. Moreover, isomerization could be envisioned to involve radical process (**Fig 4.11**).

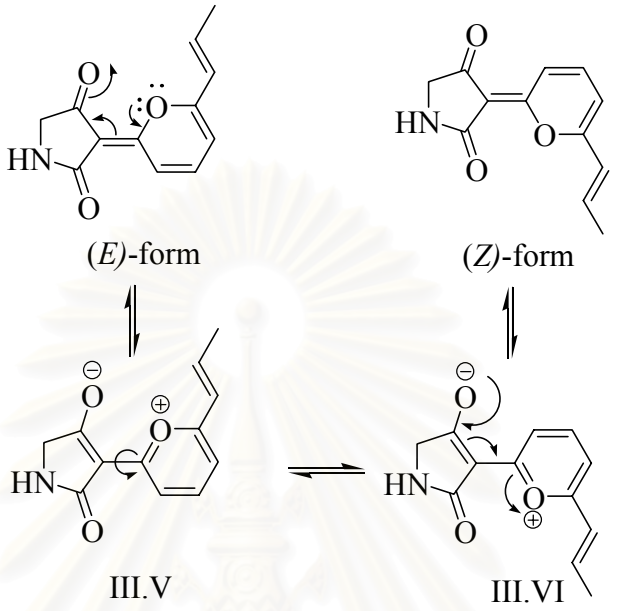

A: Electron transfer along the intramolecular electron shift

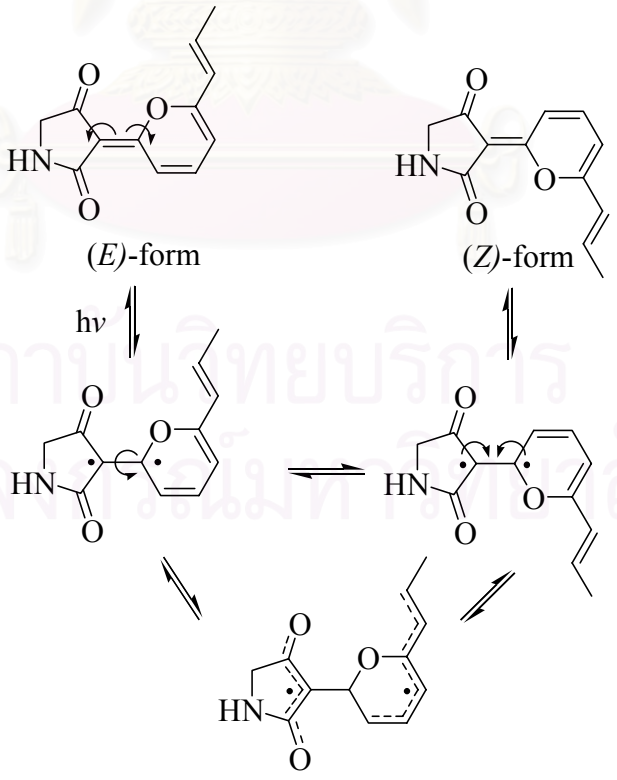

B: Radical process

Figure 4.11: Isomerization between (*E*)-form and (*Z*)-form

The biosynthesis of **compound 3** may be related to that of vermelhotin, which was previously propoded by Hosoe et al., 2006. The condensation of glycine and *β*–oxodecanoic acid is form intermediates. Dehydrogenation, hydroxylation, and cyclization lead to the formation of **compound 3** (**Fig 4.12**).

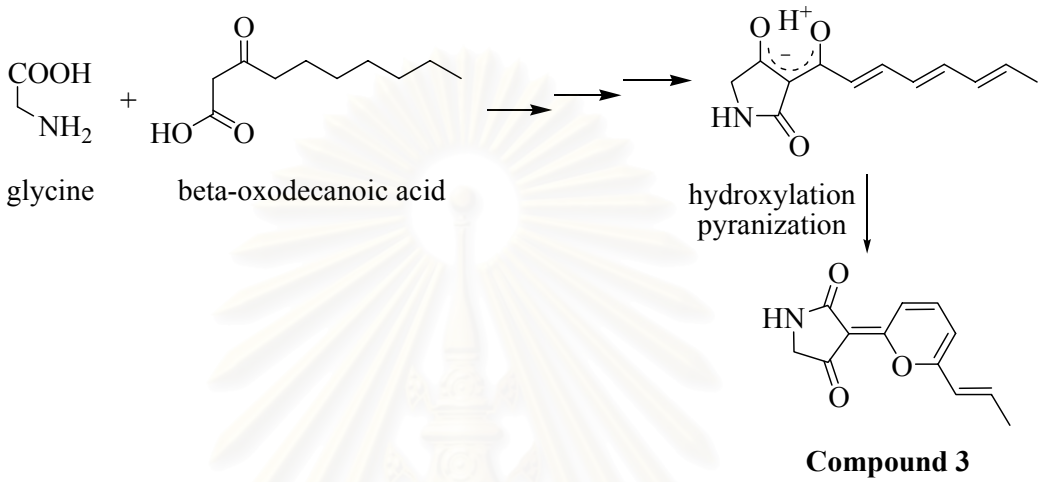

Figure 4.12: Proposed biosynthetic pathway for **compound 3**

Table 4.4: NMR spectral data for **compound 3** and vermelhotin

C no.	**(*E*)- compound 3** (DMSO-d_6)		**(*Z*)- compound 3** (DMSO-d_6)		Vermelhotin ($CDCl_3$)[a]	
	δ_C	δ_H (mult., *J* in Hz)	δ_C	δ_H (mult., *J* in Hz)	δ_C	δ_H (mult., *J* in Hz)
N*H*-1	-	7.48 (N*H*, brs)	-	7.66 (N*H*, brs)	-	5.76 (N*H*, brs)
2	170.1 (C)	-	171.4 (C)	-	172.4 (C)	-
3	98.3 (C)	-	98.4 (C)	-	98.1 (C)	-
4	195.3 C)	-	192.9 (C)	-	192.7 (C)	-
5	50.9 (CH_2)	3.61 (d, 0.7)	50.4 (CH_2)	3.57 (d, 0.6)	50.4 (CH_2)	3.79 (brs)
6	165.8 (C)	-	164.4 (C)	-	165.5 (C)	-
7	116.0 (CH)	7.98 (d, 9.3)	115.5 (CH)	8.01 (d, 9.2)	116.0 (CH)	8.18 (brd, 9.2)
8	143.3 (CH)	7.64 (dd, 7.1, 9.3)	142.6 (CH)	7.62 (dd, 7.1, 9.3)	141.5 (CH)	7.42 (dd, 7.0, 9.2)
9	108.7 (CH)	6.62 (d, 7.0)	108.6 (CH)	6.62 (d, 7.0)	107.6 (CH)	6.29 (brd, 7.0)
10	158.0 (C)	-	157.8 (C)	-	158.7 (C)	-
11	123.2 (CH)	6.37 (dq, 1.7, 15.4)	123.2 (CH)	6.37 (dq, 1.7, 15.4)	122.1 (CH)	6.16 (brd, 15.3)
12	137.4 (CH)	7.13 (dq, 7.1, 15.3)	136.6 (CH)	7.16 (dq, 7.1, 15.3)	138.6 (CH)	7.40 (dq, 7.0, 15.3)
13	18.8 (CH_3)	1.94 (3H, dd, 1.6, 7.1)	18.8 (CH_3)	1.95 (3H, dd, 1.6, 7.1)	19.0 (CH_3)	2.02 (3H, dd, 1.5, 7.0)

[a] Assignment was by Hosoe et al., (2006)

4.2 Chemical constituents of the marine-derived fungus *Hypoxylon monticulosum* CRIF1

Biological activity screening revealed that a crude EtOAc extract of the broth and mycelia of the fungus *Hypoxylon monticulosum* CRIF1 exhibited antimalarial activity with 68.46 % inhibition at 10 μg/mL and 64.29 % inhibition at 100 μg/mL for broth and mycelia extract, respectively. Both broth and cell extracts were subsequently purified by chromatographic techniques including Sephadex LH-20, silica gel column, and MPLC. **Compound 4** was isolated from both crude extracts. A structure of this compound was elucidated by analyses of spectroscopic data, especially 2D-NMR and MS spectra. **Compound 4** was derivatized to give methylester, benzylester, and hydrogenate (**compounds 5, 6** and **7**).

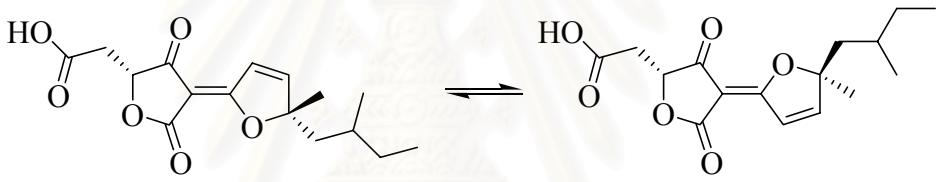

(*Z*)-form **(*E*)-form**

Compound 4

Structure elucidation of compound 4

(*2-((R)-4-((S)-5-methyl-5-(2-methylbutyl)furan-2(5H)-ylidene)-3,5-dioxo-tetrahydrofuran-2-yl)acetic acid*)

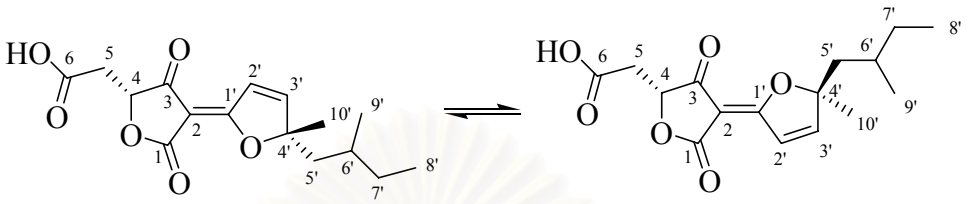

(*Z*)-form **(*E*)-form**

Compound 4 was obtained as colorless solid. UV spectrum of **compound 4** (**Fig. A42, Page 115**) displayed the maximum absorption at 317.0 nm. The infrared (IR) spectrum of **compound 4** (**Fig. A43, Page 115**) showed absorption bands at 1755 (5-membered lactone), 1696 (carboxylic acid and broad band 3433). **Compound 4** exhibited the molecular formula $C_{16}H_{20}O_6$ (seven unsaturations) as deduced from APCI MS data (**Fig. A56, Page 123**) ($[M + H]^+$ at *m/z* 309.1331, calcd. for $[C_{16}H_{20}O_6+H]^+$ 309.1338).

The ^{13}C NMR spectrum (**Fig. A46, Page 117**) showed two sets of signal with a ratio of approximately 1:1, suggesting the presence of an epimeric/isomeric mixture similar to **compound 4**. The ^{13}C NMR spectrum (**Fig. A46, Page 117**) showed signals of an α,*β*-unsaturated ketone carbonyl (δ_C 196.8), a 1,2-disubstituted olefin unit (δ_C 121.7 and 163.3), and three carbons in the carboxy carbonyl region (δ_C 167.5, 171.2 and 179.4). Signals were also observed for two non-protonated carbons in the upfield sp^2 and/or the downfield oxygenated sp^3 carbon regions (δ_C 93.4 and 101.8). In addition, the ^{13}C NMR spectrum revealed signals of three methyl groups (δ_C 11.3, 20.9 and 23.6), an oxygenated methine (δ_C 79.0), an aliphatic methine (δ_C 30.1), and three methylenes (δ_C 30.2, 43.7 and 36.0).

The ^1H-^1H COSY spectrum (**Fig. A50, Page 119**) showed couplings between H-2′ and H-3′; and between H-4 and H-5. The ^1H-^1H COSY spectrum also established the partial structure from H-5′ along the chain through H-9′.

The HMBC spectrum (**Fig. A51, Page 120**) of **compound 4** showed correlations from H-4 to C-1, C-3, C-5, and C-6; and H-5 to C-3, C-4, and C-6, enabling the assembly of a partial structure IV-I (**Fig 4.13**). The carbonyl carbon at δ_C 171.2 (C-6) and broad band at 2000-3500 cm^{-1} of IR spectrum was showing characteristic of carboxylic acid.

A second partial structure (IV-II, **Fig 4.13**) was assembled by analysis of the HMBC spectrum (**Fig. A51-A54, Page 120-121**). Both olefinic protons (H-2′ and H-3′) showed HMBC correlations to the non-protonated carbon C-4′. The downfield shift of C-4′ (δ_C 101.8) indicated its attachment to at least one oxygen atom. HMBC correlations of 3H-10′ (δ_C 23.6) to C-3′, C-4′, and C-5′ indicated the connection of C-3′, C-5′ and C-10′ to C-4′ and revealed that C-4′ must be a singly oxygenated sp^3 carbon, depite its downfield shift. The 5.8 Hz coupling constant between H-2′ and H-3′ suggested that the corresponding olefin is located in a ring, most likely to be a five-membered ring. Further ^1H-^1H COSY and HMBC correlations permitted extension of this structural unit to include an aliphatic side chain (H-5′ through H-9′).

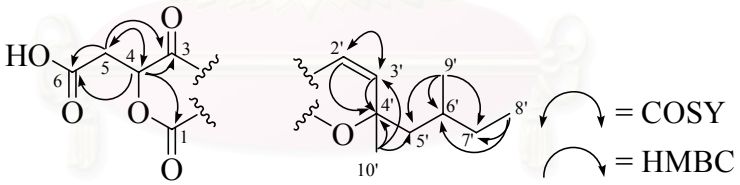

IV-I IV-II

Figure 4.13: Partial structures IV-I and IV-II

Two carbon signals (δ_C 93.4 and 179.4) remained unassigned at this stage. Both protons of the H-2′ and H-3′ olefin unit showed correlations to the signal at δ_C 179.4, suggesting its direct attachment to C-2′. Unfortunately, no other HMBC correlations were observed for this signal, and none were observed for the signal at δ_C 93.4, so these carbons could not be unambiguously located.

An upfield shift of C-3 ketone carbonyl (δ_C 196.8) suggested the presence of α,*β*- unsaturated ketone, thus there should be a double bond at C-2, which led to possible structures IV-III and IV-IV after cyclization (**Fig 4.14**).

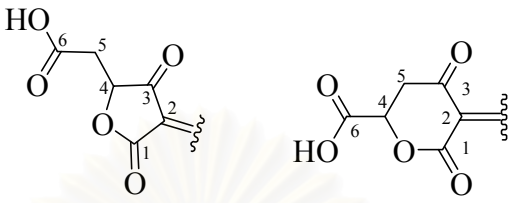

IV-III IV-IV

Figure 4.14: Cyclization of IV-I to possible structures IV-III and IV-IV

A carbon (C-1′) at δ_C 179.4 should be connected to C-2, and should be a sp^2 double bond. Considering the downfield shift of C-1′ (δ_C 179.4), it showed be an oxygenated double bond. At this stage, all carbons in **compound 4** were already placed in partial structures. The next stage was to combine partial structure IV-II with either IV-III or IV-IV through C-2 and C-1′; in order to form possible structures IV-V or IV-VI (**Fig 4.15**).

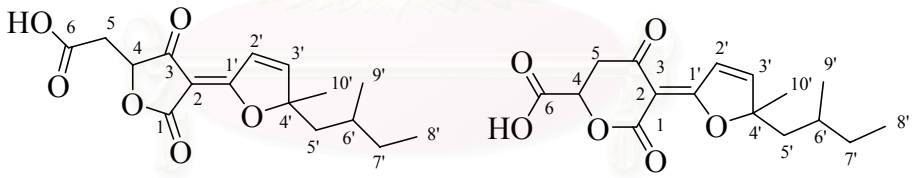

IV-V IV-VI

Figure 4.15: The possible structures of **compound 4**

The δ_H and δ_C of possible compounds IV-V and IV-VI was compared with those in the literature. The compound IV-V was related with six compounds which were tetronic acid derivatives. But compound IV-VI was not found to be related with any compound. Comparison of compound IV-V with other tetronic acid derivatives to those of carlic acid, carolic acid, dehydrocarolic acid, terrestric acid, italicic acid, and lowdenic acid (Fig 4.17); which was metabolic product of *Penicillium charlesii*, *P. charlesii*, *P. fellutanum*, *P. cinerascens*, *P. terrestre*, *P. italicum*, *Verticillium* sp. (MYC-106=NRRL 29280) (Angawi et al., 2003; Arai et al., 1989; Jacobsen et al, 1978; Simonsen, Reffstrup, and Boll, 1980). In the present work, the split signals in the ^{1}H and ^{13}C NMR spectra of compound 4 (IV-V) indicated the equilibrium mixture of *E*- and *Z*-isomers owing to the furfurylidene double bond. Thus the structure of compound 4 (IV-V) was a 1:1 mixture of the *E*- and *Z*-isomers, as shown in **Fig. 4.16**.

When compare NMR data of **compound 4** with those of tetronic acid derivatives (Jacobsen et al., 1978), the δ_C of C-1 (lactone carbonyl) in the *E*-isomer was about 3 ppm lower field than that of the *Z*-isomer. In addition, δ_H H-2′ (*Z*)-form was more downfield than that of the (*E*)-form because of the strong deshielding effect caused by the C-4 ketone.

Compound 4 exhibited negative specific rotation $[\alpha]_D^{27}$ = –28.8 (*c* 1.05 in $CHCl_3$). Previously, lowdenic acid was reported to possess negative specific rotation ($[\alpha]_D^{27}$ = –39, *c* 0.02 in $CHCl_3$), (Angawi et al., 2003). These negative specific rotations were suggested may be relatively biosynthesis. With this analogy of specific rotation, the relative configuration at C-3 and C-4 in **compound 4** may be 4*R* and 4′*R*. However, the stereochemistry at C-6′ could not be established on the basis of available spectral data (**Fig 4.17**).

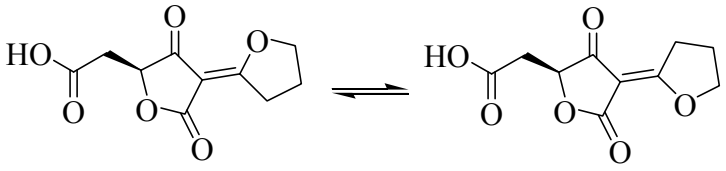

Carlic acid

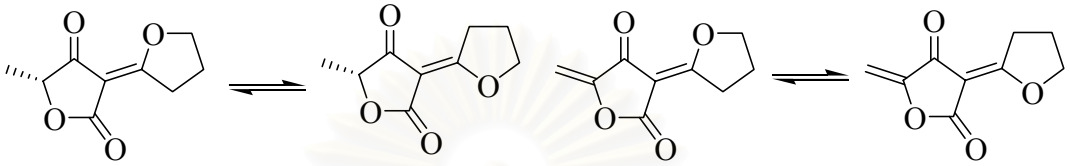

Carolic acid Dehydrocarolic acid

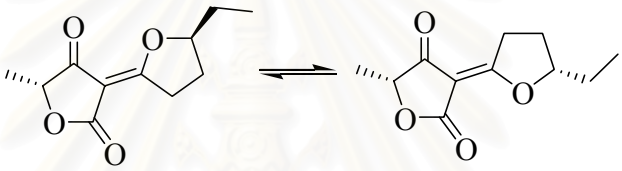

Terrestric acid

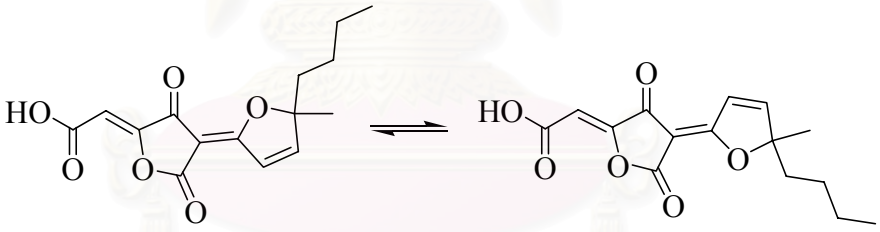

Italicic acid

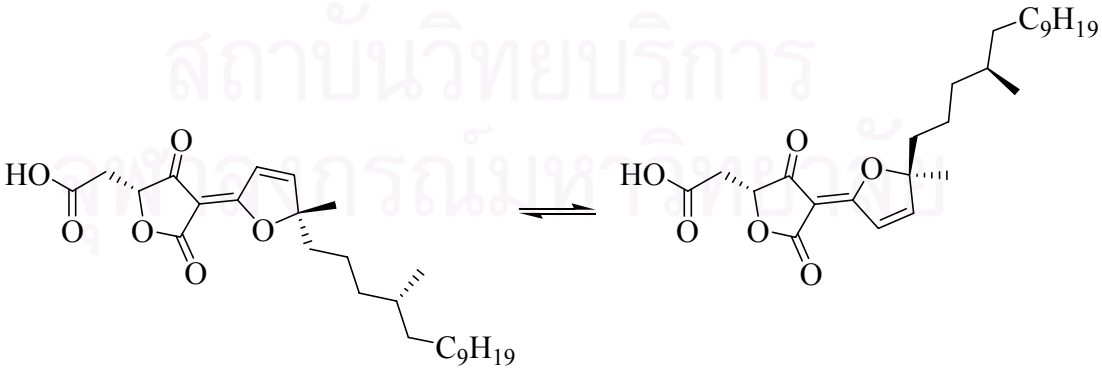

Lowdenic acid

Figure 4.16: Structures of the tetronic acids derivative

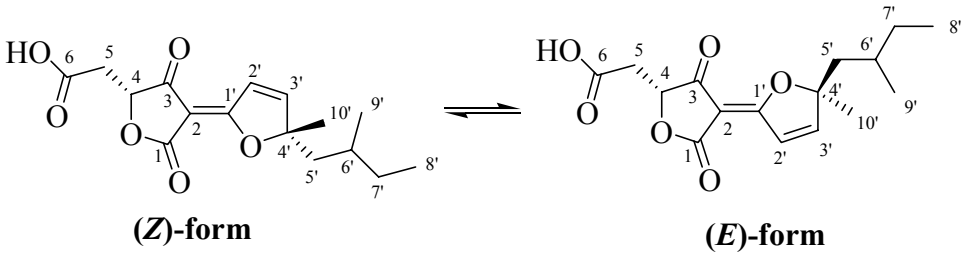

(*Z*)-form **(*E*)-form**

Figure 4.17: The structure of **compound 4**

The equilibration of **compound 4** may involve the interconversion of the external isomers [(*Z*)-form, IV-VII ⇌ IV-VIII, (*E*)-form]; however, the interconversion of the internal pairs [(*Z*)-form ⇌ IV-VII, IV-VIII ⇌ (*E*)-form] by electron resonance at C-1′, C-2, and C-3 (similar to a 1,3-diketone system) may be possible (**Fig 4.18**). Add equilibration of (*E*)- and (*Z*)-isomer occurs of carolic acid presence in traces of acid, or under the influence of light (radical) process by Jacobsen et al. (1978).

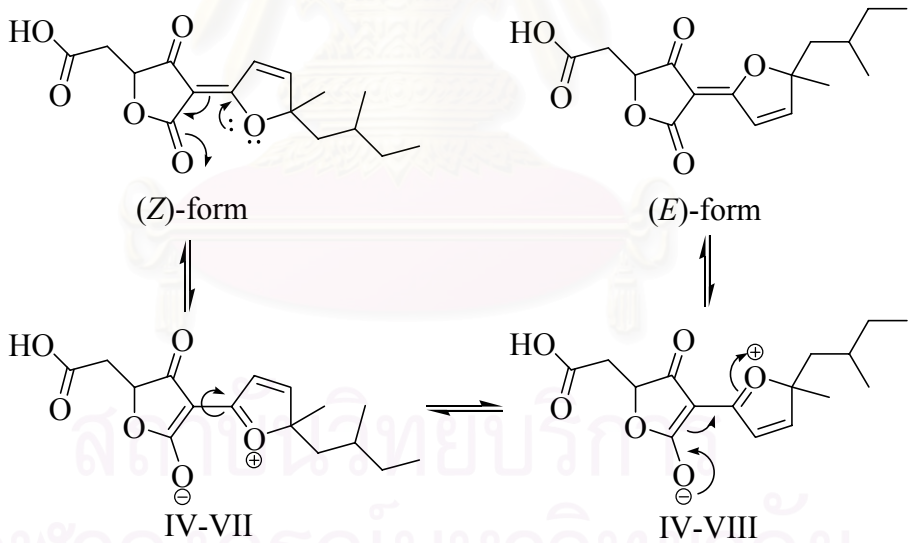

(*Z*)-form (*E*)-form

IV-VII IV-VIII

A: Electron transfer along the intramolecular electron shift

Figure 4.18: Possible isomerization of (*Z*)-form and (*E*)-form of **compound 4**

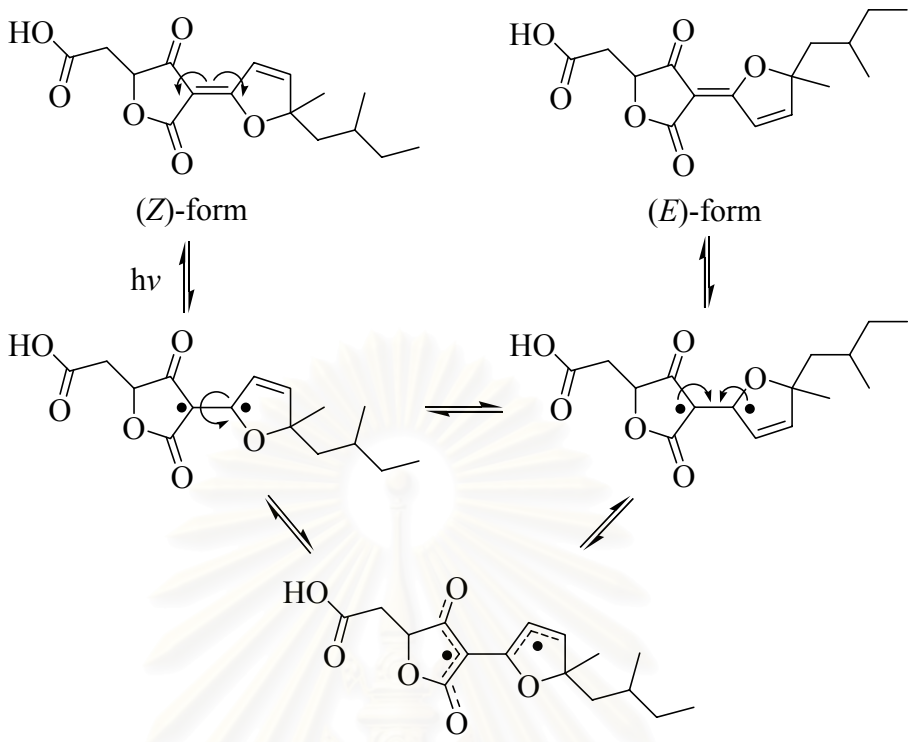

Figure 4.18: Possible isomerization of (*Z*)-form and (*E*)-form of **compound 4** (continue)

The esterification of **compound 4** with methanol and benzyl alcohol confirmed that at C-6 in **compound 4** was carboxylic group. The hydrogenation of **compound 4** yielded **compound 7** resulting the upfield shift from δ_H 7.98 (H-2′) to non-equivalent methylene δ_H 3.55, 3.44; and from δ_H 7.27 (H-3′) to methylene δ_H 2.09 in (*E*)-form.

The biosynthesis of **compound 4** may be related to that of italicic acid, which was previously proposed by Arai et al. (1989). The condensation of a modified 10-carbon polyketide unit (which forms the side chain, the furylidene ring, and C-1 and C-2 of the tetrahydrofurandione ring) with a four-carbon dicarboxylic acid unit lead to **compound 4** as shown below.

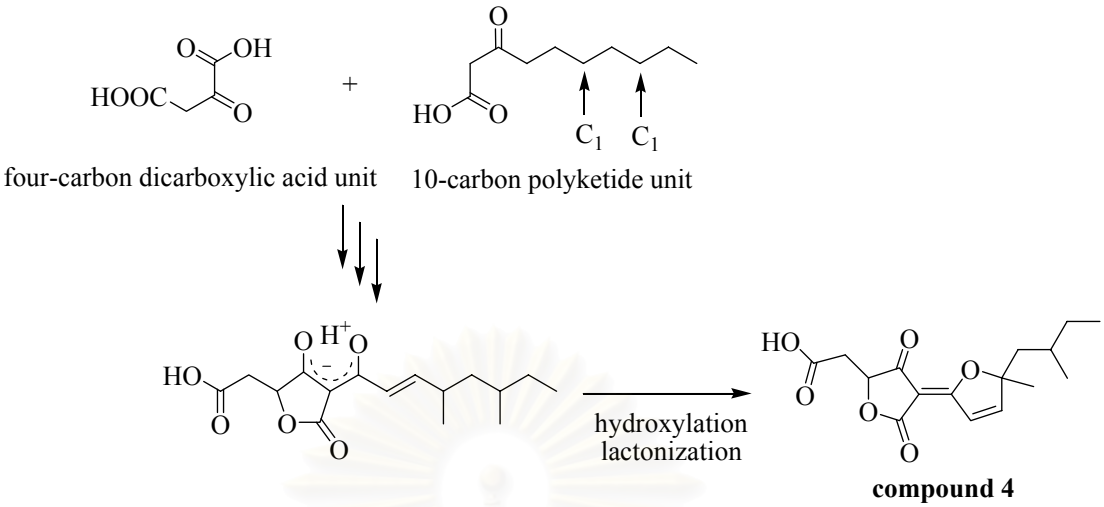

Figure 4.19: Possible biosynthetic pathway for **compound 4**

Table 4.5: NMR spectral data for **compound 4**

No.	δ_H (mult., *J* in Hz)		δ_C	
	E	*Z*	*E*	*Z*
1	-	-	170.3	167.5
2	-	-	93.8[a]	93.4[a]
3	-	-	194.3	196.8
4	4.78 (dd, 4.0, 6.3)	4.85 (dd, 4.1, 6.3)	78.8	79.0
5a	2.78 (d, 4.0)	2.82 (d, 4.0)	36.1	36.0
5b	2.68 (t, 6.1)	2.71 (t, 6.0)		
6	-	-	171.2	171.2
1′	-	-	178.4	179.4
2′	7.27 (d, 5.8)	7.37 (d, 5.8)	121.7	121.7
3′	7.98 (d, 5.8)	7.98 (d, 5.8)	163.4[b]	163.3[b]
4′	-	-	102.4	101.8
5′a	1.98 (dd, 3.7, 9.1)	2.01 (dd, 3.9, 9.1)	43.7	43.7
5′b	1.60 (t, 7.4)	1.64 (t, 7.4)		
6′	1.22 (m)	1.22 (m)	30.1	30.1
7′a	1.22 (m)	1.22 (m)	30.2	30.2
7′b	1.09 (m)	1.09 (m)		
8′	0.76 (q, 7.2)	0.76 (q, 7.2)	11.3	11.3
9′	0.83 (d, 6.4)	0.83 (d, 6.4)	21.0	20.9
10′	1.50 (s)	1.51 (s)	23.7	23.6

[a] Assignment was by comparison with lowdenic aid.

[b] The assignments are interchangeable.

Table 4.6: NMR spectral data for (*E*)-**compound 4** with COSY and HMBC

(*E*)-**Compound 4** (DMSO-d_6)				
position	δ_C	δ_H (mult., *J* in Hz)	COSY (H to H)	HMBC (H to C)
1	170.3 (C)	-	-	-
2	93.8 (C)[a]	-	-	-
3	194.3 (C)	-	-	-
4	78.8 (CH)	4.78 (dd, 4.0, 6.3)	5a,5b	1, 3, 5, 6
5a	36.1 (CH_2)	2.78 (d, 4.0)	4, 5b	3, 4, 6
5b		2.68 (t, 6.1)	4, 5a	
6	171.2 (C)	-	-	-
1′	178.4 (C)	-	-	-
2′	121.7 (CH)	7.27 (d, 5.8)	2′	1′, 3′, 4′, 10′
3′	163.4 (CH)[b]	7.98 (5.8)	3′	1′, 2′, 4′, 5′, 10′
4′	102.4 (C)	-	-	-
5′a	43.7 (CH_2)	1.98 (dd, 3.7, 9.1)	5′b, 6′	3′, 4′, 6′, 7′, 9′, 10′
5′b		1.60 (t, 7.4)	5′a, 6′	
6′	30.1 (CH)	1.22 (m)	5′, 7′, 9′	5′, 7′, 8′, 9′
7′a	30.2 (CH_2)	1.22 (m)	6′, 7′b, 8′	5′, 6′, 8′, 9′
7′b		1.09 (m)	6′, 7′a, 8′	
8′	11.3 (CH_3)	0.76 (q, 7.2)	7′	6′, 7′
9′	21.0 (CH_3)	0.83 (d, 6.4)	6′	5′, 6′, 7′
10′	23.7 (CH_3)	1.50 (s)	-	3′, 4′, 5′

[a] Assignment was by comparison with lowdenic aid.

[b] The assignments are interchangeable with (*Z*)-**compound 4**.

Table 4.7: NMR spectral data for (*Z*)-**compound 4** with COSY and HMBC

(*Z*)-**Compound 4** (DMSO-d_6)				
position	δ_C	δ_H (mult., *J* in Hz)	COSY (H to H)	HMBC (H to C)
1	167.5 (C)	-	-	-
2	93.4 (C)[a]	-	-	-
3	196.8 (C)	-	-	-
4	79.0 (CH)	4.78 (dd, 4.0, 6.3)	5a,5b	1, 3, 5, 6
5a	36.0 (CH_2)	2.78 (d, 4.0)	4, 5b	3, 4, 6
5b		2.68 (t, 6.1)	4, 5a	
6	171.2 (C)	-	-	-
1′	179.4 (C)	-	-	-
2′	121.7 (CH)	7.27 (d, 5.8)	2′	1′, 3′, 4′, 10′
3′	163.3 (CH)[b]	7.98 (5.8)	3′	1′, 2′, 4′, 5′, 10′
4′	101.8 (C)	-	-	-
5′a	43.7 (CH_2)	1.98 (dd, 3.7, 9.1)	5′b, 6′	3′, 4′, 6′, 7′, 9′, 10′
5′b		1.60 (t, 7.4)	5′a, 6′	
6′	30.1 (CH)	1.22 (m)	5′, 7′, 9′	5′, 7′, 8′, 9′
7′a	30.2 (CH_2)	1.22 (m)	6′, 7′b, 8′	5′, 6′, 8′, 9′
7′b		1.09 (m)	6′, 7′a, 8′	
8′	11.3 (CH_3)	0.76 (q, 7.2)	7′	6′, 7′
9′	20.9 (CH_3)	0.83 (d, 6.4)	6′	5′, 6′, 7′
10′	23.6 (CH_3)	1.50 (s)	-	3′, 4′, 5′

[a] Assignment was by comparison with lowdenic aid.

[b] The assignments are interchangeable with (*E*)-**compound 4**.

^{1}H and ^{13}C NMR spectra of ergosterol (**Fig. A64-A65, Page 125**) and adenosine (**Fig. A66-A67, Page 126**) were identical to those reported in the literature (Pouchert and Behnke, 1993: 222; 570.).

Biological activities of the isolated compounds

Antimalarial activity

The isolated compounds were tested for antimalarial activity against *Plasmadium falciparum* 94 with the assay method described by Trager and Jensen (1976) method. The IC_{50} values reported in **Table 4.7** are classified as follows: for excellence activity (10^{-9} – $<10^{-8}$M), very good (10^{-8} – $<10^{-7}$M), good (10^{-7} – $<10^{-6}$M), fair (10^{-6} – $<10^{-5}$M), and negative ($>10^{-5}$M). An IC_{50} value of 2.98×10^{-7} M was observed for the standard sample, chloroquine hydrochloride. The antimalarial results are shown in **Table 4.8**.

The isolated **compounds 1-4** and derivatives **compound 5, 6** and **7** exhibited weak antimalarial activity. Among the compounds tested, **compound 7** exhibited strongest activity with the % inhibition of 82.2 at 1×10^{-5} M.

Cytotoxic activity

The isolated compounds were tested for cytotoxic activity against HuCCA-1 (human cholangiocarcinoma), KB (human epidermoid carcinoma in mouth), HeLA (human cervical carcinoma), MDA-MB-231(hormone-independent breast cancer), T47D (hormone-dependent breast cancer), H69AR (lung cancer, small cell, multidrug resistance), HL-60 (human promyelocytic leukemia cell), P388 (mouse lymphoid neoplasm), HepG2 (human hepatoblastoma carcinoma), A549 (human lung adenocarcinoma, non-small cell ATCC No. CCL-185), and S102 (human hepatocellular carcinoma). Etoposide and doxorubicin were used as a positive control. The results are shown in **Table 4.9**. **Compounds 3**, **5** and **6** exhibited potent cytotoxicity against all cell lines tested.

Derivatives **5** and **6** more exhibited potent cytotoxicity against than **compound 4** may be they were non-polar molecule which transfer into cell easier.

Cancer chemoprevention

The isolated compounds were tested for cancer chemoprevention property with the following assay models: DPPH, HL-60 Antioxidation, XXO, IXO, ORAC, and LOX. The results are shown in **Table 4.11**.

For radical scavenging, all pure compounds show weak scavenging of diphenyl picrylhydrazyl radicals (DPPH).

With respect to antioxidant effects, **compounds 5** and **6** inhibited TPA-induced superoxide burst in differentiated HL-60 cells (HL-60 Antioxidation) the concentration of 13.2 and 4 μM, respectively. **Compound 3** could scavenge of $O_2^{\cdot-}$ generating by xanthine/xanthine oxidase (XXO) at IC_{50} = 122.1 μM. **Compounds 3**, **4**, and **5** could inhibit xanthine oxidase (IXO) at IC_{50} = 113.0, 478.6, and 456.2 μM, respectively. **Compounds 1**, **3**, and **4** scavenged oxygen radicals absorbance capacity (ORAC) at 0.3, 1.0, and 0.1 unit.

There are four possible pathways of **compounds 6** for the reduction of $O_2^{\cdot-}$ production in HL-60 Antioxidation (Kim et al., 2002):

1. Radical scavenging by directly reacting with reactive oxygen species (ROS).
2. Inhibition of ROS-generating enzyme induction, for instance, the expression of enzyme proteins and assembly of enzyme components
3. Inhibition of enzyme reactions, including pseudo-substrates and modifiers of the active enzyme sites
4. Induction of antioxidant enzymes

Compound 6 showed potent antioxidant with the HL-60 Antioxidation model, but did not exhibit activity in the XXO and IXO system. **Compound 6** may be inhibited the signal transduction cascade, resulting from the generation of superoxide anion radicals after stimulation of granulocytes by TPA (Gerhäuser et al., 2003).

In anti-inflammatory mechanism, all pure compounds showed only weak inhibition of lipoxygenase activity (LOX).

Table 4.8: Antimalarial activity of **compounds 1-7**

Concentration (M)	% Inhibitory of the compounds						
	1	**2**	**3**	**4**	**5**	**6**	**7**
1×10^{-9}	0	ND	0	13.9	1.6	2.5	0
1×10^{-8}	0.8	ND	7.4	21.2	3.3	5.0	6.9
1×10^{-7}	12.6	ND	39.8	24.7	3.3	5.0	43.3
1×10^{-6}	29.0	ND	43.7	28.6	6.6	7.5	46.8
1×10^{-5}	61.5	ND	58.0	52.0	27.9	55.0	82.3
IC_{50}	$10^{-6} - 10^{-5}$	ND	$10^{-6} - 10^{-5}$	$10^{-6} - 10^{-5}$	$>10^{-5}$	$10^{-6} - 10^{-5}$	$10^{-6} - 10^{-5}$
Result	Fair	ND	Fair	Fair	Negative	Fair	Fair

ND = not determined

Chloroquine hydrochloride (standard), $IC_{50} = 2.98\times10^{-7}$ M

Table 4.9: Cytotoxic activity of **compound 1-7**

Cell lines	IC_{50} of the compounds							
	Etoposide (positive control)	**1**	**2**	**3**	**4**	**5**	**6**	**7**
HuCCA-1	5.3±1.53	>50	>50	2.9±0.17	>50	2.3±0.10	2.1±0.21	>50
KB	0.46±0.15	21.0±2.12	>50	0.5±0.00	>50	2.2±0.30	3.2±0.44	>50
HeLA	0.40±0.12	23.0±2.83	>50	0.33±0.08	>50	2.7±0.17	2.6±0.12	>50
MDA-MB231	0.40±0.10	>50	>50	0.31±0.08	>50	2.5±0.46	0.38±0.04	>50
T47D	0.04±0.01	50.0±0.00	>50	1.25±0.35	>50	1.7±0.25	0.14±0.02	>50
H69AR	36.0±1.41	>50	ND	2.5±0.42	>50	ND	ND	>50
HepG2	0.19±0.02[a]	>50	>50	2.5±0.70	>50	2.3±0.35	2.0±0.42	>50
A549	0.48±0.03[a]	>50	>50	8.2±2.54	>50	7.5±0.71	2.2±0.28	>50
S102	1.2±0.14[a]	>50	>50	13.5±0.70	>50	6.0±1.41	4.8±0.14	>50
HL-60	0.77±0.35	>50	>50	1.60±0.03	>50	1.01±0.2	1.18±0.14	>50
P388	0.10±0.01	48.28±1.41	>50	1.23±0.02	>50	0.77±0.0	0.70±0.06	>50

ND = not determined, [a] Doxorubicin (positive control)

Table 4.10: Cytotoxic activity of **compound 4 and derivatives 5, 6 and 7**

Cell lines	**Compounds**				
	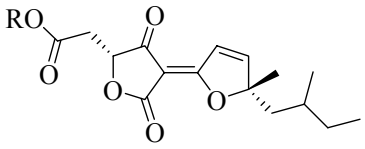			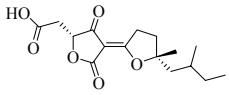	
	4; R = H	**5**; R = CH_3	**6**; R = 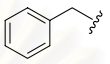	**7**;	Etoposide (positive control)
HuCCA-1	>50	2.3±0.10	2.1±0.21	>50	5.3±1.53
KB	>50	2.2±0.30	3.2±0.44	>50	0.46±0.15
HeLA	>50	2.7±0.17	2.6±0.12	>50	0.40±0.12
MDA-MB231	>50	2.5±0.46	0.38±0.04	>50	0.40±0.10
T47D	>50	1.7±0.25	0.14±0.02	>50	0.04±0.01
H69AR	>50	ND	ND	>50	36.0±1.41
HepG2	>50	2.3±0.35	2.0±0.42	>50	0.19±0.02[a]
A549	>50	7.5±0.71	2.2±0.28	>50	0.48±0.03[a]
S102	>50	6.0±1.41	4.8±0.14	>50	1.2±0.14[a]
HL-60	>50	1.01±0.2	1.18±0.14	>50	0.77±0.35
P388	>50	0.77±0.0	0.70±0.06	>50	0.10±0.01

ND = not determined

[a] Doxorubicin (positive control)

Table 4.11: Cancer chemoprevention activity of **compound 1-7**

Assay	Summary of radical-scavenging, antioxidant effect, and anti- inflammatory mechanism of compounds						
	1	**2**	**3**	**4**	**5**	**6**	**7**
DPPH (μM)	>250 (6%)	ND	>250 (11%)	>250 (13%)	>250 (3%)	>250 (9%)	>250 (21%)
HL-60 Antiox. (μM)	>100 (1%)	ND	>100 (26%)	>100 (1%)	13.2	4.0	>100 (0%)
XXO (μM)	>500 (0%)	ND	122.1	>500 (11%)	ND	>500 (0%)	>500 (0%)
IXO (μM)	>500 (0%)	ND	113.0	478.6	456.2	>500 (6%)	>500 (0%)
ORAC (unit)[a]	0.3	ND	1.0	0.1	0	0	0
LOX (μM)	>100 (2%)	ND	>100 (2%)	>100 (2%)	>100 (0%)	>100 (5%)	>100 (0%)

ND = not determined

(%) = % activities at that concentrate

CHAPTER V

CONCLUSION

The objective of this thesis was the investigation of secondary metabolites produced by marine-derived fungi isolated from the sponge and soft coral collected from Surin Island, Pang-nga Province, Thailand. Biological activities of the isolated compounds were also evaluated.

Two fungal stains were isolated from a sponge and soft coral, respectively. Crude extracts of these fungi showed cytotoxic and antimalarial activities. Isolation of fungal extracts give 4 pure compounds representing different structural sub-classes within the polyketides i.e. isocoumarin (**compounds 1** and **2**), tetronic acid derivatives (**compound 4**), and amino acid pathway i.e. tetramic acid derivatives (**compound 3**). **Compounds 2** and **4** were new natural products.

6-Methoxymellin (**compound 1**), (-)-4-hydroxy-6-methoxymellin (**compound 2**) and vermilhotin (**compound 3**) were isolated from an unidentified sponge-derived fungus strain CRI 247-01. **Compounds 1** and **2** showed weak cytotoxic and antimalarial activities, while **compound 3** showed potent cytotoxic activity. In addition, a new **compound 4** was isolated from *Hypoxylon monticulosum* CRIF1 which was isolated from the soft coral. The compound showed weak cytotoxic activity, however its synthetic derivatives **5** and **6** showed potent cytotoxic activity. Moreover, **compound 6** also inhibited antioxidant activity (HL-60 Antioxidation).

This study demonstrates that marine-derived fungi are an excellent source for the discovery of novel bioactive compuonds. Besides, the prominent biological activity as well as the diversity of structures obtained during this project is a motivation for further investigation of marine-derived fungi.

REFERENCES

Abell, C., Sutkowski, A. C., and Staunton, J. (1987). Studies on the biosynthesis of hydroxymellein using ^{17}O N.M.R. and ^{2}H N.M.R. spectroscopy to determine the origin of the C-4 hydroxy group. J. Chem, Soc., Chem. Commun. (8): 586-587.

Abraham, E. P., and Loder, P. B. (1972). Cephalosporin C. in E. H. Flynn (ed), Cephalosporins and penicillins: Chemistry and biology. New York: Academic Press. Cited in Bugni, T. S., and Ireland C. M. (2004). Marine-derived fungi: a chemically and biologically diverse group of microorganisms. Nat. Prod. Rep. 21(1): 143-163.

Amagata, T., Minoura, K., and Numata, A. (2006). Gymnastatins F-H, cytostatic metabolites from the sponge-derived fungus *Gymnascella dankaliensis*. J. Nat. Prod. 69(10): 1384-1388.

Angawi, R. F., Swenson, D. C., Gloer, J. B., and Wicklow, D. T. (2003). Lowdenic acid: a new antifungal polyketide-derived metabolite from a new fungicolous *Verticillium* sp. J. Nat. Prod. 66(9): 1259-1262.

Arai, K., Miyajima, H., Mushiroda, T., and Yamamoto, Y. (1989). Metabolites of *Penicillium italicum* WEHMER: isolation and structures of new metabolites including naturally occurring 4-ylidene-acyltetronic acids, italicinic acid and italicic acid. Chem. Pharm. Bull. 37(12): 3229-3235.

Ayer, W., A., Lu, P.-P., and Orszanska, H. (1993). Deoxyscytalidin and lignicol: new metabolites from *Scytalidium* species. J. Nat. Prod. 56(10): 1835-1838.

Belofsky, G. N., Jensen, P. R., and Fenical, W. (1999). Sansalvamide: a new cytotoxic cyclic depsipeptide produced by a marine fungus of the genus *Fusarium*. Tetrahedron Lett. 40(15): 2913-2916.

Bugni, T. S., and Ireland C. M. (2004). Marine-derived fungi: a chemically and biologically diverse group of microorganisms. Nat. Prod. Rep. 21(1): 143-163.

Cabras, A., Mannoni, M. A., Serra, S. Andolfi, A., and Fiore, M. (2006). Occurrence, isolation and biological activity of phytotoxic metabolites produced in vitro by *Sphaeropsis sapinea*, pathogenic fungus of *Pinus radiate*. Eur. J. Plant Pathol. 115: 187-193.

Camarda, L., Merlini, L., and Nasini, G. (1976). Metabolites of *Cercospora taiwapyrone*, an α-pyrone of unusual structure from *Cercospora taiwanensis*. Phytochemistry. 15(4): 537-539.

Cao, G., and Prior, R.L. (1999). Measurement of oxygen-radical absorbing capacity in biological samples. Meth Enzymol. 299: 50-62.

Chen, G., Lin, Y., Vrijmoed, L. L. P., and Fong, W. (2006). A new isochroman from the marine endophytic fungus 1893#. Chem. Nat. Compd. 42(2): 138-141.

Cueto, M., MacMillan, J. B., Jensen, P. R., and Fenical, W. (2006). Tropolactones A–D, four meroterpenoids from a marine-derived fungus of the genus *Aspergillus*. Phytochemistry. 67(16): 1826–1831.

Czepa, A., and Hofmann, T. (2003). Structural and sensory characterization of compounds contributing to the bitter off-taste of carrots (*Daucus carota* L.) and carrot puree. J. Agric. Food Chem. 51(13):3865-3873.

Du, L., Zhu, T., Fang, Y., Liu, H., Gu, Q., and Zhu, W. (2007). Aspergiolide A, a novel anthraquinone derivative with naphtho[1,2,3-de]chromene-2,7-dione skeleton isolated from a marine-derived fungus *Aspergillus glaucus*. Tetrahedron. 63(5): 1085–1088.

Feng, Z., and Yongcheng, L. (2006). Marinamide, a novel alkaloid and its methyl ester produced by the application of mixed fermentation technique to two mangrove endophytic fungi from the South China Sea. Chinese Science Bulletin. 51(12): 1426-1430.

Florey, H. W., et al. (1949). Antibiotics. vol 1. Oxford: Oxford University Press. Cited in Bugni, T. S., and Ireland C. M. (2004). Marine-derived fungi: a chemically and biologically diverse group of microorganisms. Nat. Prod. Rep. 21(1): 143-163.

Garo, E., Starks, C. M., Jensen, P. R. Fenical, W., Lobkovsky, E., and Clardy, J. (2003). Trichodermamides A and B, cytotoxic modified dipeptides from the marine-derived fungus *Trichoderma virens*. J. Nat. Prod. 66(3): 423-426.

Gerhäuser, C., et al. (2003). Mechanism-based in vitro screening of potential cancer chemopreventive agents. Mutat. Res. 253-254: 163-172.

Gleason, M.M., Rojas, C.J., Learn K.S., Perrone, M.H., and Bilder G.E. (1995). Characterization and inhibition of 15-lipoxygenase in human monocytes:

comparison with soybean 15-lipoxygenase. Am. J. Physiol. 268(5): 1301-1307

Hart, C., (1999). Forged in St. Anthony's fire: drugs for migraine. Mod. Drug Discovery. 2(2): 20-21, 23-24, 28, 31.

Hosoe, T., Fukushima, K., Takizawa, K., Itabashi, T., Yoza, K., and Kawai, K. (2006). A new pyrrolidine-2,4-dione derivative, vermelhotin, isolated from unidentified fungus IFM 52672. Heterocycles. 68(9): 1949-1953.

Jacobsen, J. P., Reffestrup, T., Cox, R. E., Holker, J. S. E., and Boll, P. M. (1978). Revision of the structures of the naturally occurring acyl tetronic acids: dehydrocarolic aicd, terrestric acid and carlic acid. Tetrahedron Lett. 19(12); 1081-1084.

Kasai, Y., Komatsu, K., Shigemori, H., Tsuda, M., Mikami, Y., and Kobayashi, J. (2005). Cladionol A, a polyketide glycoside from marine-derived fungus *Gliocladium* species. J. Nat. Prod. 68(5): 777-779.

Kato, H., et al. (2007). Notoamides A–D: prenylated indole alkaloids isolated from a marine-derived fungus, *Aspergillus* sp. Angew. Chem. Int. Ed. 46(13): 2254 –2256.

Kim, H. W., Murakami, A., Nakamura, Y., and Ohigashi, H. (2002). Screening of edible Japanese plants for suppressive effects on phorbol ester-induced superoxide generation in differentiated HL-60 cells and AS52 cells. Cancer Lett. 176(1): 7-16.

Kohlmeyer, J. (1974). Veröff. Inst. Meeresforsch. Bremerh. 5: 339-356. Cited in Claudia Osterhage. (2001). Isolation, structure determination and biological activity assessment of secondary metabolites from marine-derived fungi. Doctoral dissertation. Institut für Pharmazeutische Biologie, 03 - Chemistry and Pharmacy, Braunschweig University.

Kohlmeyer, J., and Volkmann-Kohlmeyer, B. (1991). Illustrated key to the filamentous higher marine fungi. Bot. Mar. 34: 1-61.

Kralj, A., Kehraus, S., Krick, A., Echten-Deckert, G. v., and König, G. M. (2007). Two new depdipeptides from the marine fungus *Spicellum roseum*. Planta Med. 73(4): 366-371.

Krick, A., et al. (2007). Potential cancer chemopreventive in vitro activities of monomeric xanthone derivatives from the marine algicolous fungus *Monodictys putredinis*. J. Nat. Prod. 70(3): 353-360.

Kriengsak Lirdprapamongkol, et al. (2003). Anti-metastatic effects of aqueous extract of *Helixanthera parasitica*. J. Ethnopharmacol. 86(2-3): 253-256.

Kupka, J., Anke, T., Steglich, W., and Zechlin, L. (1981). Antibiotics from basidiomycetes. XI: The biological activity of siccayne, isolated from the marine fungus *Halocyphina villosa* J. & E. Kohlmeyer. J. Antibiot. 34(3): 298-304.

Kurosaki, F., and Nishi, A. (1988). A methyltransferase for synthesis of the phytoalexin 6-methoxymellein in carrot cells. FEBS Lett. 227(2): 183-186.

Lambros, C., and Vanderberg, J. P. (1979). Synchronization of Plasmodium falciparum erythrocytic stages in culture. J. Parasitol. 65(3), 418-20.

Li, H., Lin, Y., Wang, L., Zhou, S., and Vrijmoed, L. L. P. (2001). Metabolites of the marine fungus *Hypoxylon oceanicum* from the South China Sea. Zhongshan Daxue Xuebao, Ziran Kexueban. 40(4): 70-72.

Li, X., Kim, S., Nam, K. W., Kang, J. S., Choi, H. D., and Son, B. W. (2006). A new antibacterial dioxopiperazine alkaloid related to gliotoxin from a marine isolate of the fungus *Pseudallescheria.* J. Antibiot. 59(4): 248–250.

Li, X., Zheng, Y., Sattler, I., and Lin, W. (2006). Griseusin C, a novel quinone derivative from a marine-derived fungus *Penicillium* sp. Arch. Pharm. Res. 29(11): 942-945.

Li, X., Zhang, D., Lee, U., et al. (2007). Bromomyrothenone B and botrytinone, cyclopentenone derivatives from a marine isolate of the fungus *Botrytis.* J. Nat. Prod. 70(2): 307-309.

Liu, R., et al. (2006). 10-Phenyl-[12]-cytochalasins Z7, Z8, and Z9 from the marine-derived fungus *Spicaria elegans*. J. Nat. Prod. 69(6): 871-875.

Malmstrøma, J., Christophersena, C., and Frisvadb, J. C. (2000). Secondary metabolites characteristic of *Penicillium citrinum*, *Penicillium steckii* and related species. Phytochemistry. 54(3): 301-309.

McDonald, L. A., et al. (1999). Spiroxins, DNA cleaving antitumor antibiotics from a marine-derived fungus. Tetrahedron Lett. 40(13), 2489-2492.

Mosmann, T. (1983). Rapid colorimetric assay for cellular growth and survival: Application to proliferation and cytotoxicity assays. J. Immunol. Methods. 65(1-2): 55-63.

Munn C. B. (2004). Marine microbiology : ecology and applications. UK and New York: Garland Science/BIOS Scientific Publishers.

Nagao, A., Seki, M., and Kobayashi, H. (1999). Inhibition of xanthine oxidase by flavonoids. Biosci. Biotechnol. Biochem. 63 (10): 1787-1790.

Oh, D.-C., Kauffman, C. A., Jensen, P. R., and Fenical, W. (2007). Induced production of emericellamides A and B from the marine-derived fungus *Emericella* sp. in competing co-culture. J. Nat. Prod. 70(4): 515-520.

Osterhage., C. (2001). Isolation, structure determination and biological activity assessment of secondary metabolites from marine-derived fungi. Doctoral dissertation. Institut für Pharmazeutische Biologie, 03 - Chemistry and Pharmacy, Braunschweig University.

Pick, E., and Mizel, D. (1981). Rapid microassays for the measurement of superoxide and hydrogen peroxide production by macrophages in culture using an automatic enzyme immunoassay reader. J. Immunol. Methods. 46(2): 211-226.

Pouchert, C. J., and Behnke, J. (1993). The aldrich library of ^{13}C and ^{1}H FT NMR spectra. vol. III. I nd ed. USA: Aldrich Chemical Company.

Sasaki, M., Tsuda, M., Sekiguchi, M., Mikami, Y., and Kobayashi, J. (2005). Perinadine A, a novel tetracyclic alkaloid from marine-derived fungus *Penicillium citrinum*. Org. Lett. 7(19): 4261-4264.

Schlingmann, G., Milne, L., Williams, D. R., and Carter, G. T. (1998). Cell wall active antifungal compounds produced by the marine fungus *Hypoxylon oceanicum* LL-15G256. II. Isolation and structure determination. J. Antibiot. 51(3): 303-316.

Schlingmann, G., Milne, L., and Carter, G. T. (2002). Isolation and identification of antifungal polyesters from the marine fungus *Hypoxylon oceanicum* LL-15G256. Tetrahedron. 58(34): 6825–6835.

Scudiero, D. A., et al. (1988). Evaluation of a soluble tetrazolium/formazan assay for cell growth and drug sensitivity in culture using human and other tumor cell line. Cancer Res. 48: 4827-4833.

Shibano, M., Naito, H., Taniguchi, M., Wang, N. and Baba, K. (2006). Two isocoumarins from *Pleutospermun angelicoides*. Chem. Pharm. Bull. 54(5): 717-718.

Shu, Y., et al. (1997). Bripiodionen, a new inhibitor of human cytomegalovirus protease from *Streptomyces* sp. WC 76599. J. Nat. Prod. 60(5): 529-532.

Simonsen, O., Reffstrup, T., and Boll, P. M. (1980). The molecular structure of carolic acid. Tetrahedron. 36(6): 795-797.

Sondheimer, E. (1957). The isolation and identification of 3-methyl-6-methoxy-8-hydroxy-3,4-dihydroisocoumarin from carrots. J. Am. Chem. Soc. 79(18): 5036-5039.

Stoessa, A., and Stothers, J. B. (1978). A carbon-13 biosynthetic study of stress metabolites from carrot roots: eugenin and 6-methoxymellein. Can. J. Bot. 56: 2589-2593.

Takahashi, S., et al. (1992). Apiodionen, inhibitor of topoisomerase and suppressor of chemiluminescence: taxonomy, fermentation, isolation, structural elucidation and biological activity. Sankyo Kenkyusho Nenpo. 44: 119-27.

Takeuchi, T., Nakajima, M., and Morimoto, K. (1994). Establishment of a human system that generates O_2^- and induces 8-hydroxydeoxyquanosine, typical of oxidative DNA damage, by a tumor promotor. Cancer Res. 54(22): 5837-5840.

Trager, W., and Jensen, J. B. (1976). Human malaria parasites in continuous culture. Science. 193(4254): 673-675.

Tsuda, M., et al. (2005). Scalusamides A-C, new pyrrolidine alkaloids from the marine-derived fungus *Penicillium citrinum*. J. Nat. Prod. 68(2): 273-276.

Tsukamoto, S., Miura, S., Yamashita Y., and Ohta, T. (2004). Aspermytin A: a new neurotrophic polyketide isolated from a marine-derived fungus of the genus *Aspergillus*. Bioorg. Med. Chem. Lett. 14(2): 417–420.

Ukeda, H., Maeda, S., Ishii, T., and Sawamura, M. (1997). Spectrophotometric assay for superoxide dismutase based on tetrazolium salt 3′-{1-[(phenylamino) - carbonyl] - 3,4 - tetrazolium}- bis(4-methoxy-6-nitro)benzenesulfonic acid hydrate reduction by xanthine/xanthine oxidase. Anal. Biochem. 251(2): 206-209

van Amsterdam, F. T., Roveri, A., Maiorino, M., Ratti, E., and Ursini, F. (1992). Lacidipine: a dihydropyridine calcium antagonist with antioxidant activity. Free Radic. Biol. Med. 12(3): 183-187.

Venkatwubbaiah., P. and Chilton., W. S. (1990). Phytotoxins of *Botryosphaeria obtusa*. J. Nat. Prod. 53(6): 1628-1630.

Wu, X. Y., et al. (2005). Xyloketal F: a strong L-calcium channel blocker from the mangrove fungus *Xylaria* sp. (#2508) from the South China Sea Coast. Eur. J. Org. Chem. 2005(19): 4061–4064.

Xin, Z. H., et al. (2007). Aurantiomides A-C, quinazoline alkaloids from the sponge-derived fungus *Penicillium aurantiogriseum* SP0-19. J. Nat. Prod. 70(5): 853-855.

APPENDIX

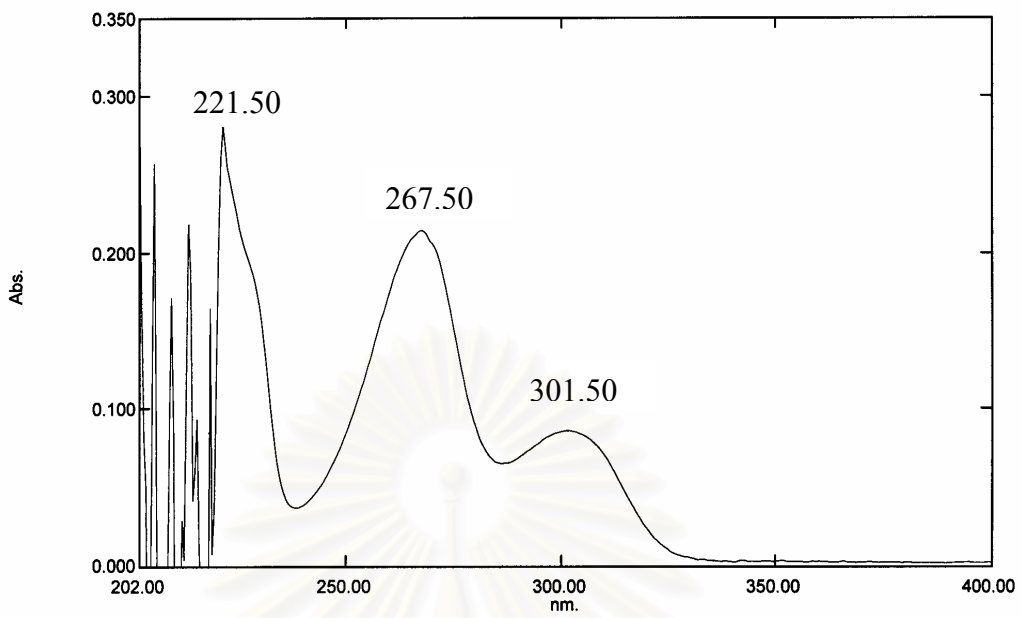

Figure A1: UV spectrum of **compound 1** (6-methoxymellein)

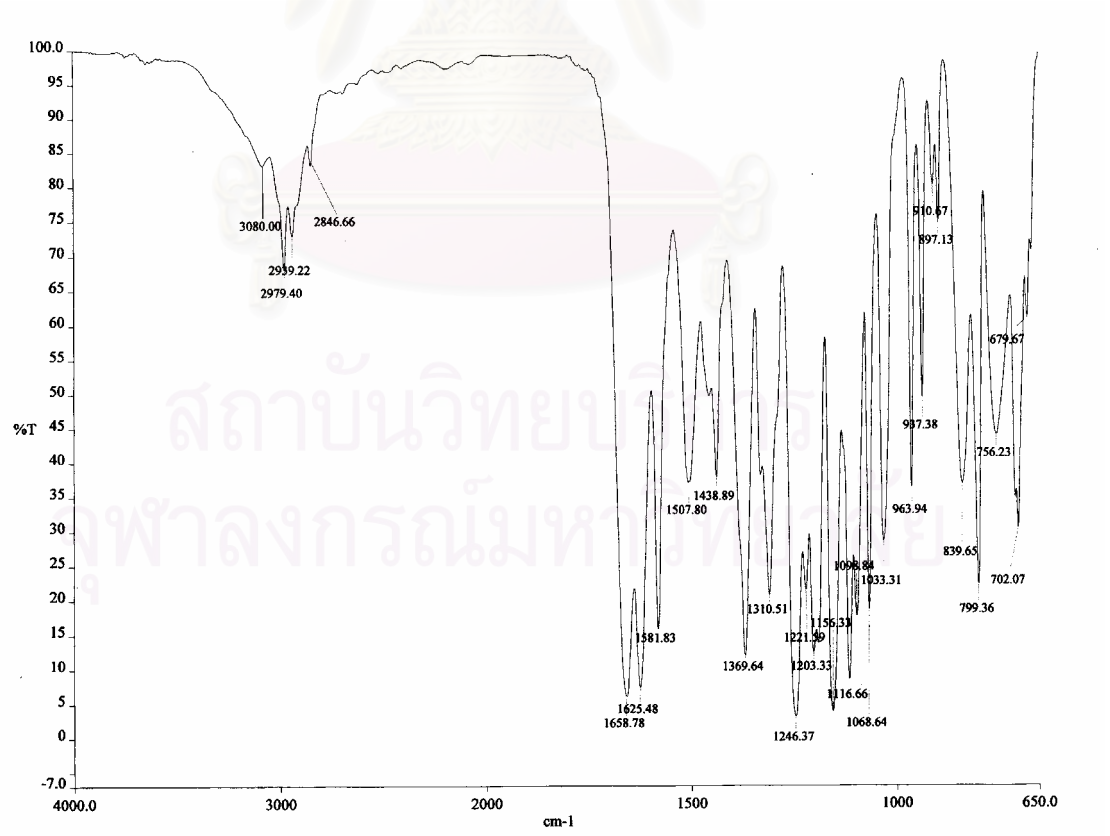

Figure A2: IR spectrum of **compound 1** (6-methoxymellein)

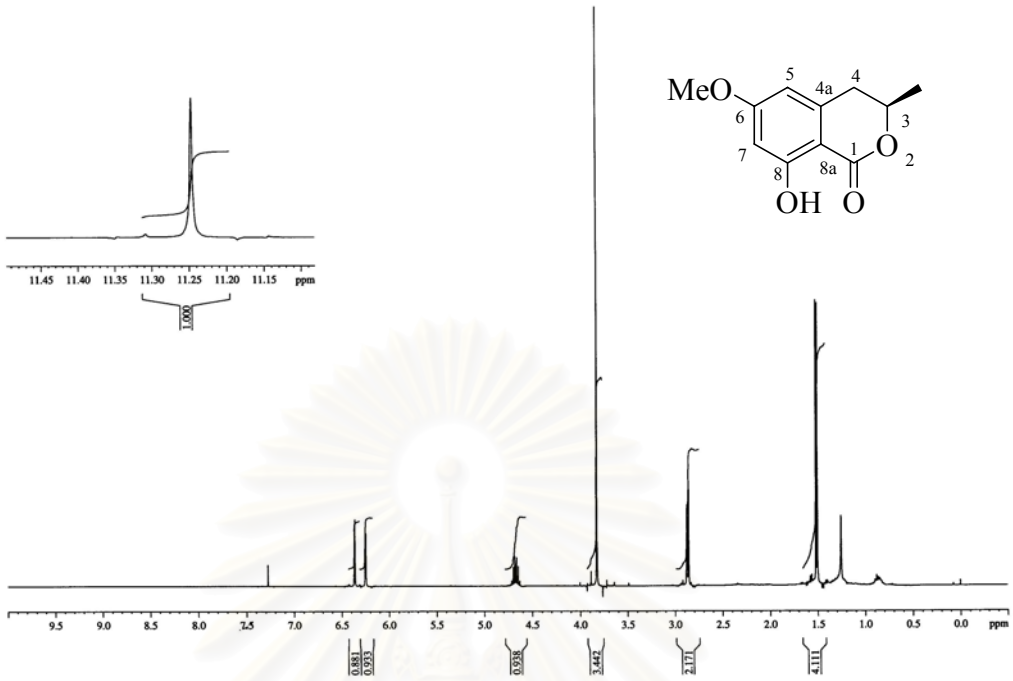

Figure A3: ^{1}H NMR ($CDCl_3$) spectrum of **compound 1** (6-methoxymellein)

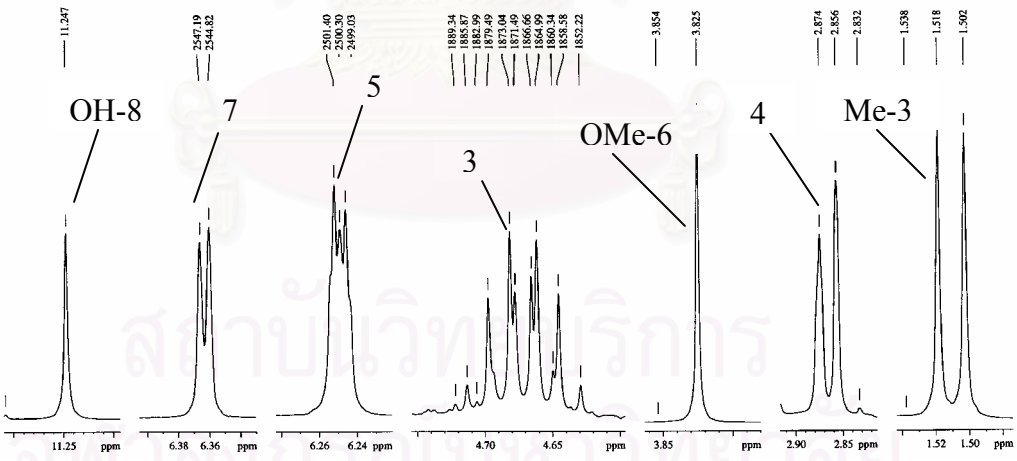

Figure A4: Expansion of **Fig. A3**

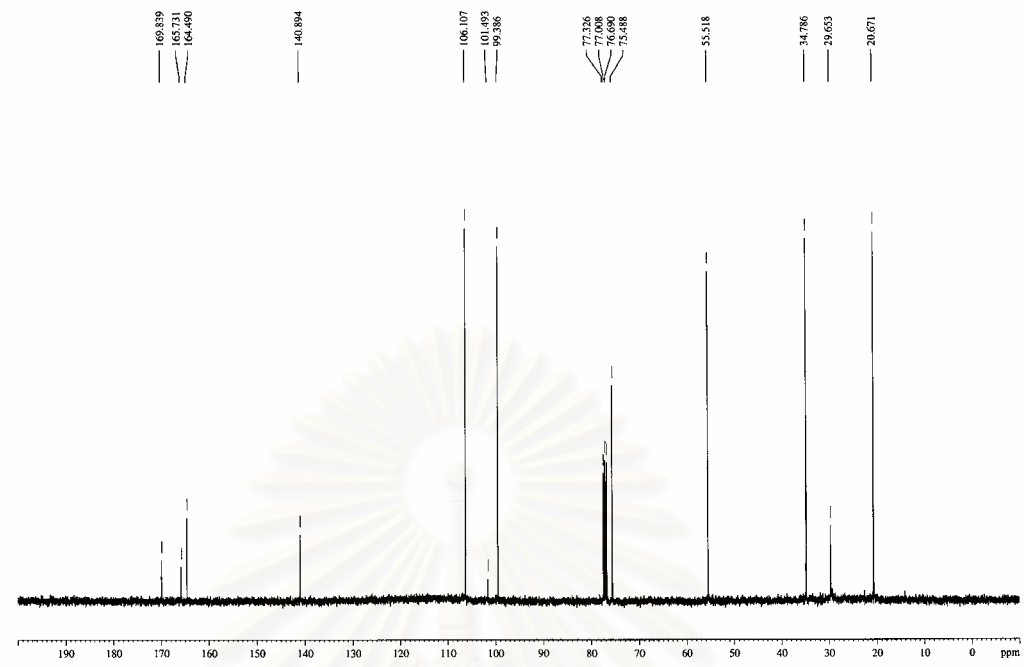

Figure A5: ^{13}C NMR ($CDCl_3$) spectrum of **compound 1** (6-methoxymellein)

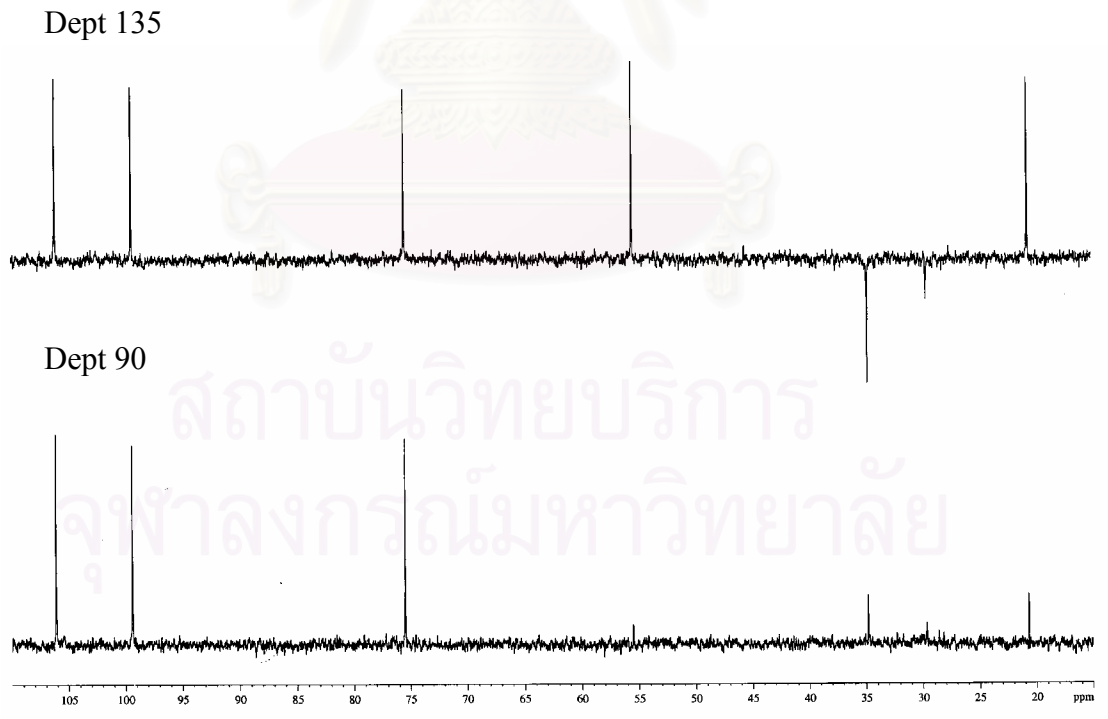

Figure A6: Depts spectra of **compound 1** (6-methoxymellein)

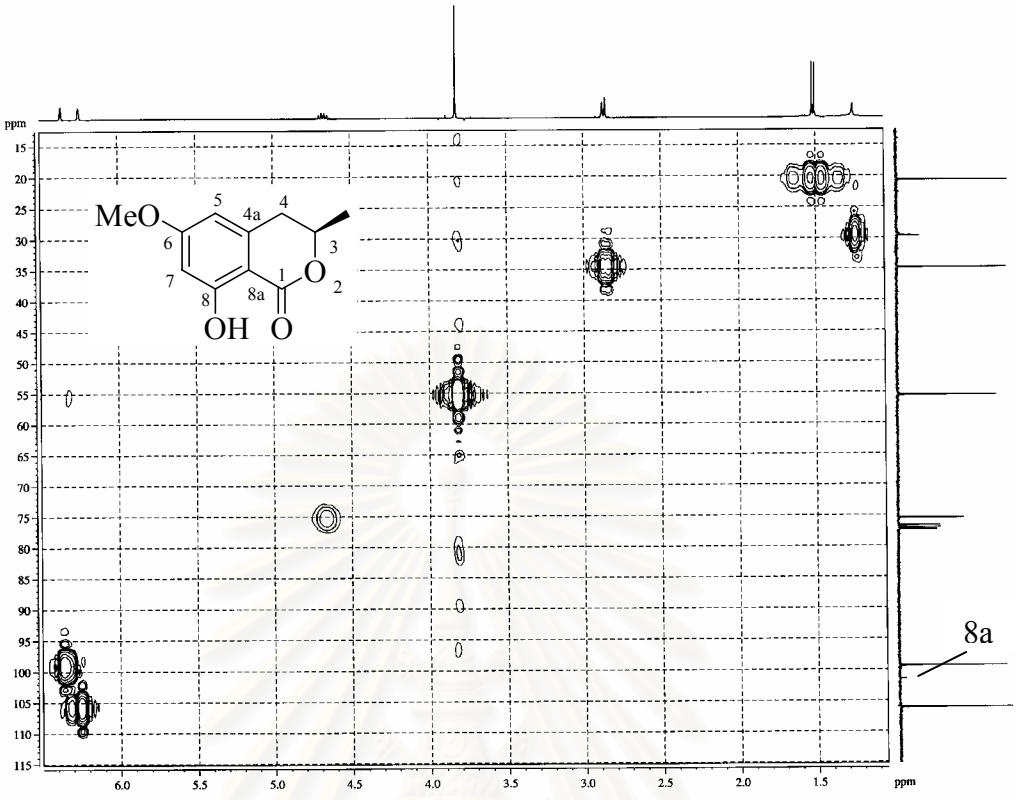

Figure A7: HMQC spectrum of **compound 1** (6-methoxymellein)

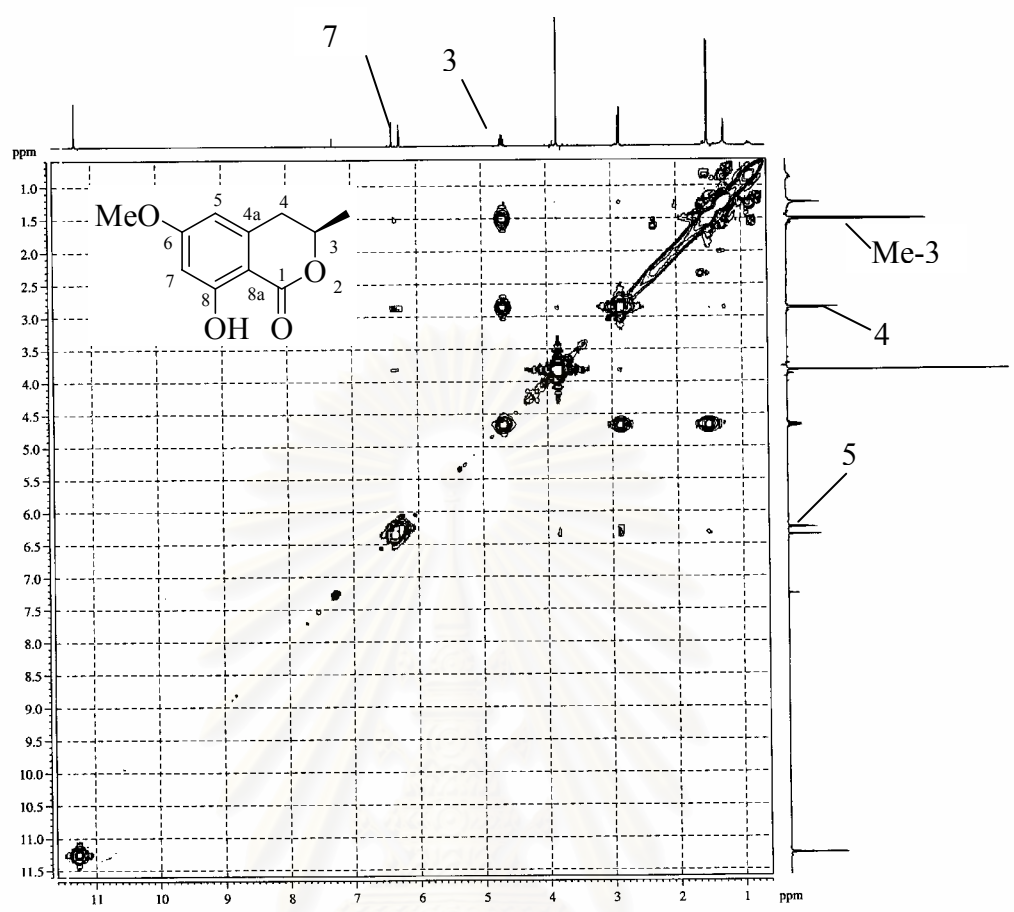

Figure A8: COSY spectrum of **compound 1** (6-methoxymellein)

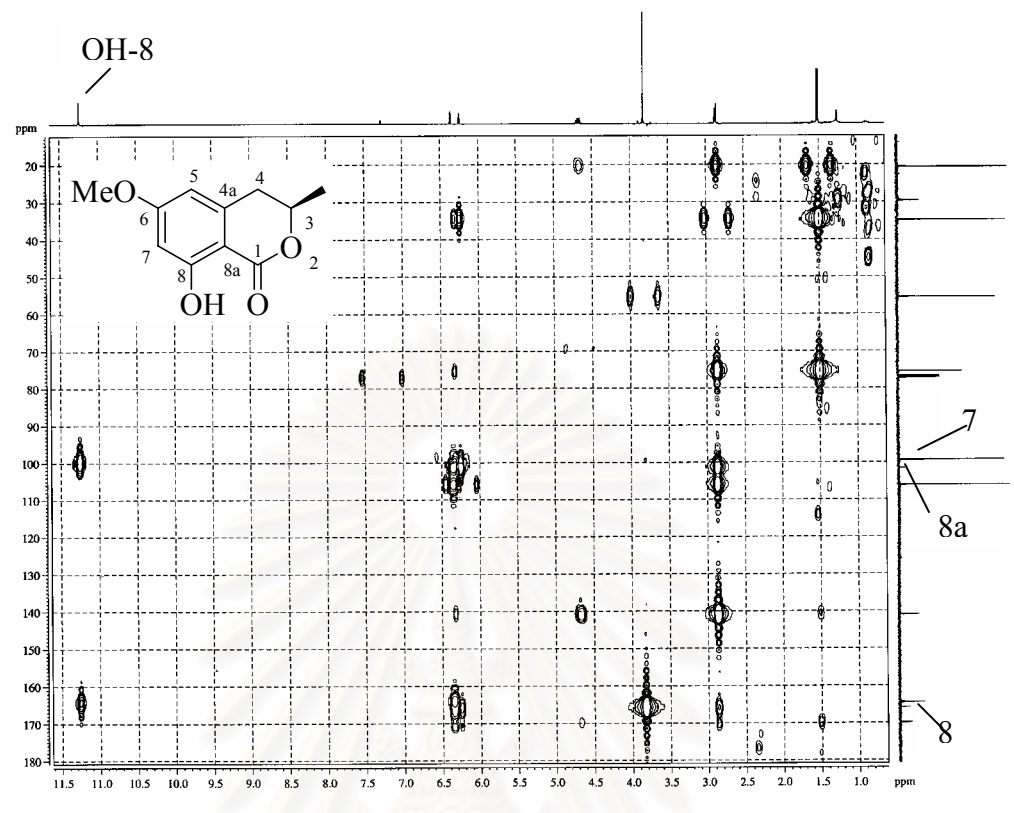

Figure A9: HMBC spectrum of **compound 1** (6-methoxymellein)

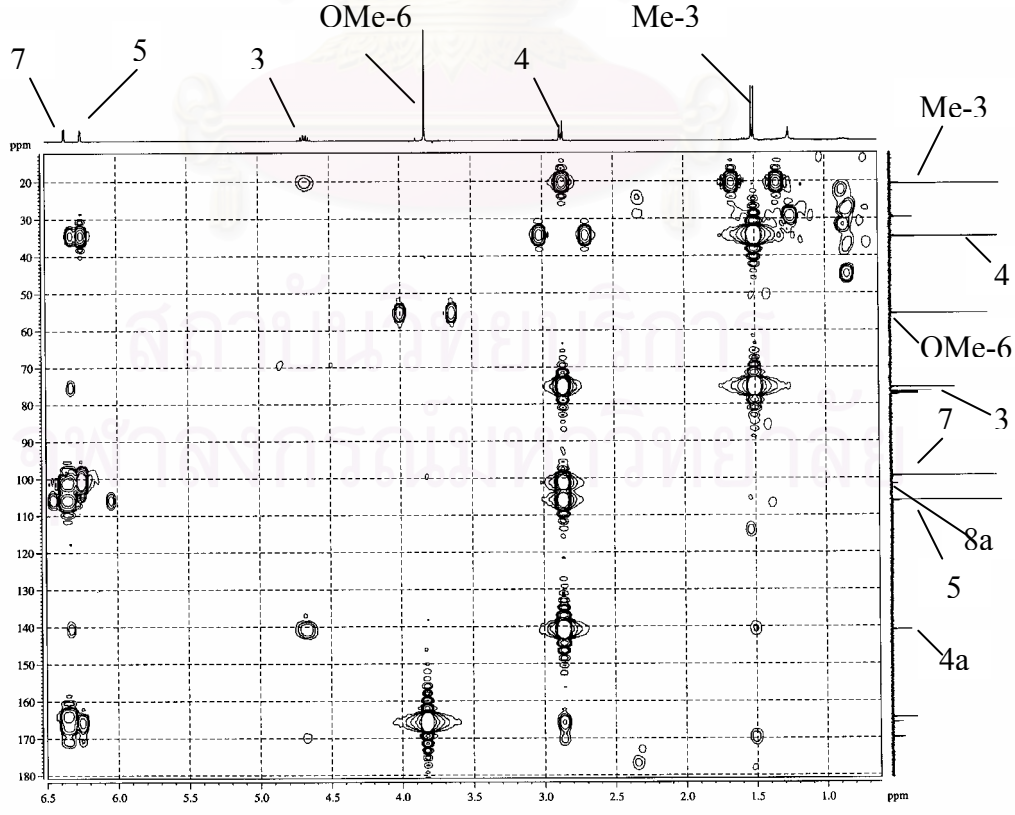

Figure A10: Expansion of **Fig. A8**

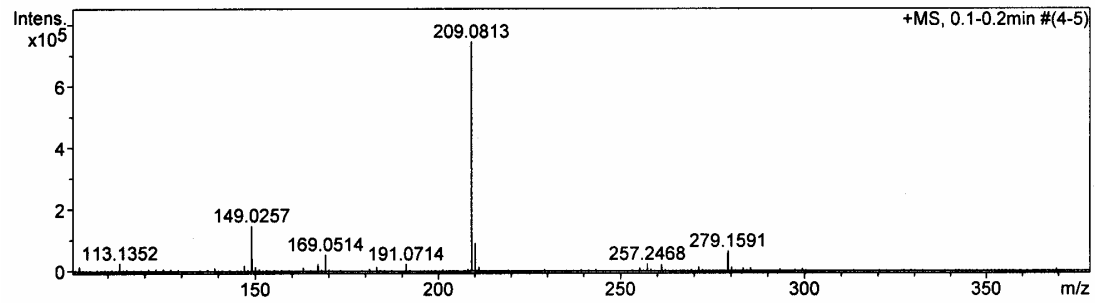

Figure A11: APCI-TOF spectrum of **compound 1** (6-methoxymellein)

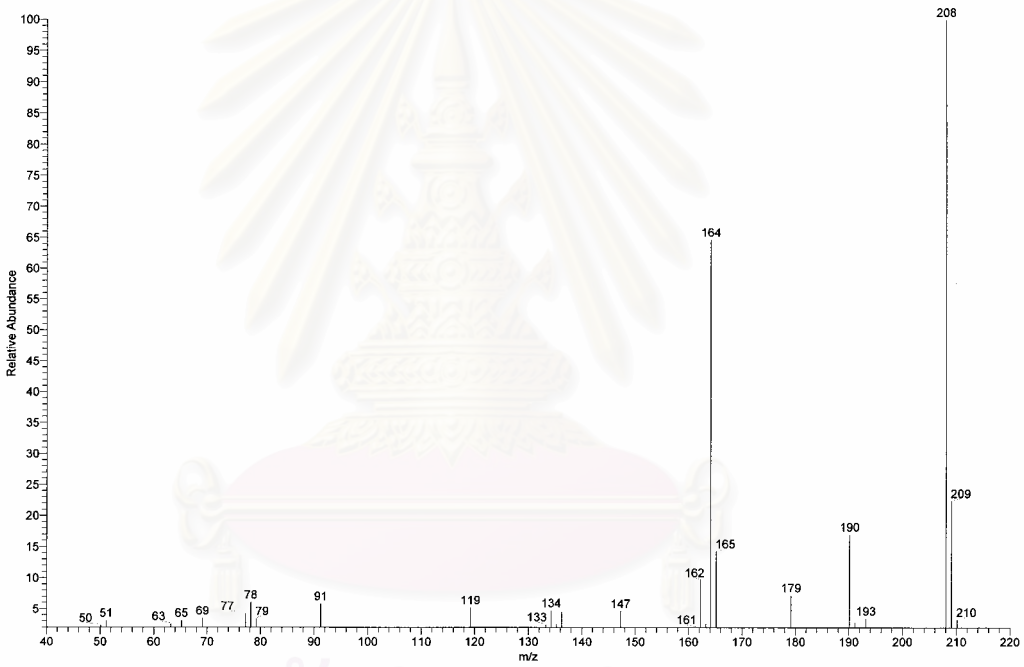

Figure A12: EI-MS spectrum of **compound 1** (6-methoxymellein)

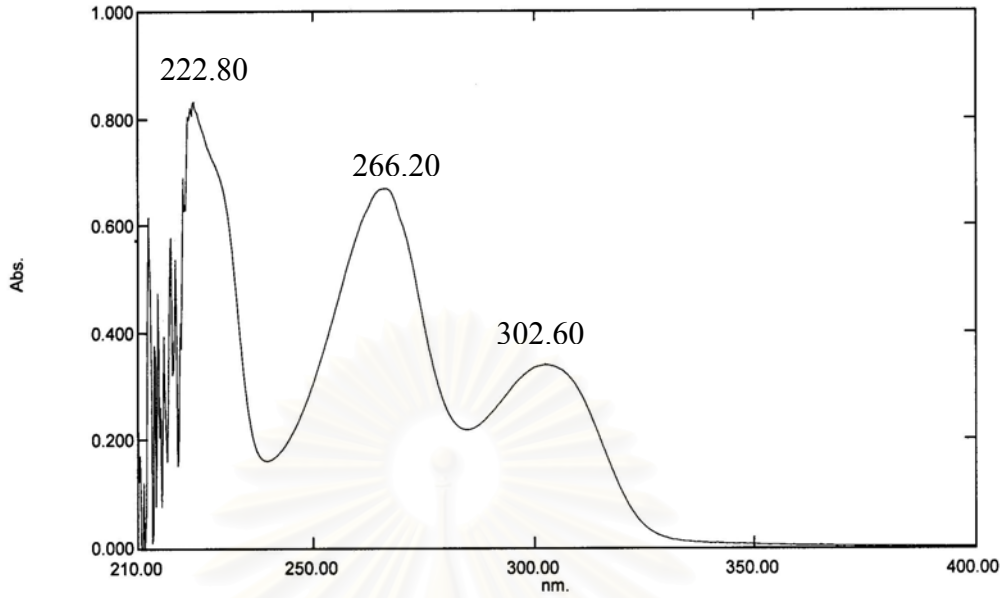

Figure A13: UV spectrum of **compound 2**

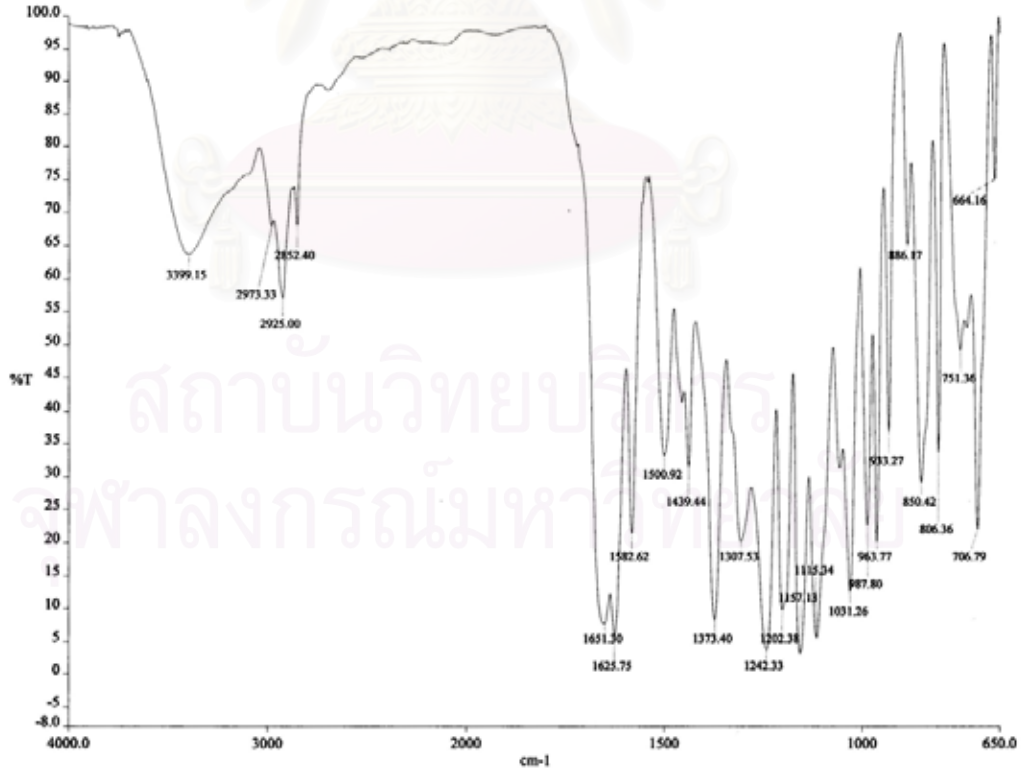

Figure A14: IR spectrum of **compound 2**

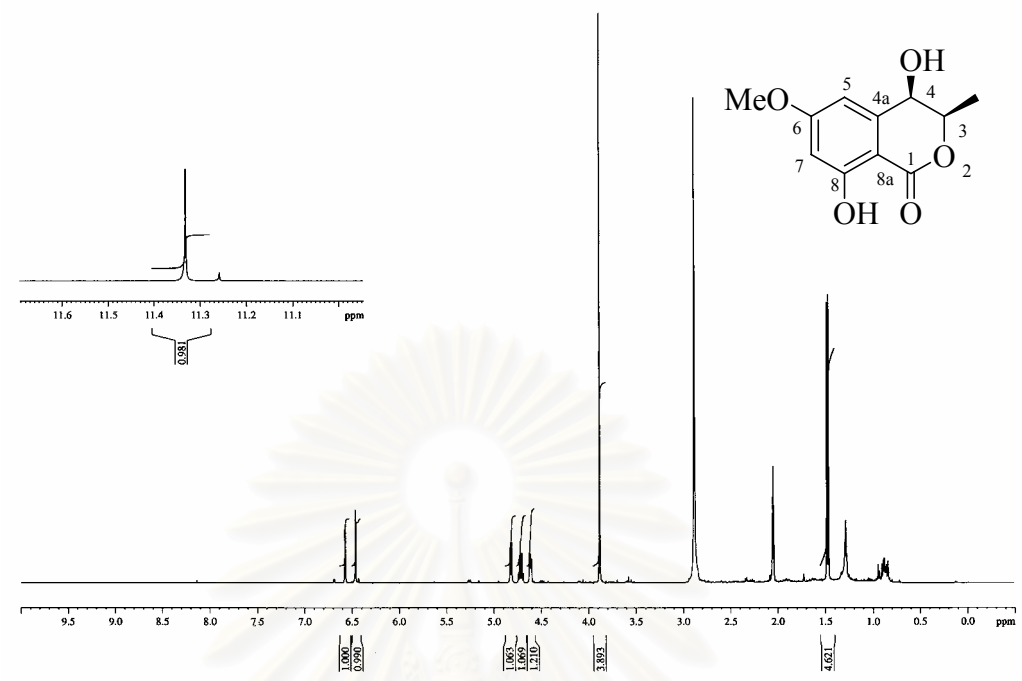

Figure A15: ^{1}H NMR (acetone-d_6) spectrum of **compound 2**

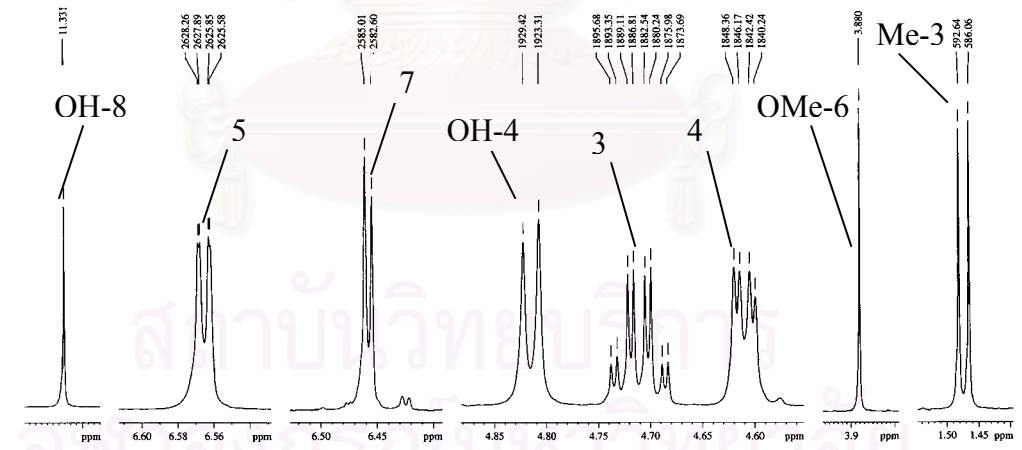

Figure A16: Expansion of **Fig. A15**

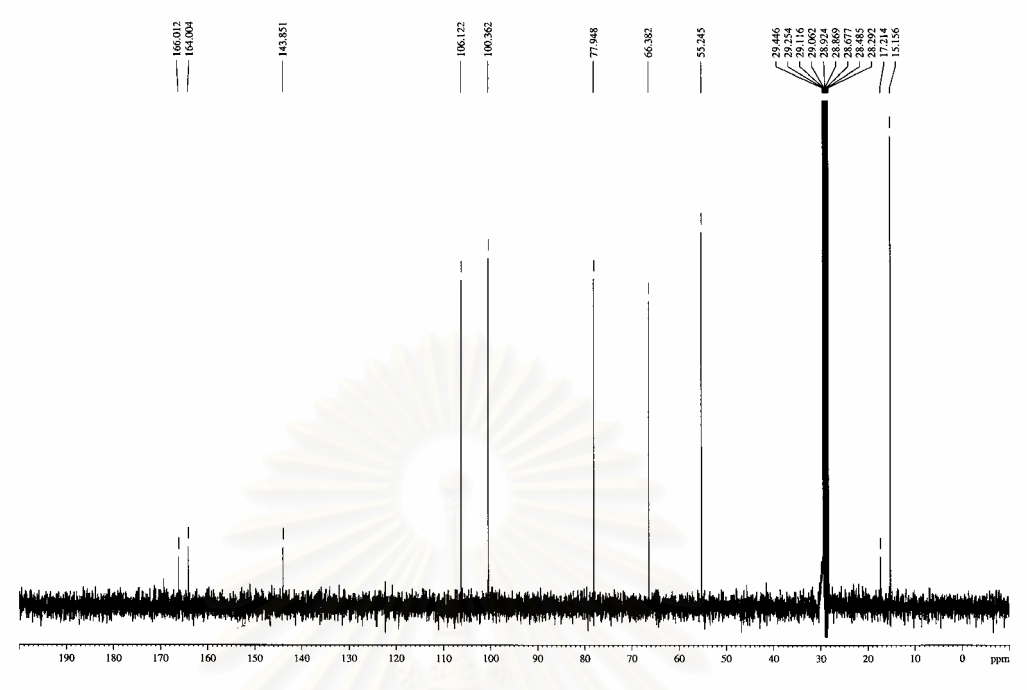

Figure A17: ^{13}C NMR (acetone-d_6) spectrum of **compound 2**

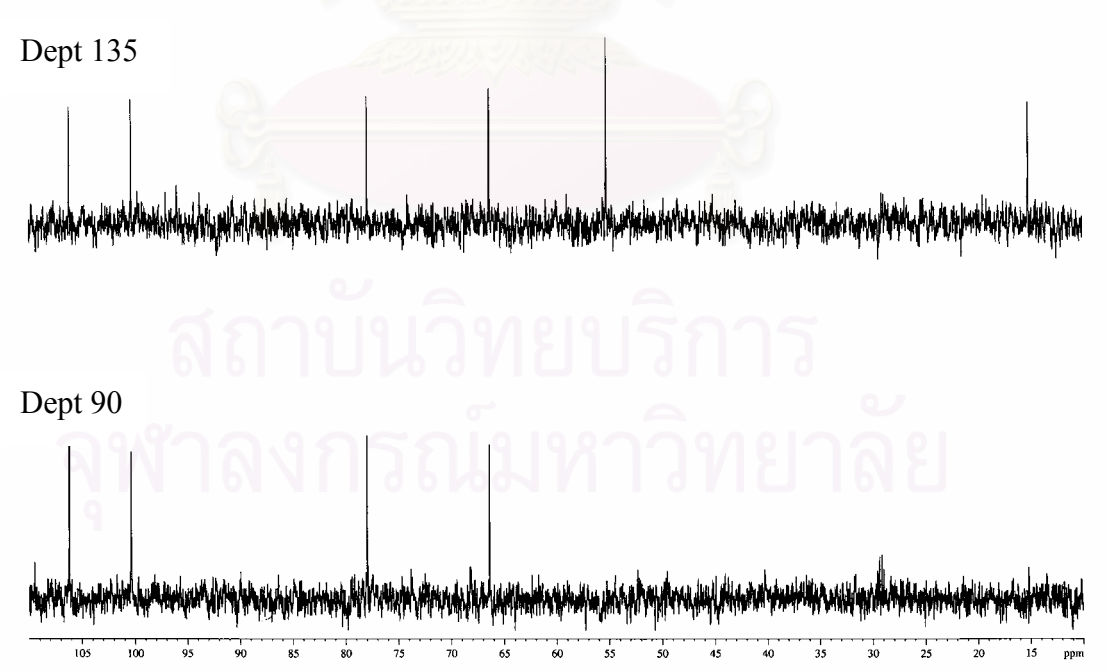

Figure A18: Depts spectra of **compound 2**

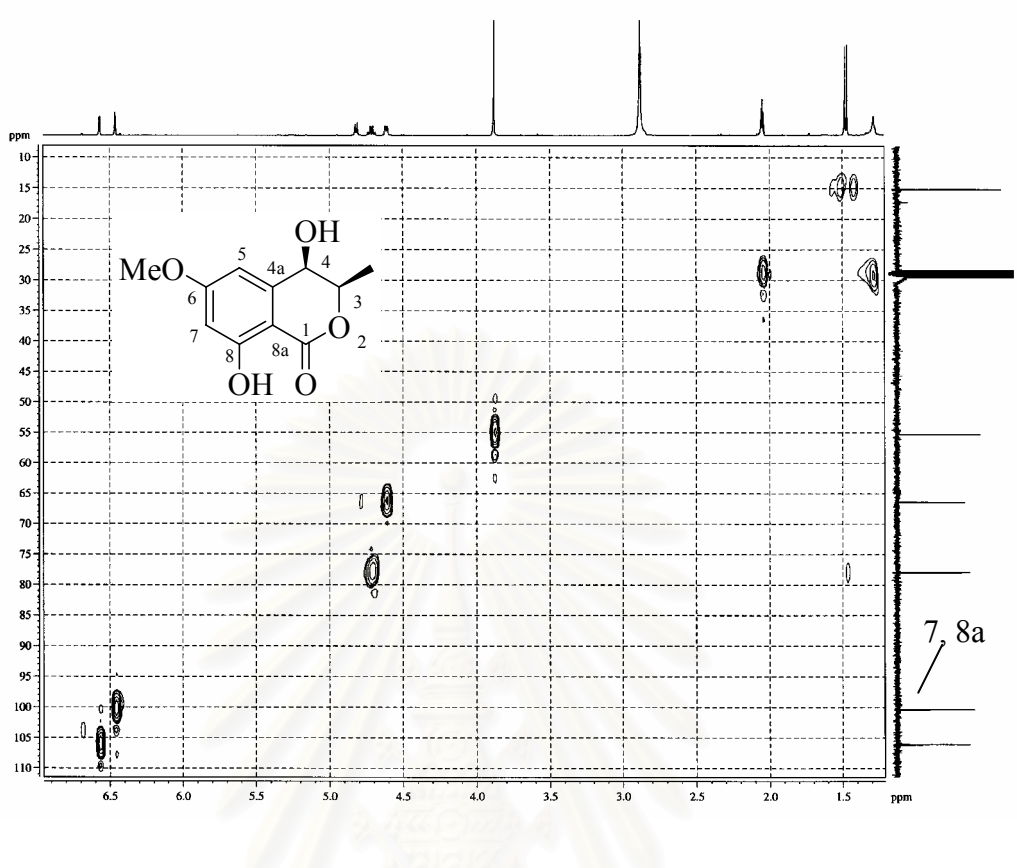

Figure A19: HMQC spectrum of **compound 2**

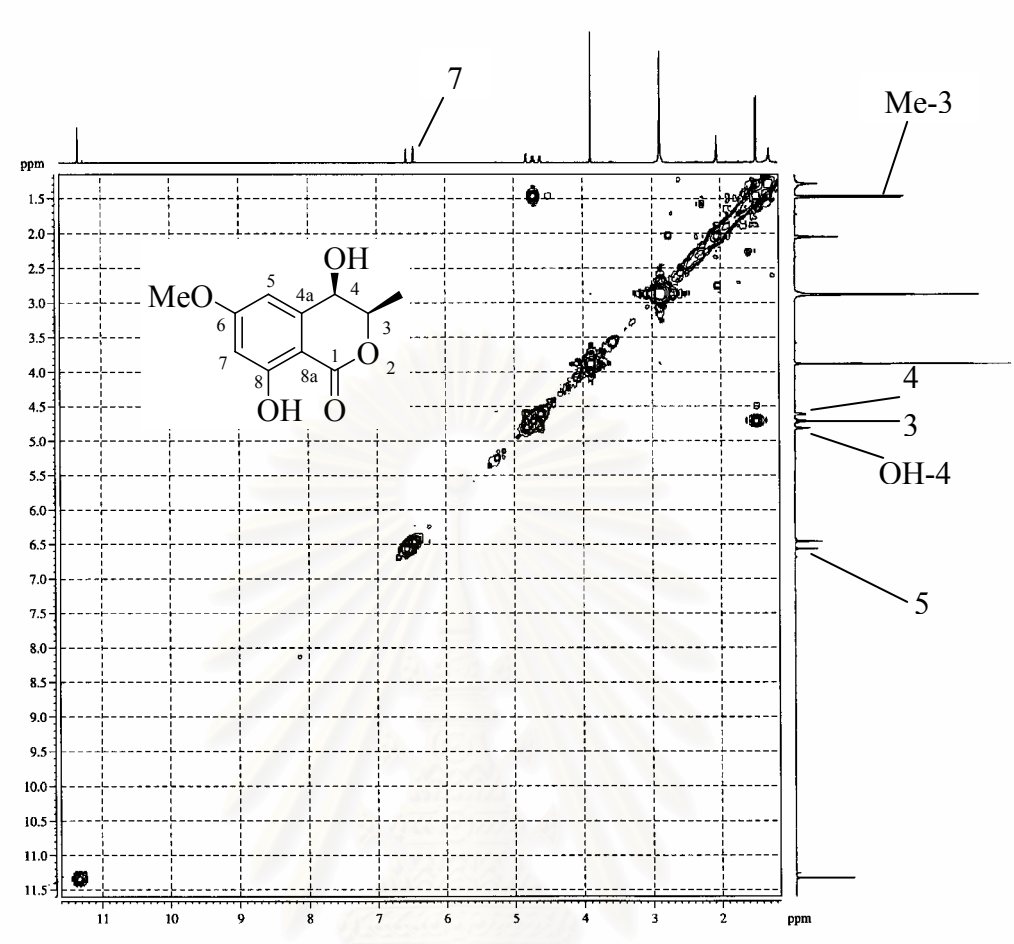

Figure A20: COSY spectrum of **Compound 2**

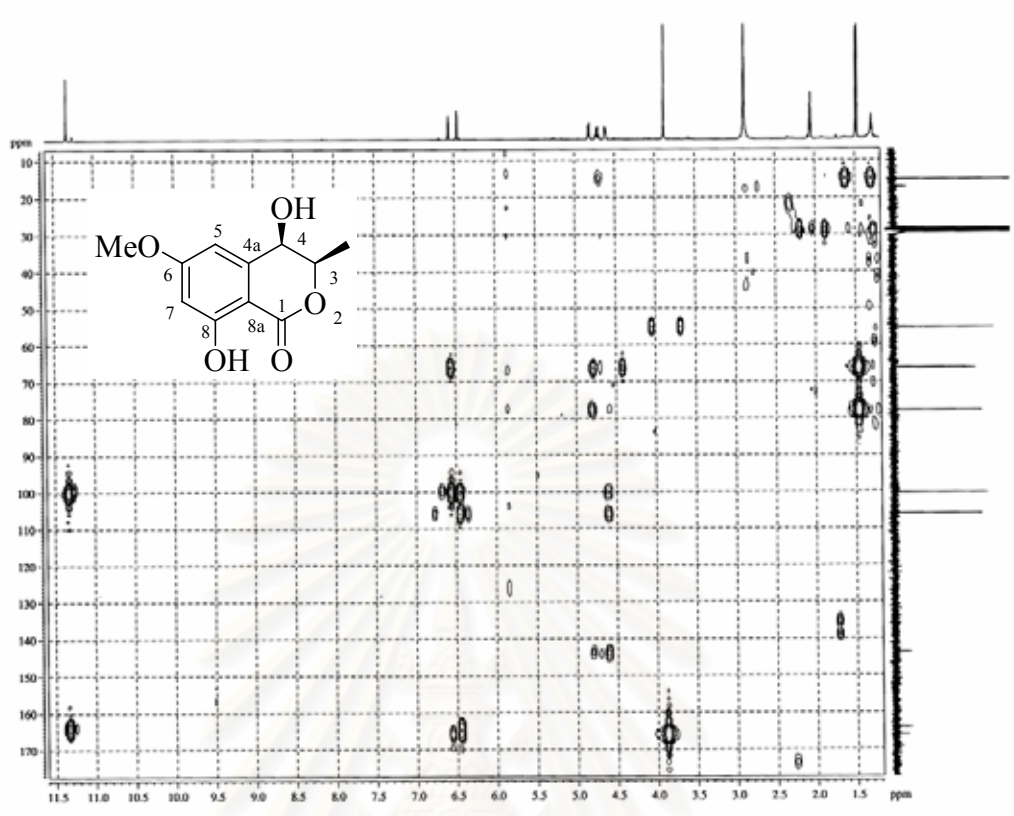

Figure A21: HMBC spectrum of **compound 2**

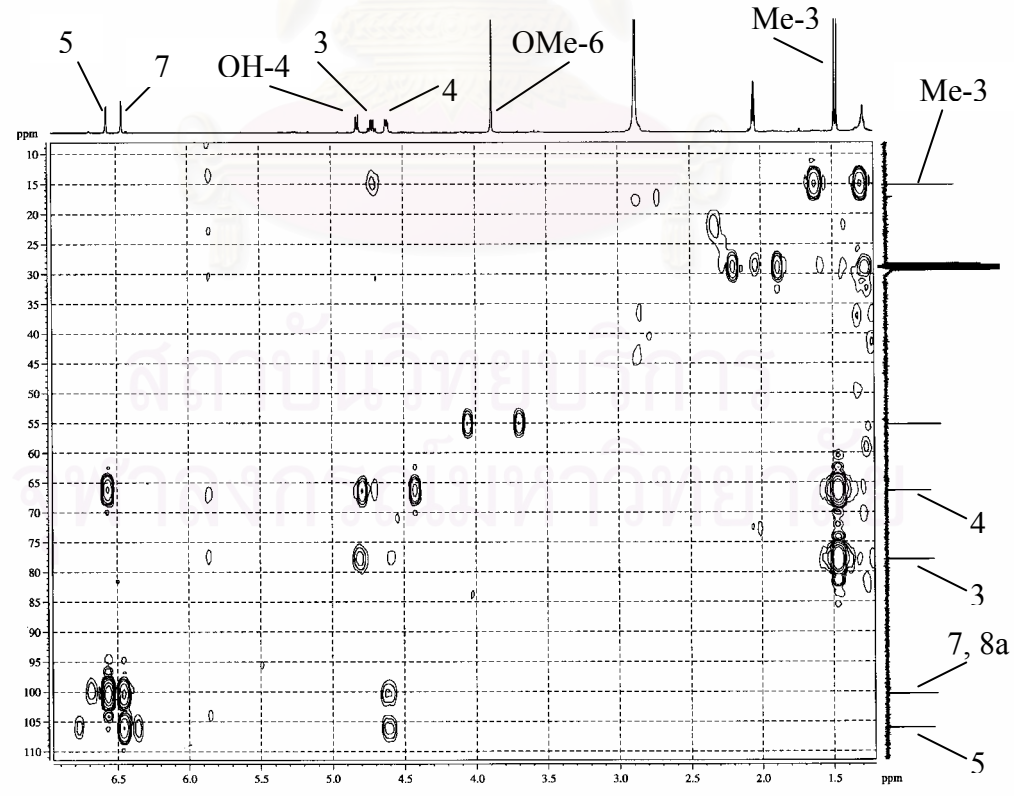

Figure A22: Expansion of **Fig. A21**

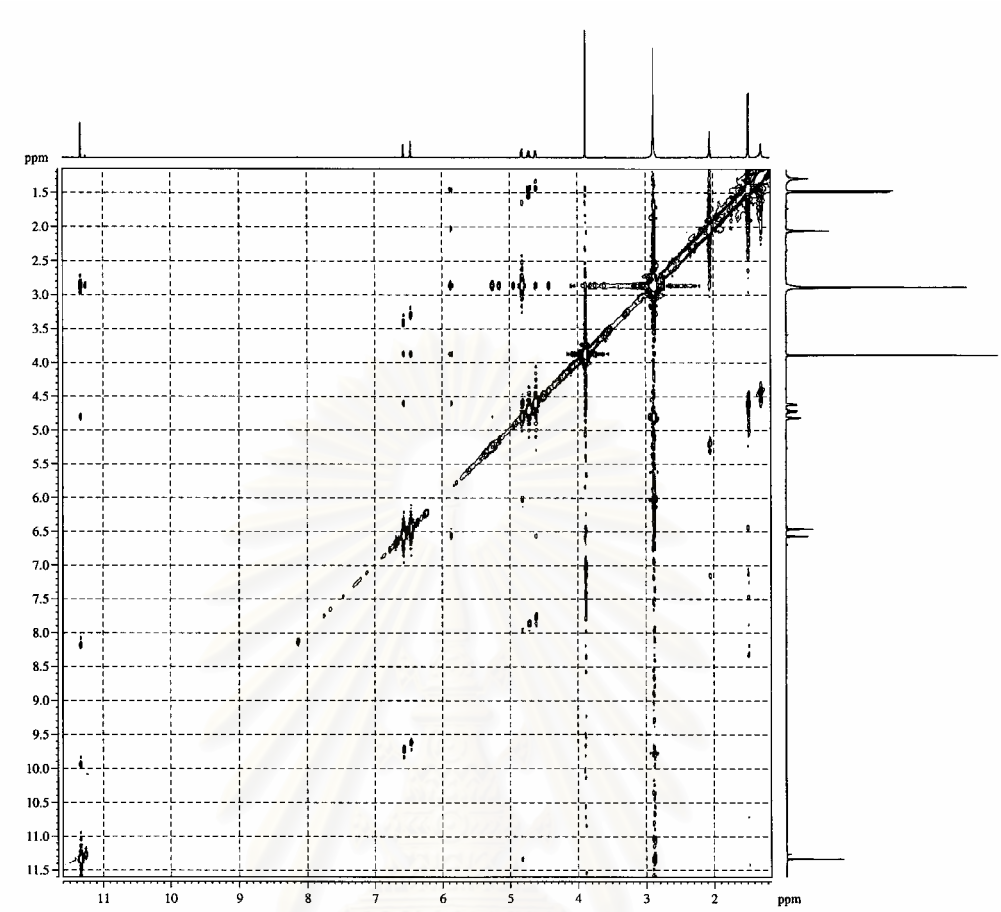

Figure A23: NOESY spectrum of **compound 2**

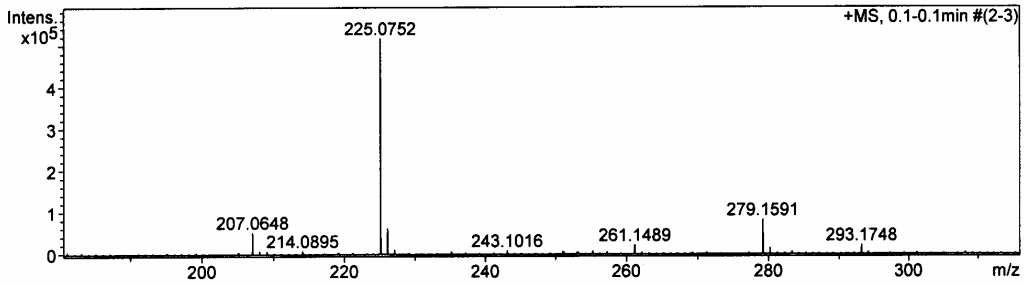

Figure A24: APCI-TOF spectrum of **compound 2**

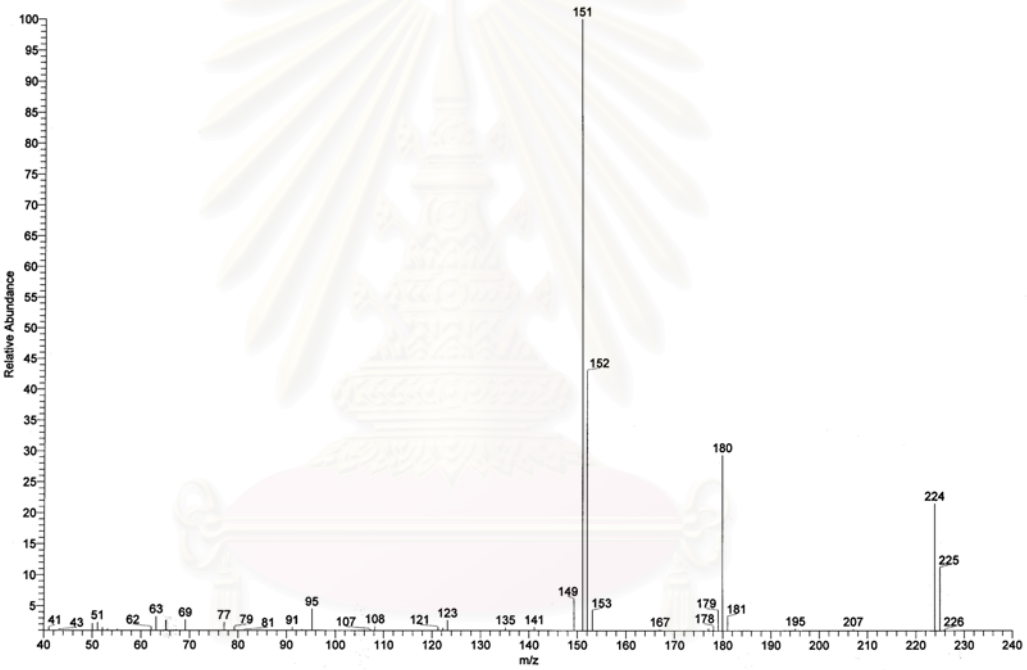

Figure A25: EI-MS spectrum of **compound 2**

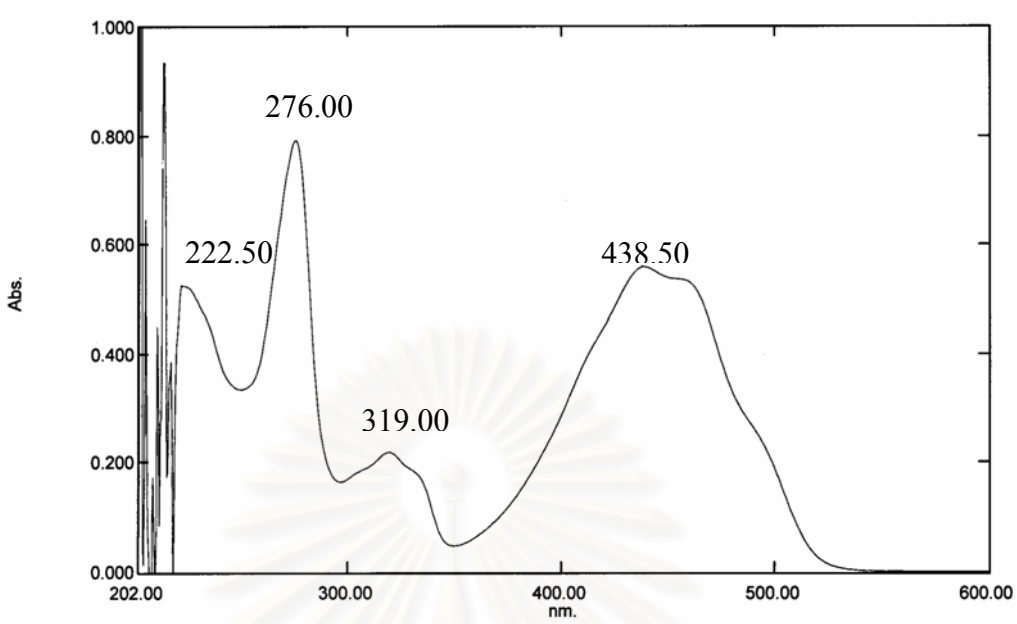

Figure A26: UV spectrum of **compound 3** (vermilhotin)

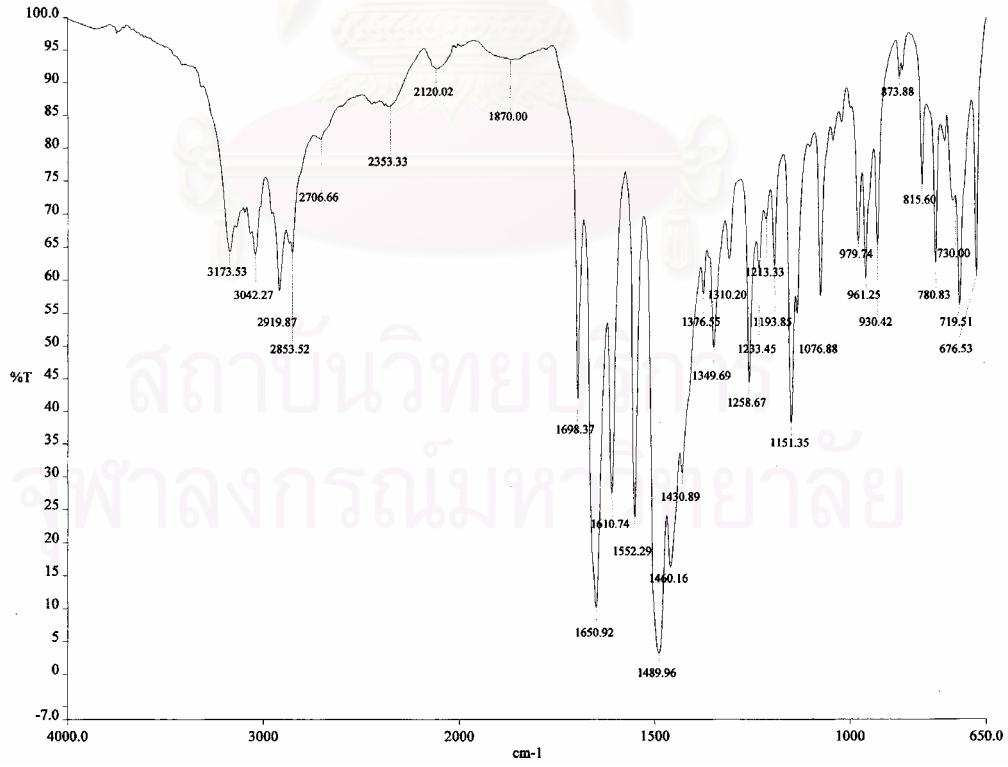

Figure A27: IR spectrum of **compound 3** (vermilhotin)

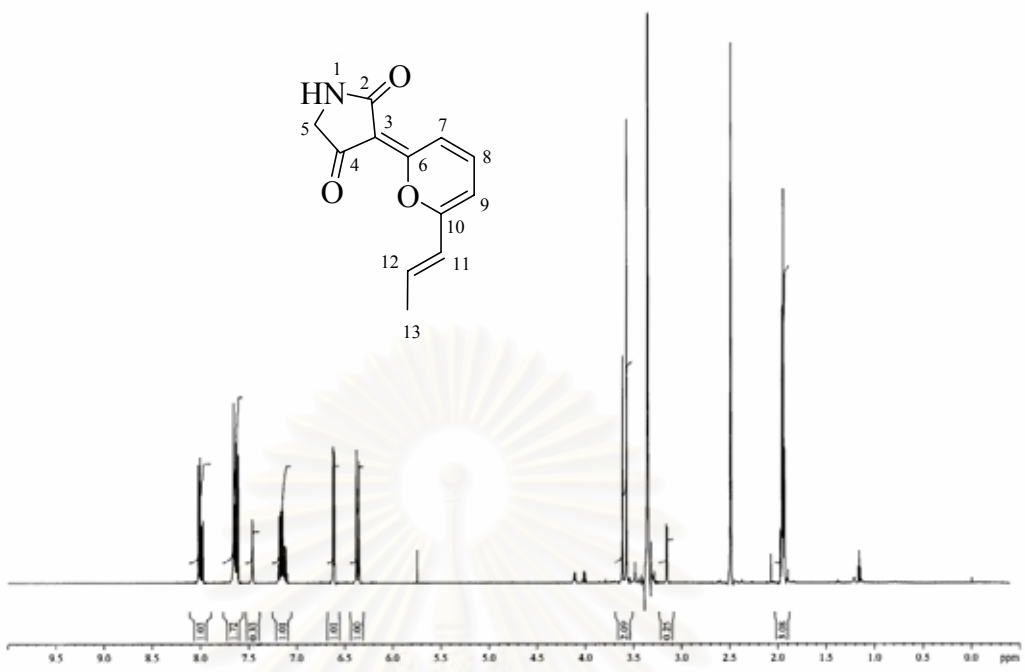

Figure A28: ^{1}H NMR (DMSO-d_6) spectrum of **compound 3** (vermilhotin)

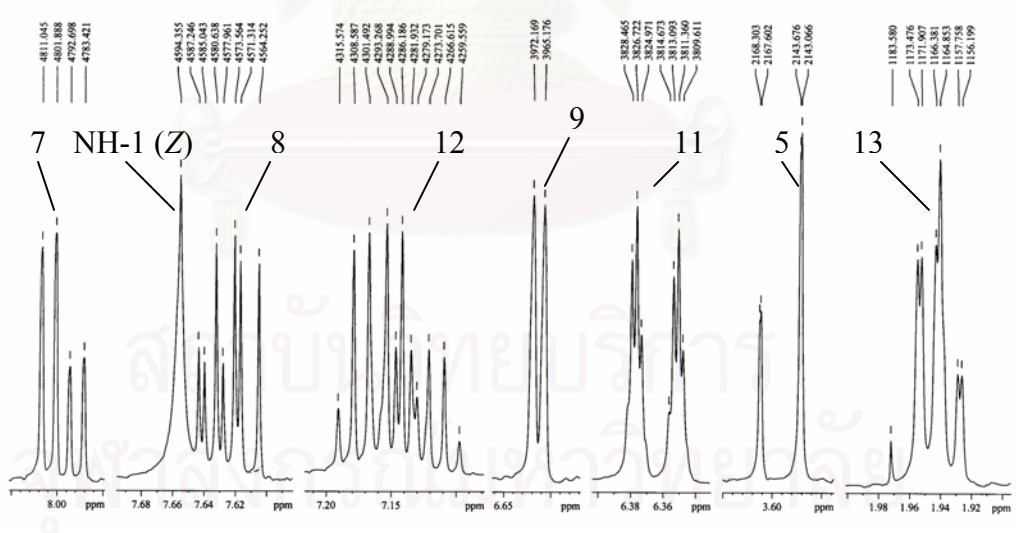

Figure A29: Expansion of **Fig. A28**

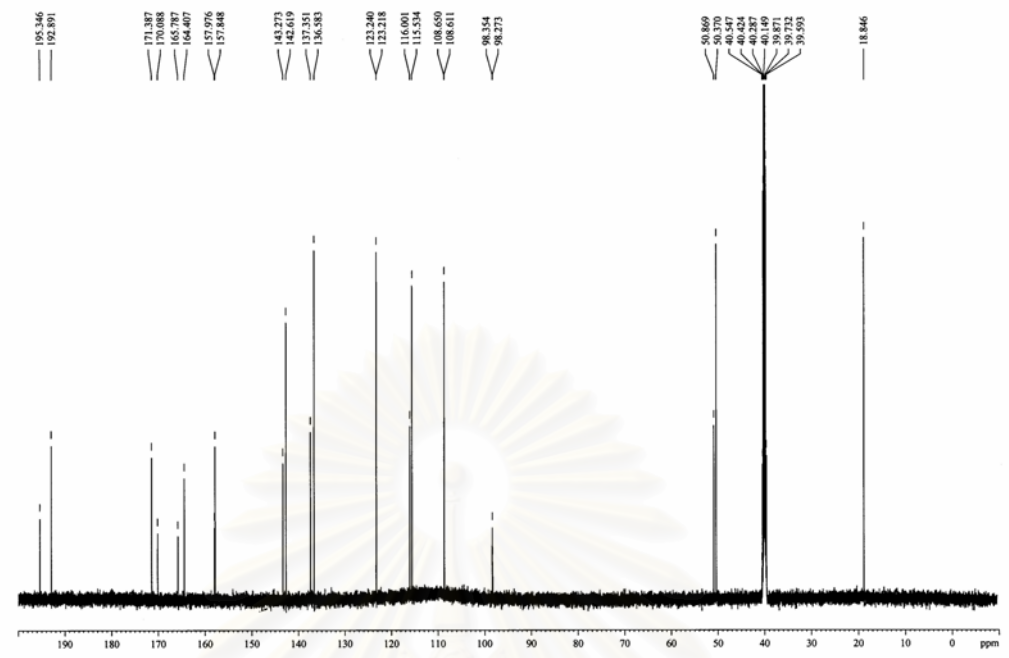

Figure A30: ^{13}C NMR (DMSO-d_6) spectrum of **compound 3** (vermilhotin)

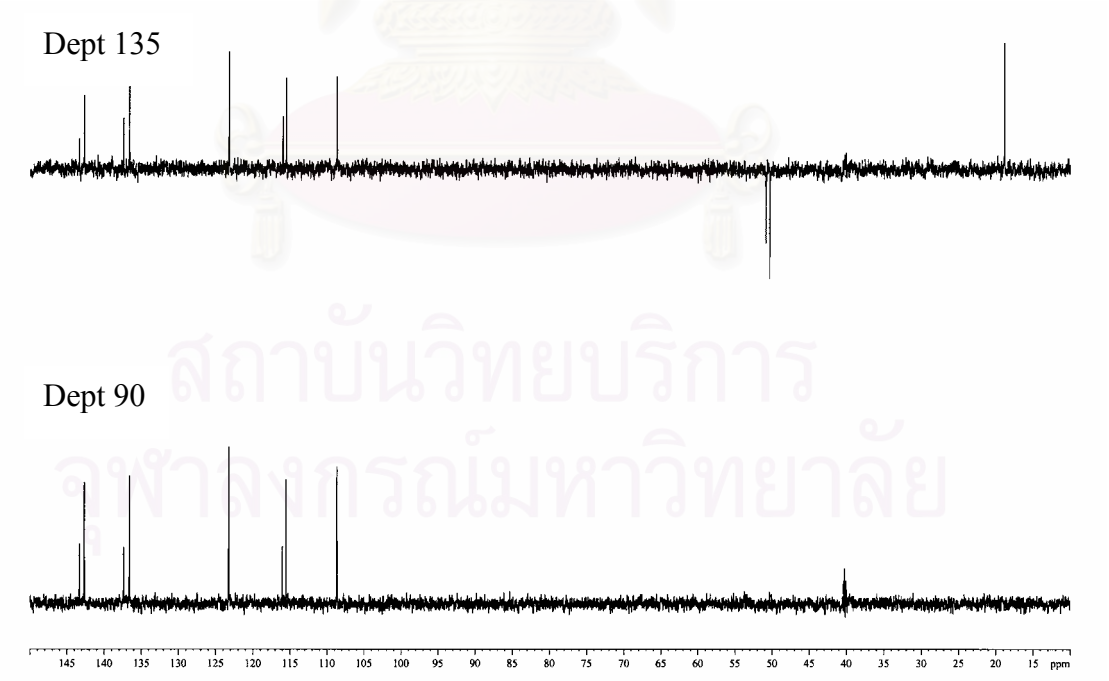

Figure A31: Depts spectra of **compound 3** (vermilhotin)

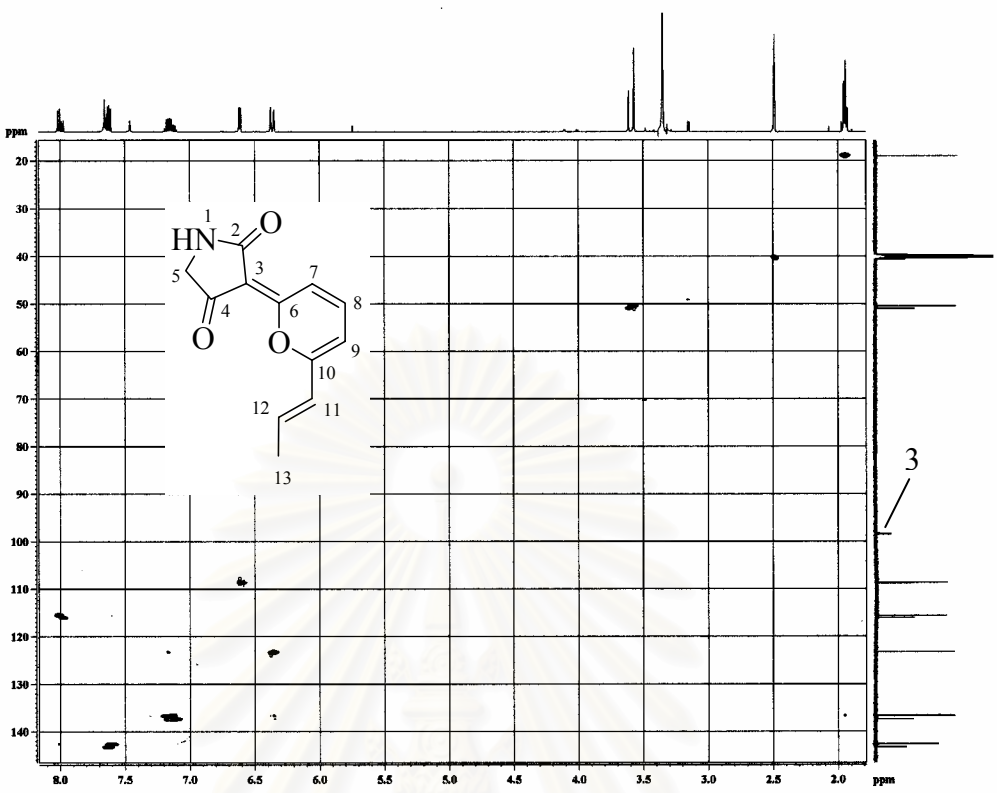

Figure A32: HMQC spectrum of **compound 3** (vermilhotin)

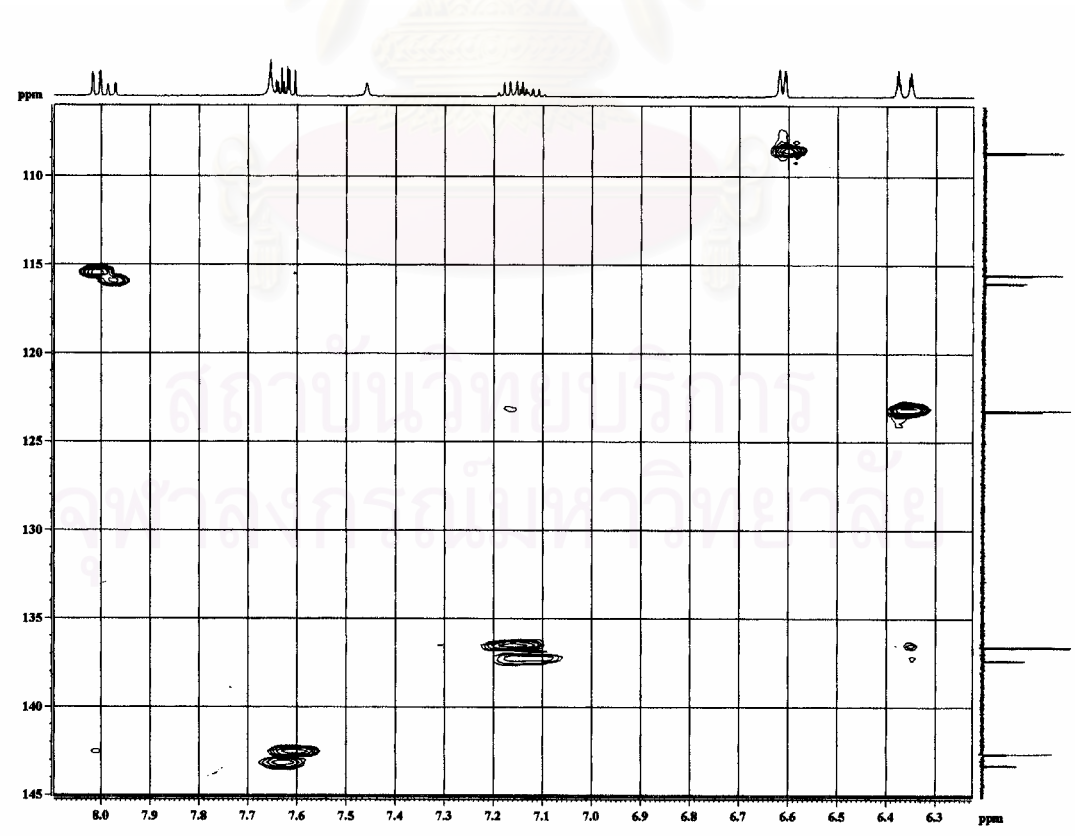

Figure A33: HMQC Expansion of **Fig. A32**

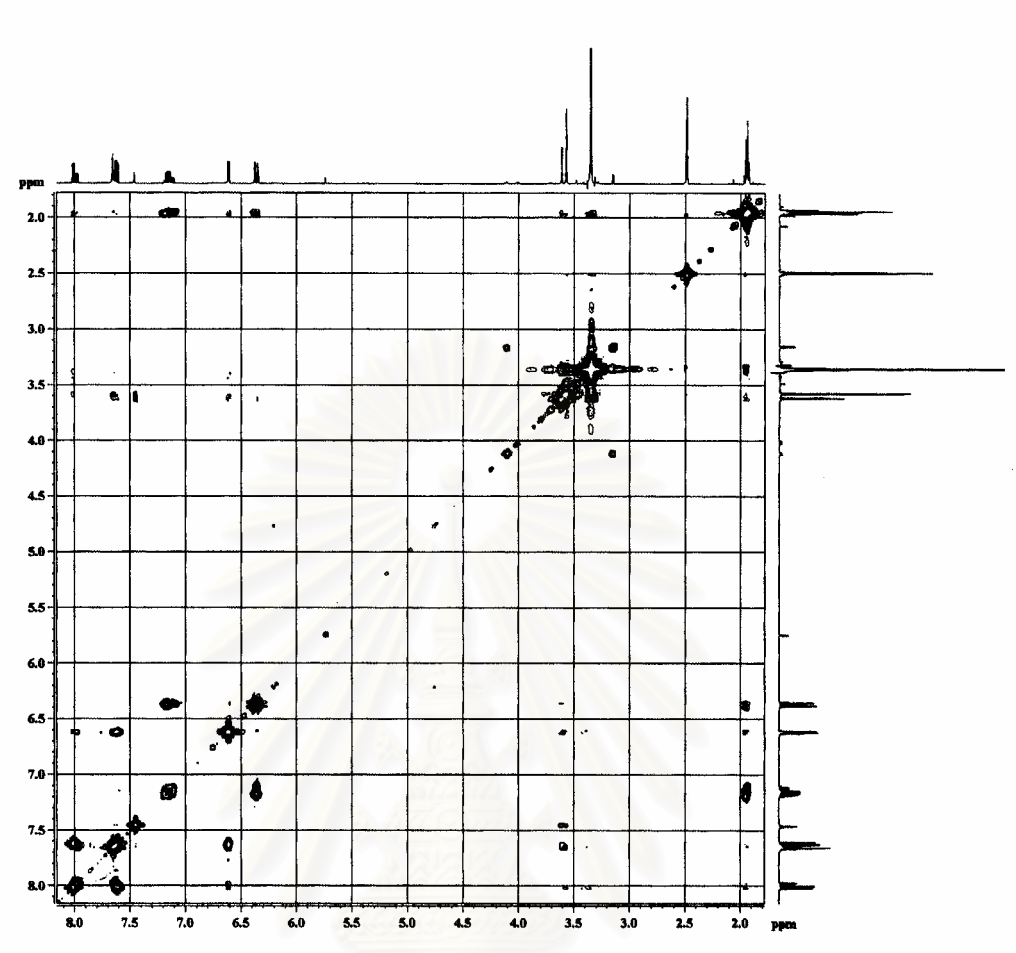

Figure A34: COSY spectrum of **compound 3** (vermilhotin)

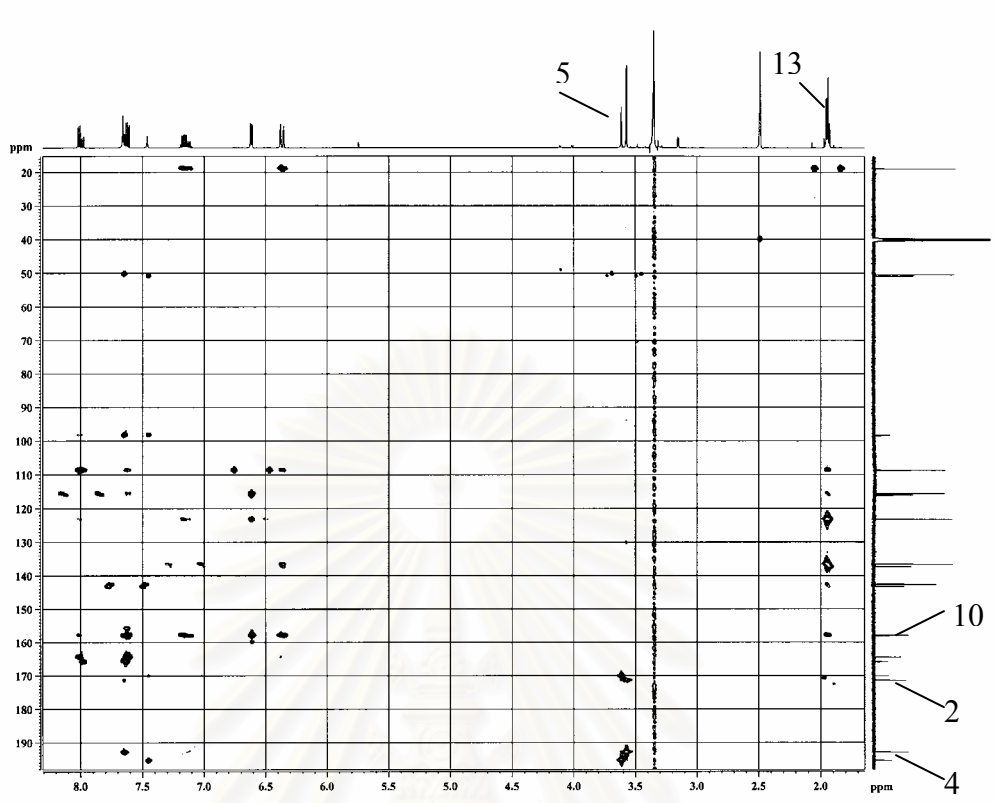

Figure A35: HMBC spectrum of **compound 3** (vermilhotin)

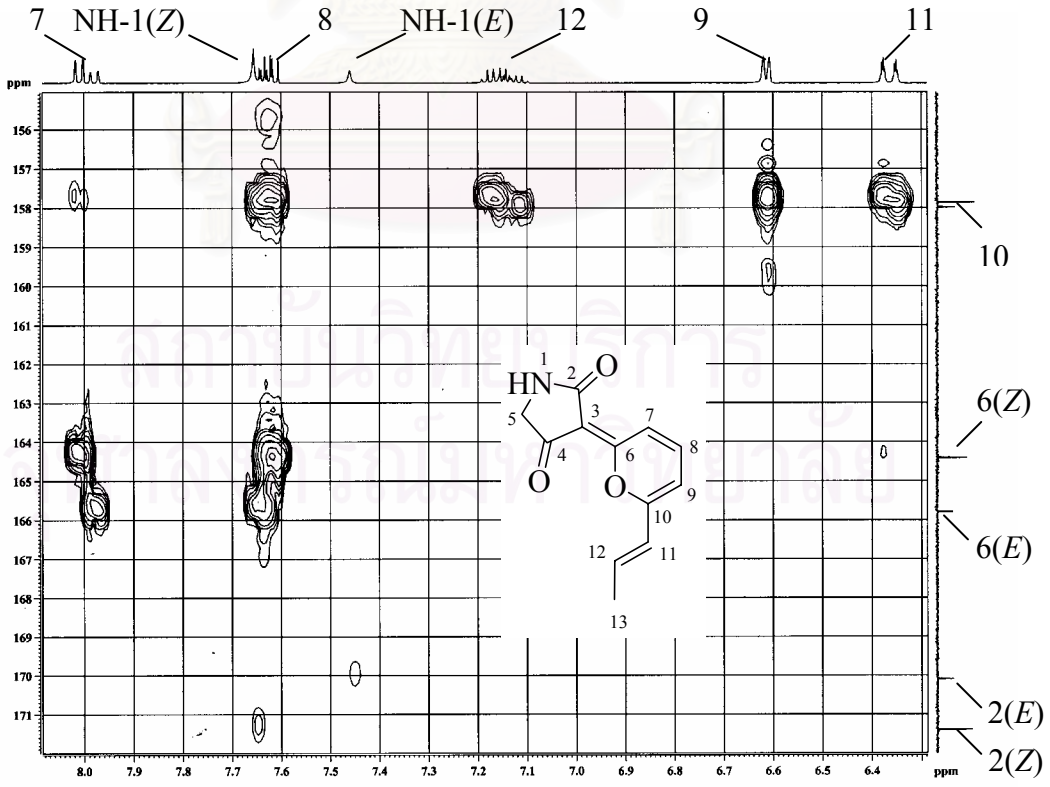

Figure A36: Expansion of **Fig. A35**

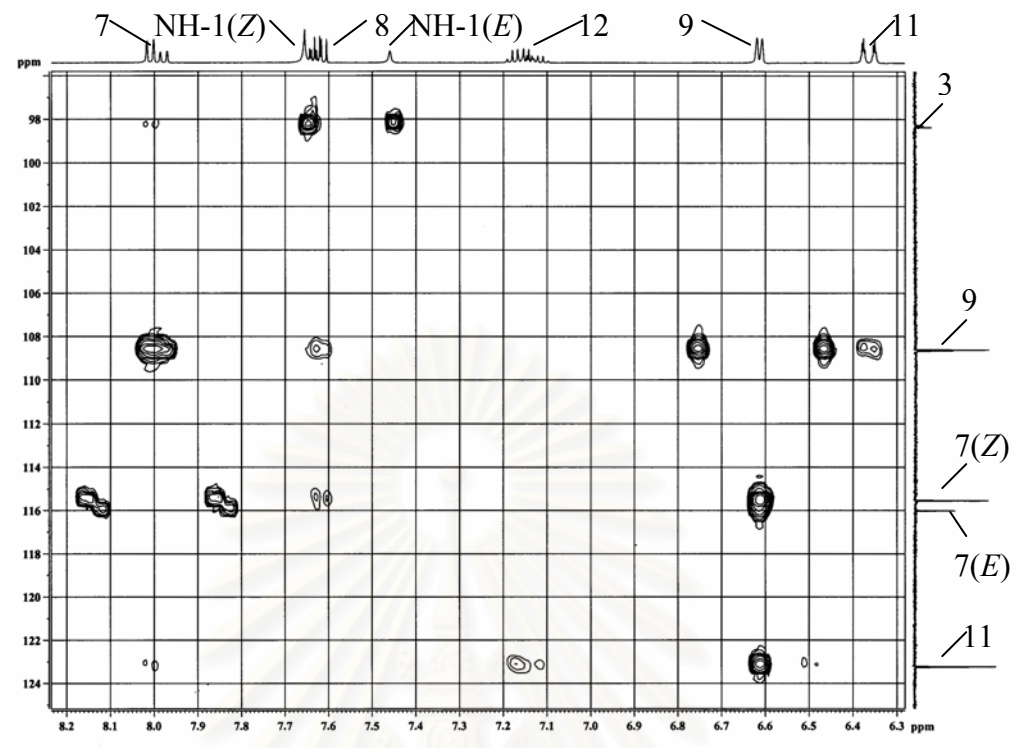

Figure A37: Expansion of **Fig. A35** (continue)

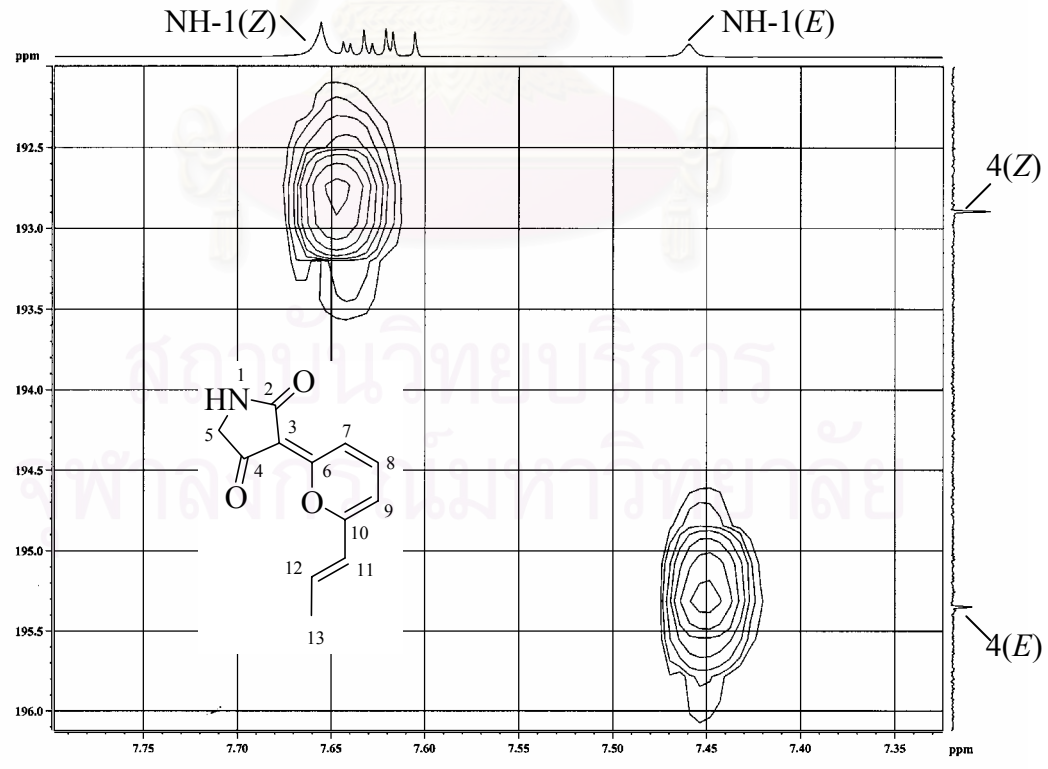

Figure A38: Expansion of **Fig. A35** (continue)

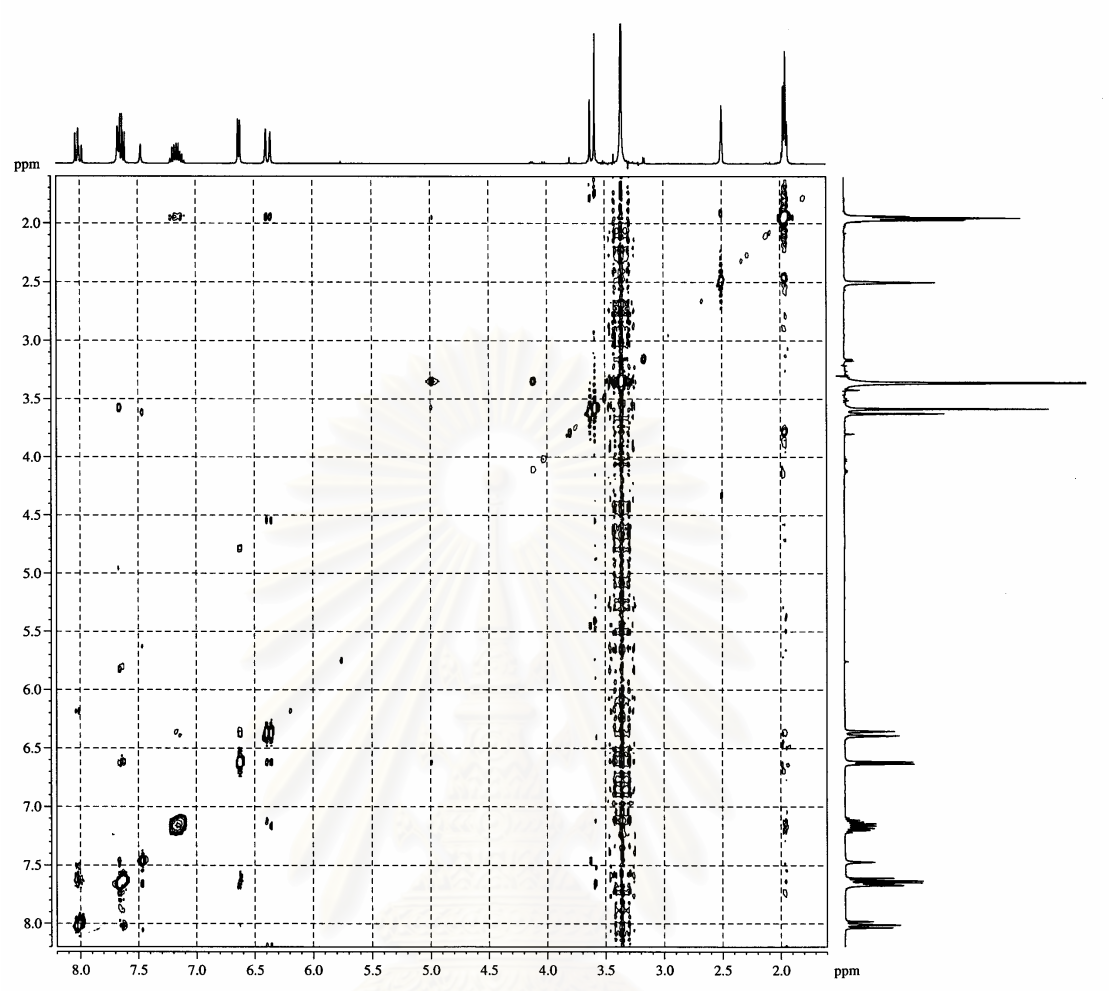

Figure A39: NOESY spectrum of **compound 3** (vermilhotin)

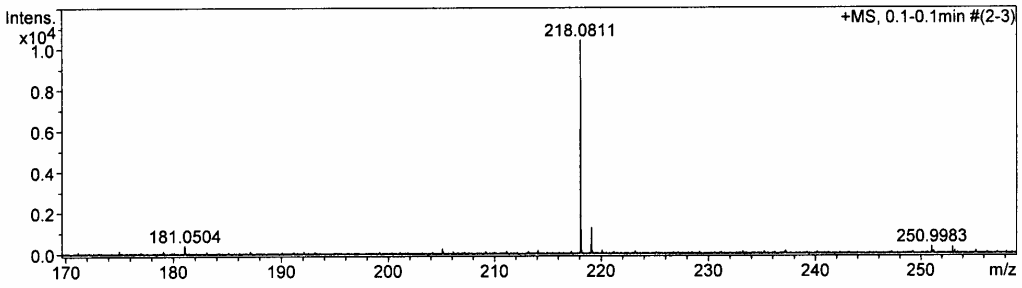

Figure A40: APCI-TOF spectrum of **compound 3** (vermilhotin)

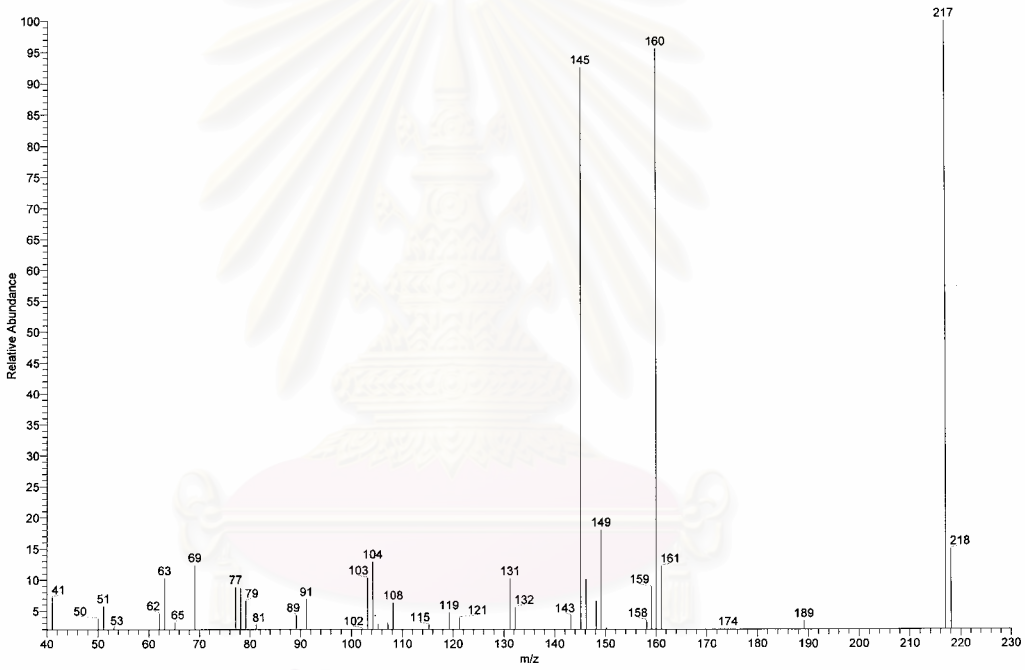

Figure A41: EI-MS spectrum of **compound 3** (vermilhotin)

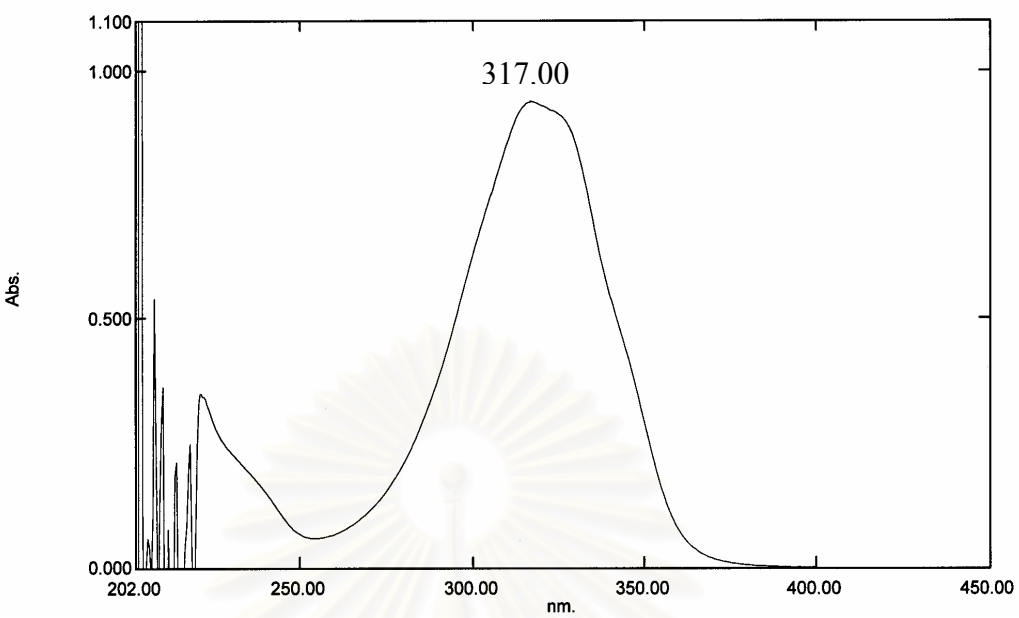

Figure A42: UV spectrum of **compound 4**

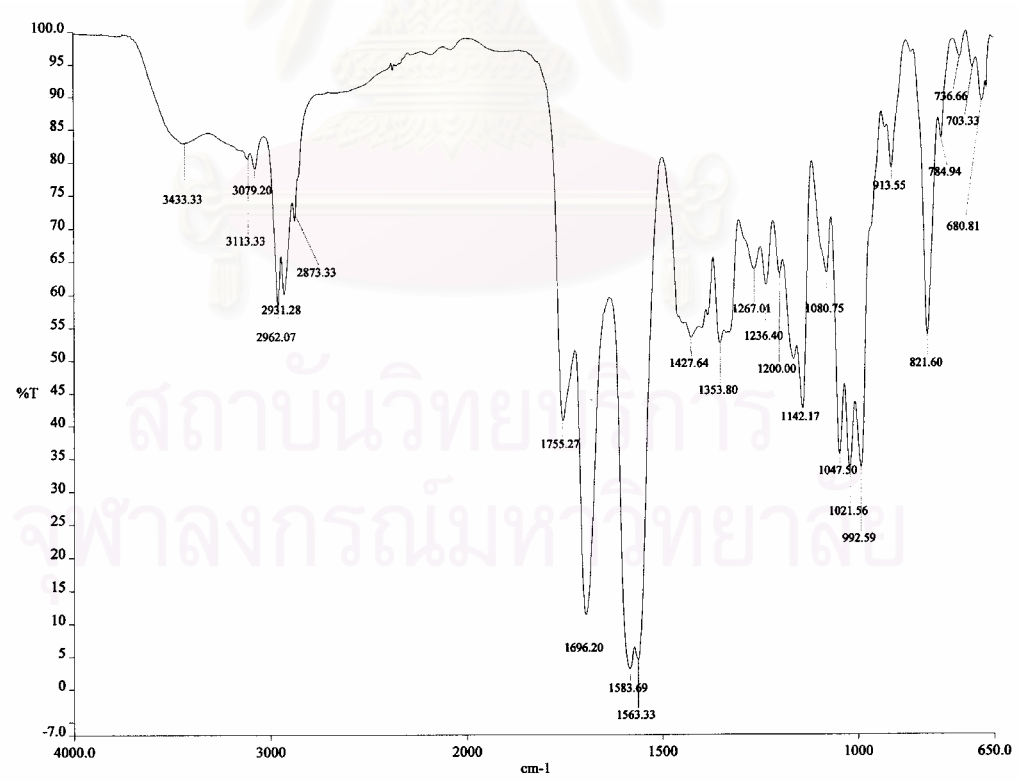

Figure A43: IR spectrum of **compound 4**

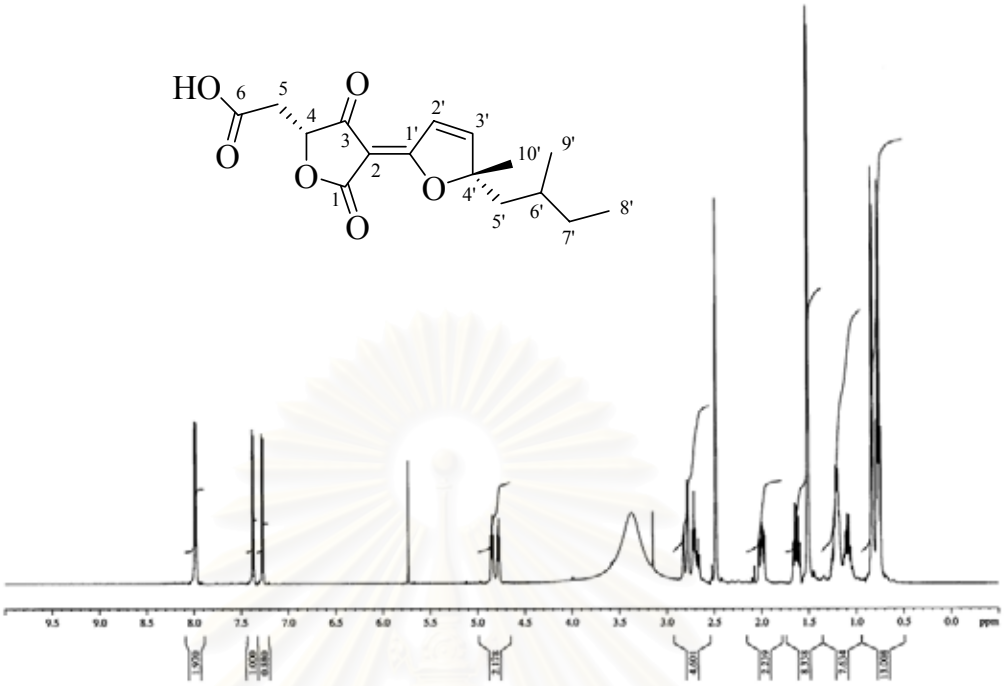

Figure A44: ^{1}H NMR (DMSO-d_6) spectrum of **compound 4**

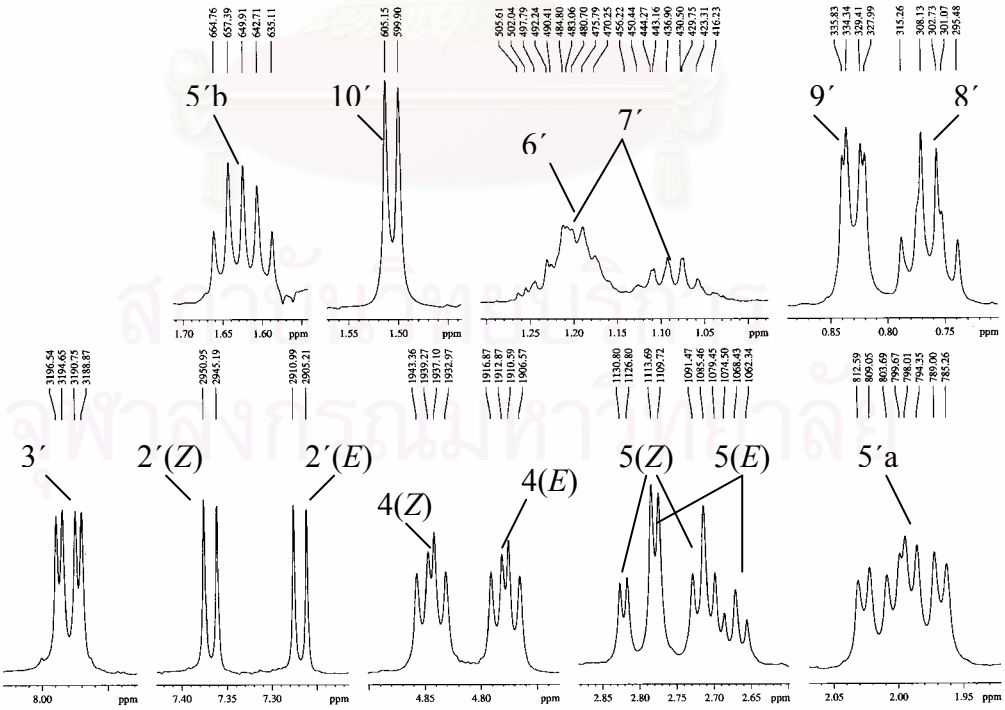

Figure A45: Expansion of **Fig. A44**

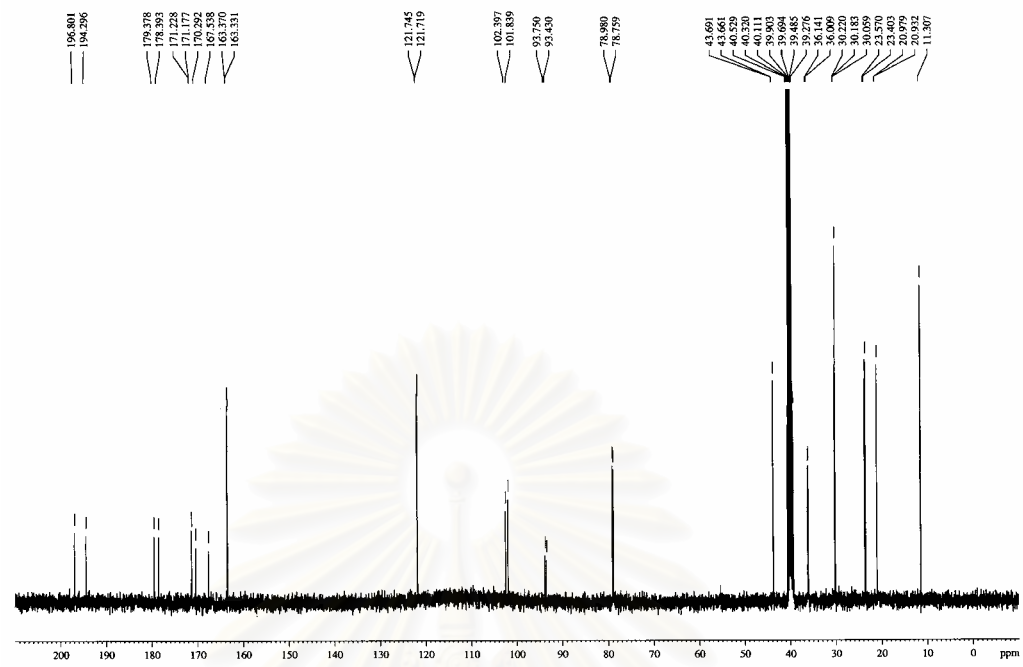

Figure A46: ^{13}C NMR (DMSO-d_6) spectrum of **compound 4**

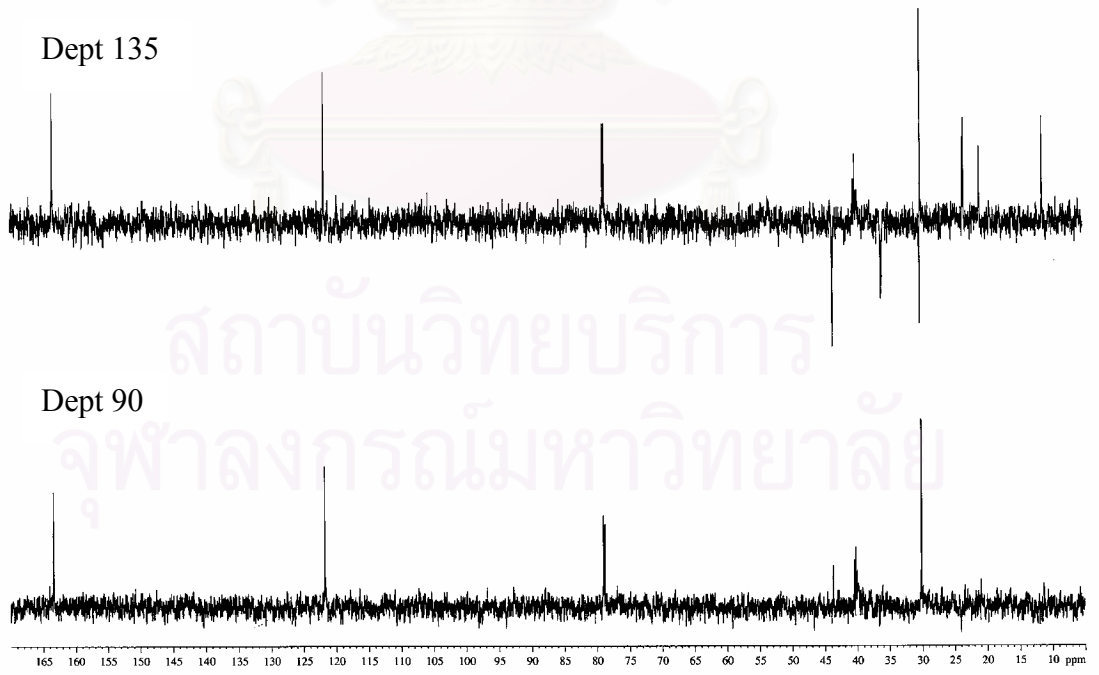

Figure A47: Depts spectra of **compound 4**

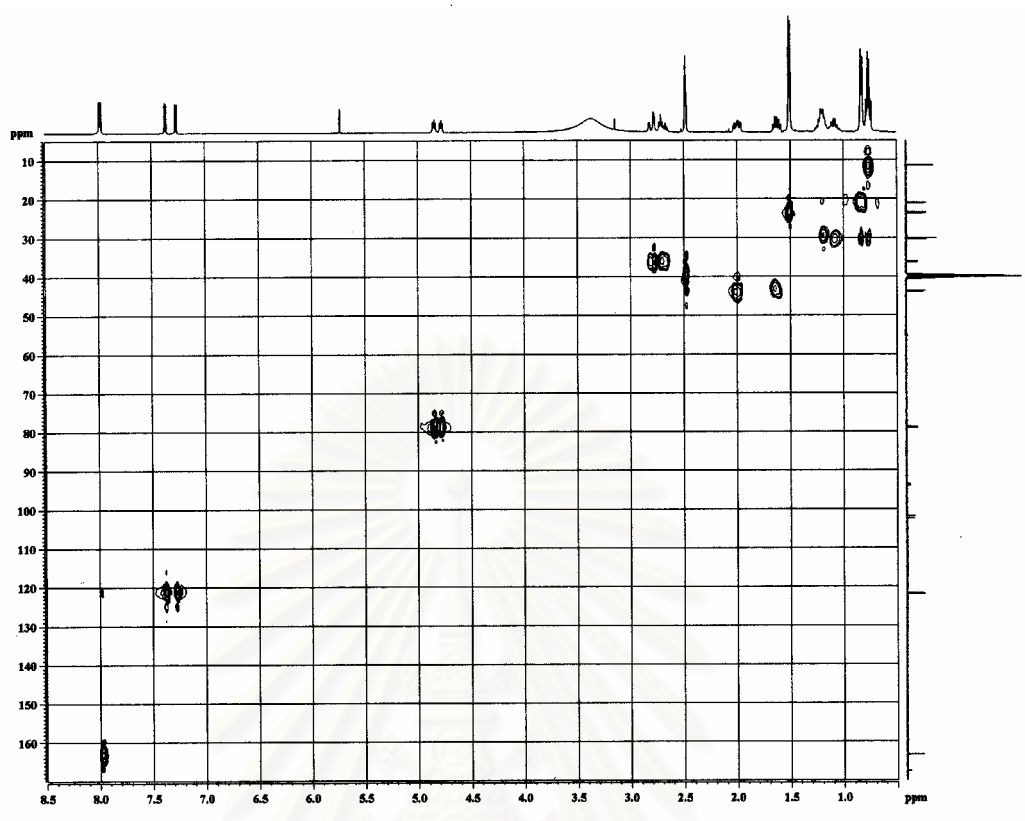

Figure A48: HMQC spectrum of **compound 4**

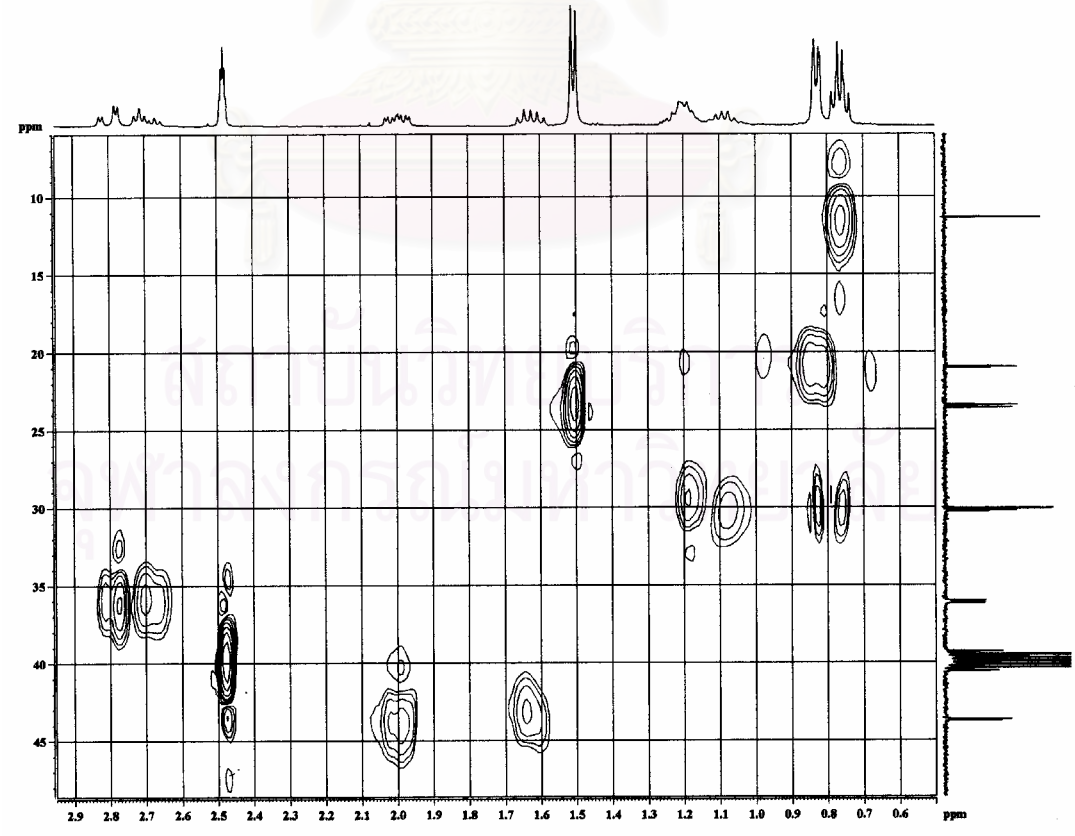

Figure A49: Expansion of **Fig. A48**

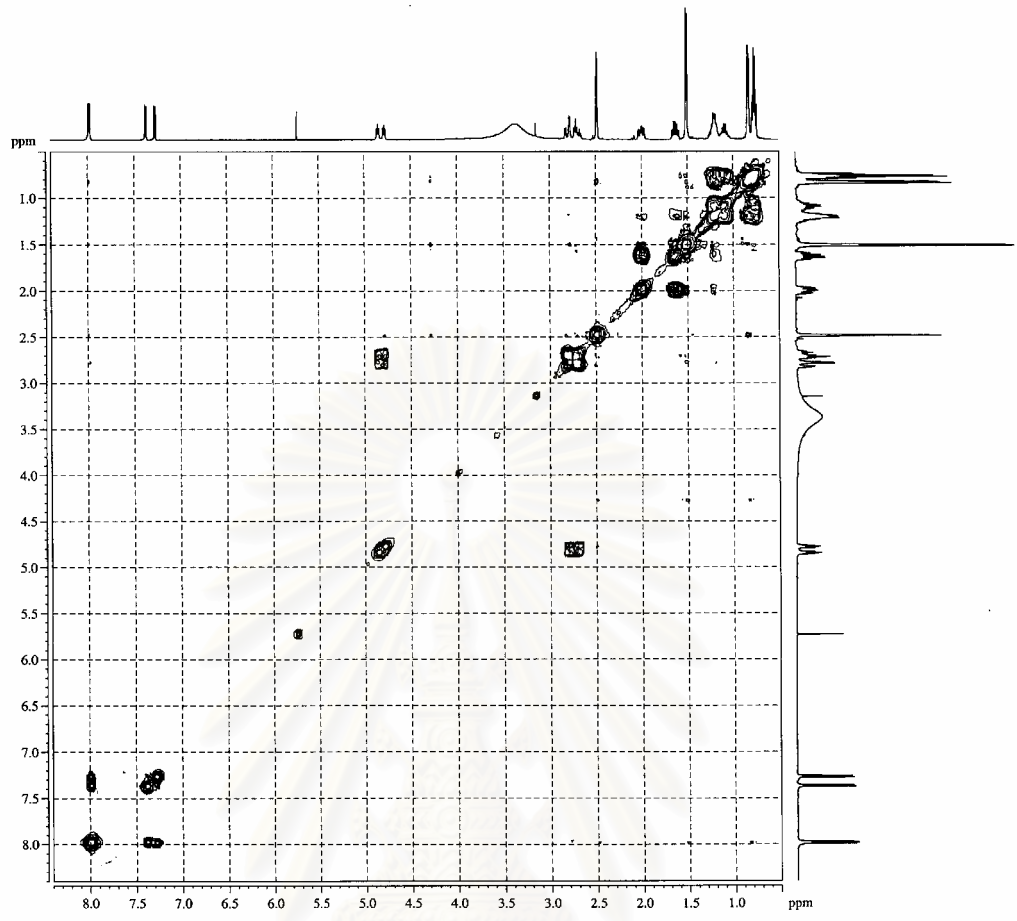

Figure A50: COSY spectrum of **compound 4**

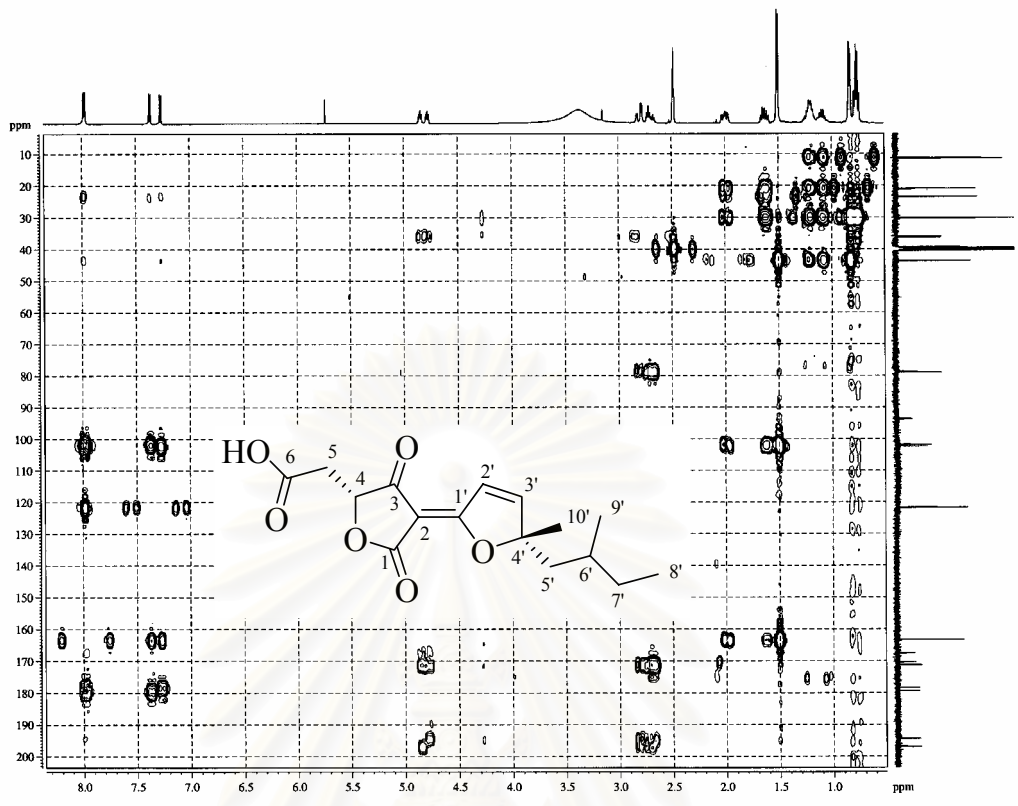

Figure A51: HMBC spectrum of **compound 4**

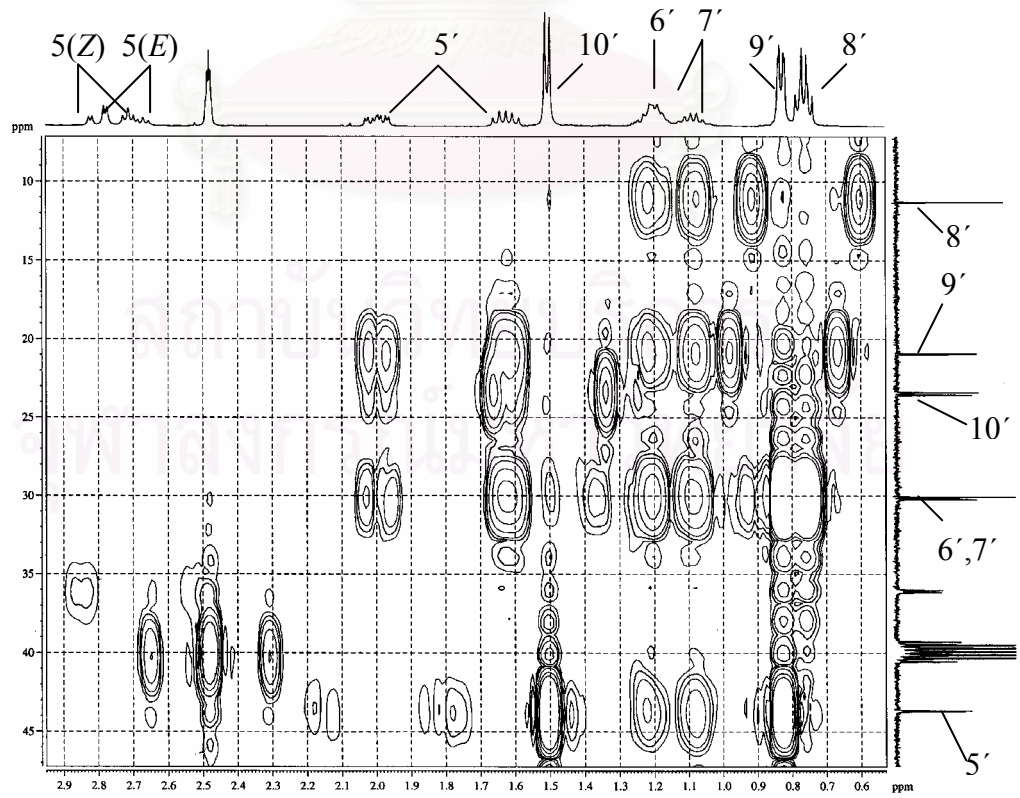

Figure A52: Expansion of **Fig. A51**

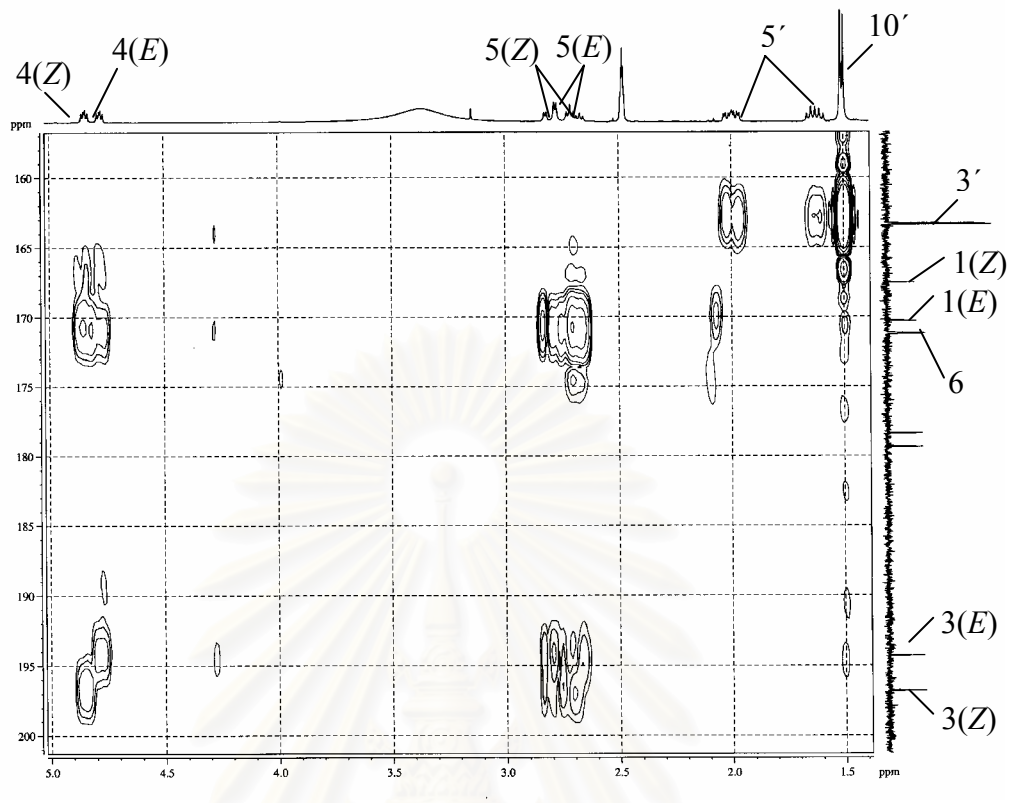

Figure A53: Expansion of **Fig. A51** (continue)

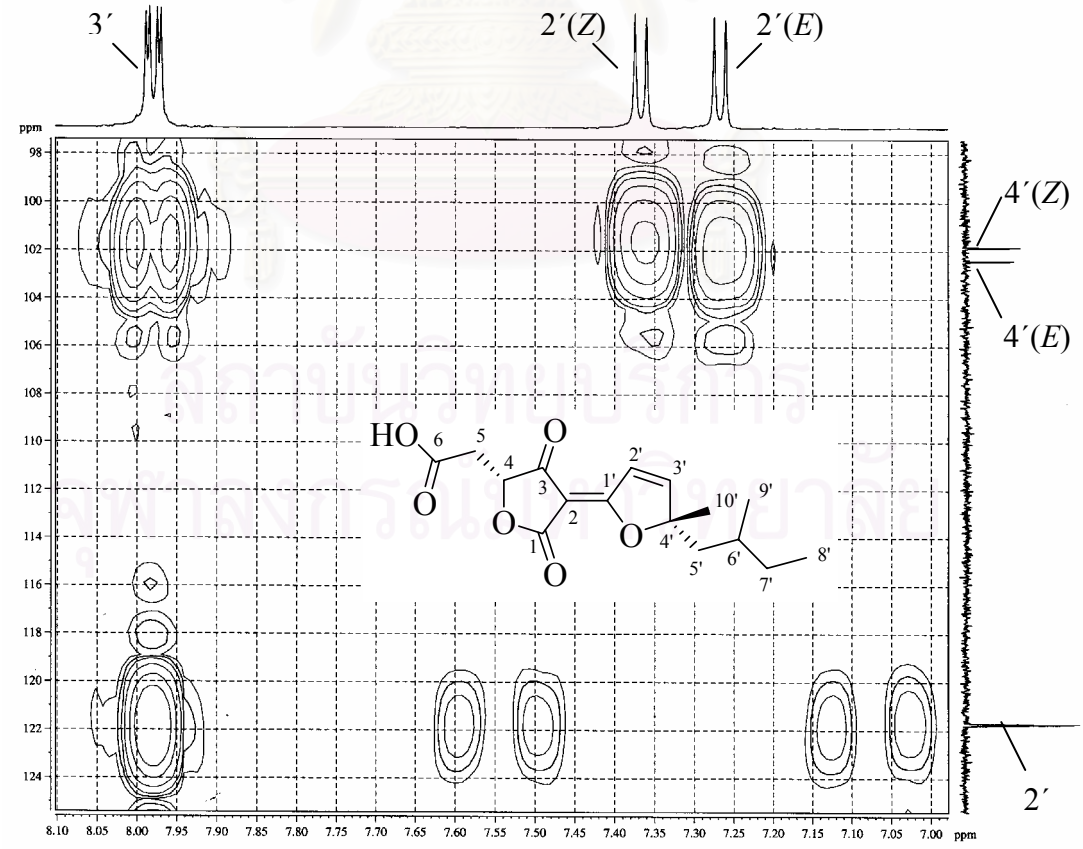

Figure A54: Expansion of **Fig. A51** (continue)

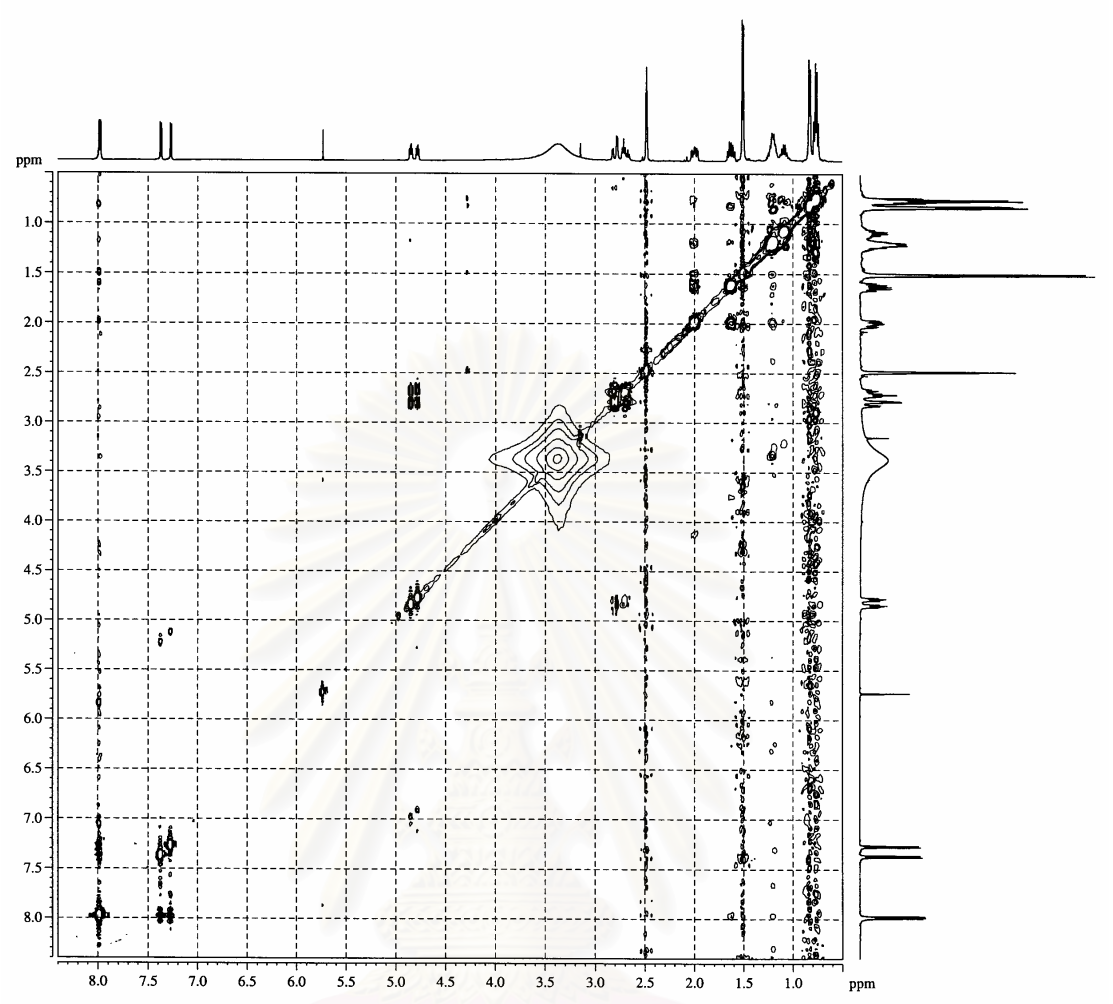

Figure A55: NOESY spectrum of **compound 4**

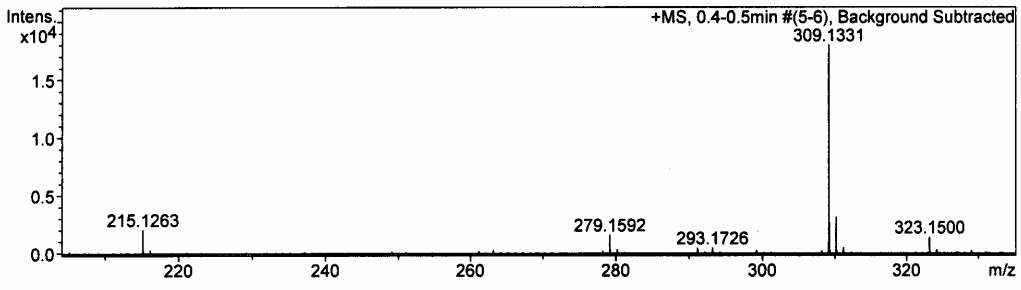

Figure A56: APCI-TOF spectrum of **compound 4**

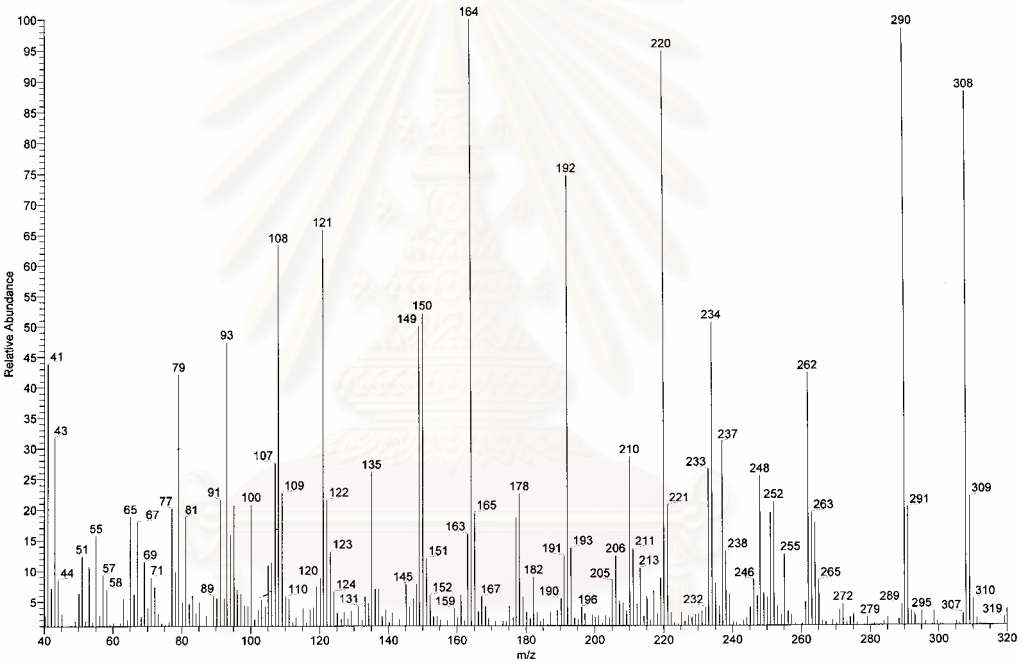

Figure A57: EI-MS spectrum of **compound 4**

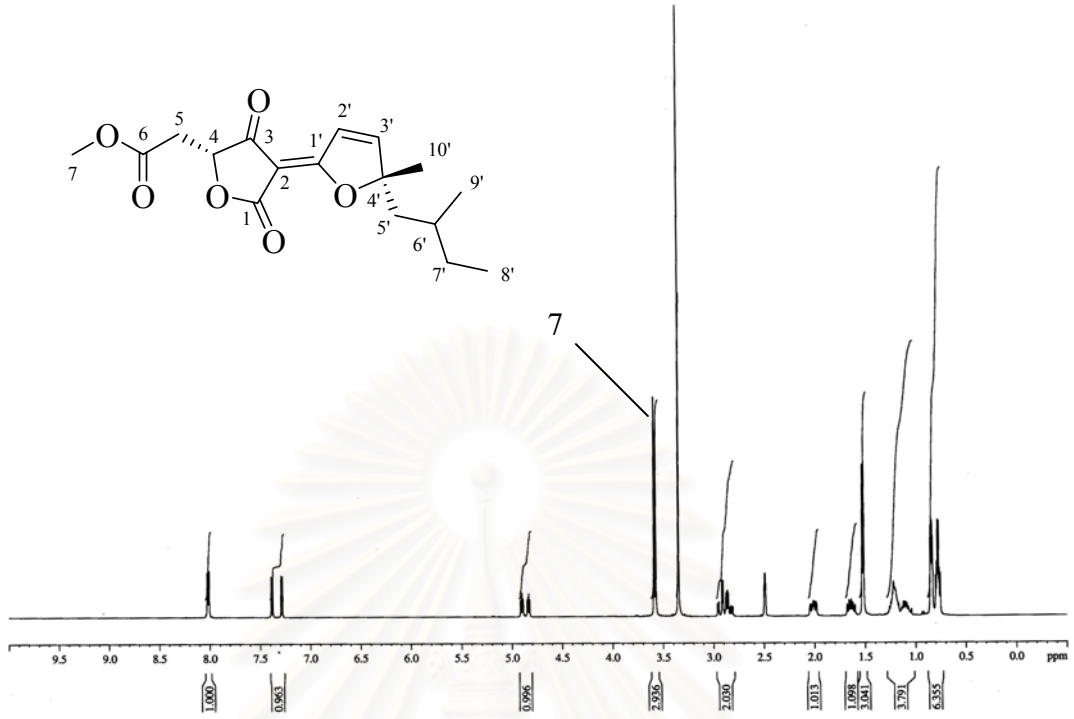

Figure A58: ^{1}H NMR (DMSO-d_6) spectrum of **compound 6**

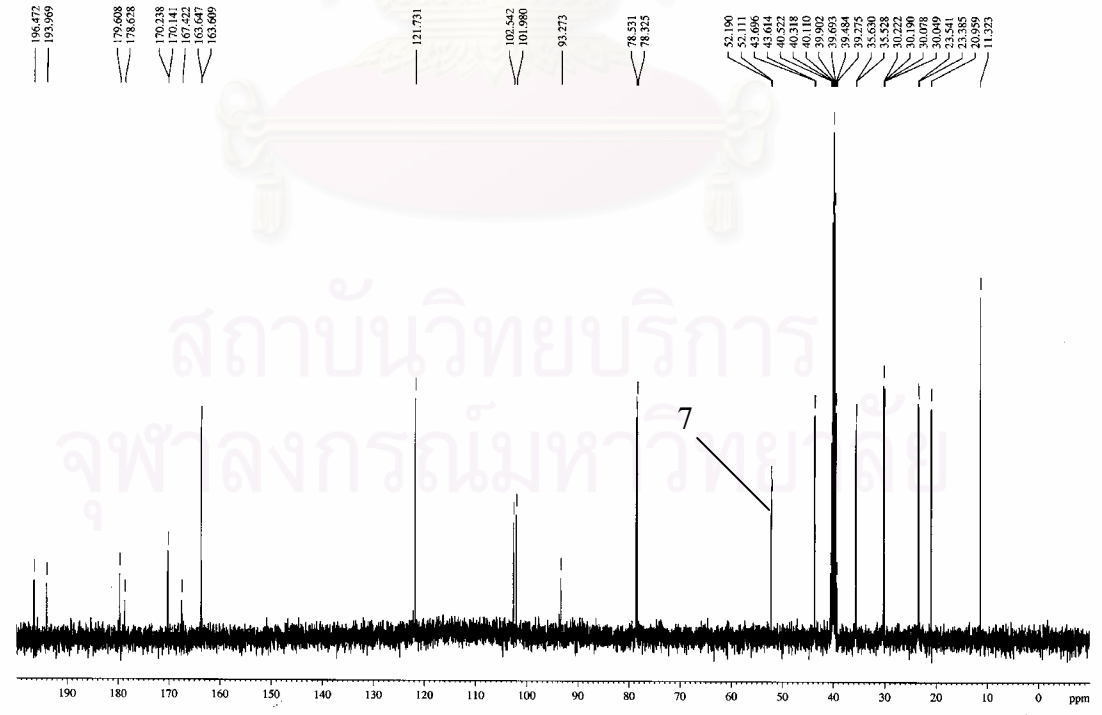

Figure A59: ^{13}C NMR (DMSO-d_6) spectrum of **compound 6**

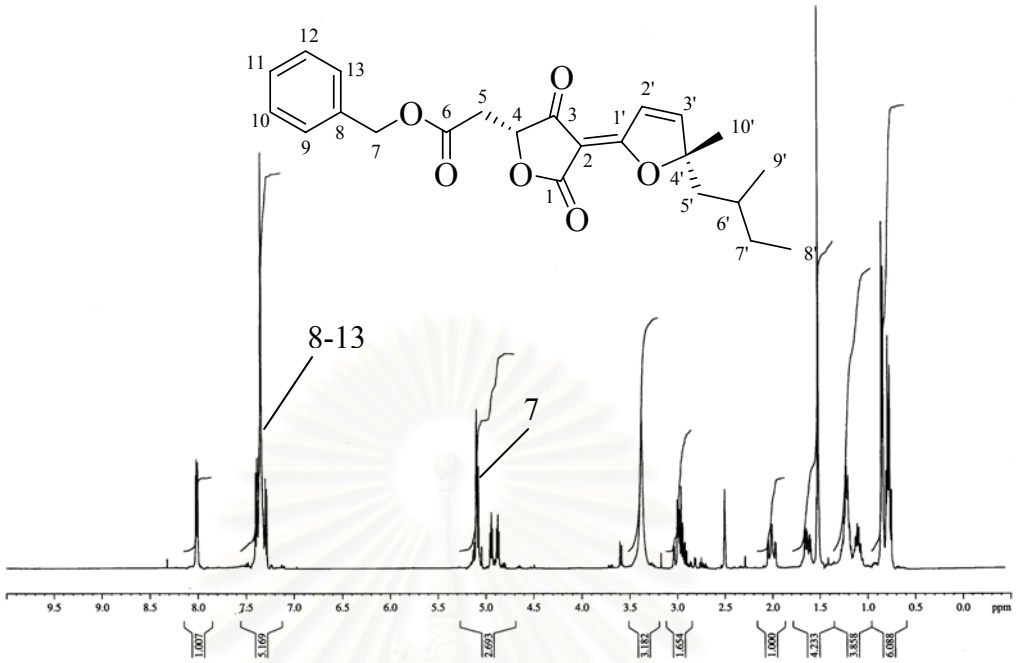

Figure A60: ^{1}H NMR (DMSO-d_6) spectrum of **compound 6**

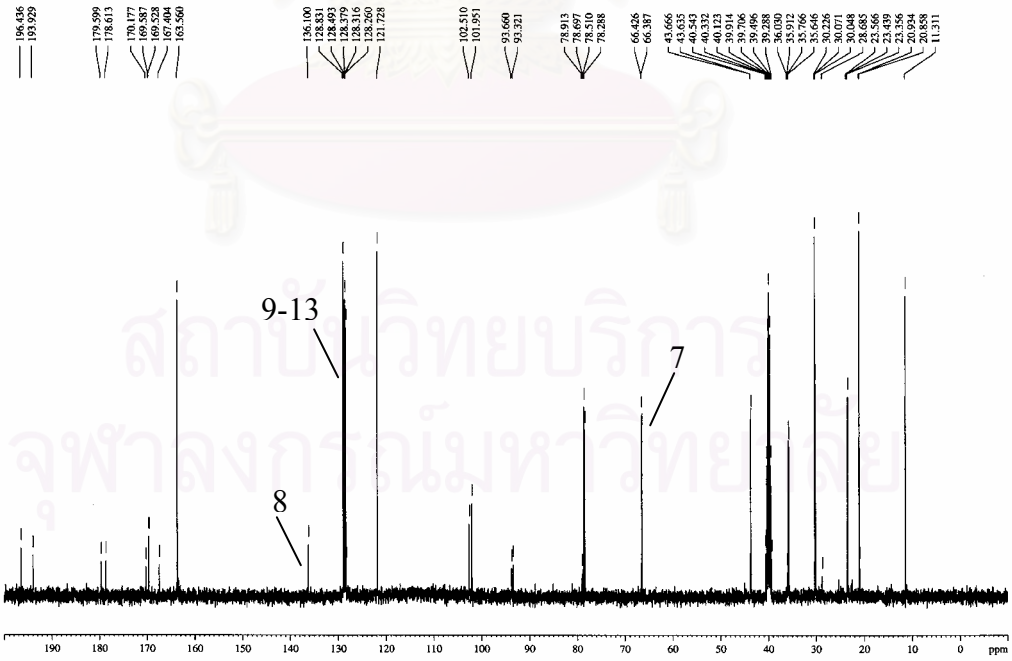

Figure A61: ^{13}C NMR (DMSO-d_6) spectrum of **compound 6**

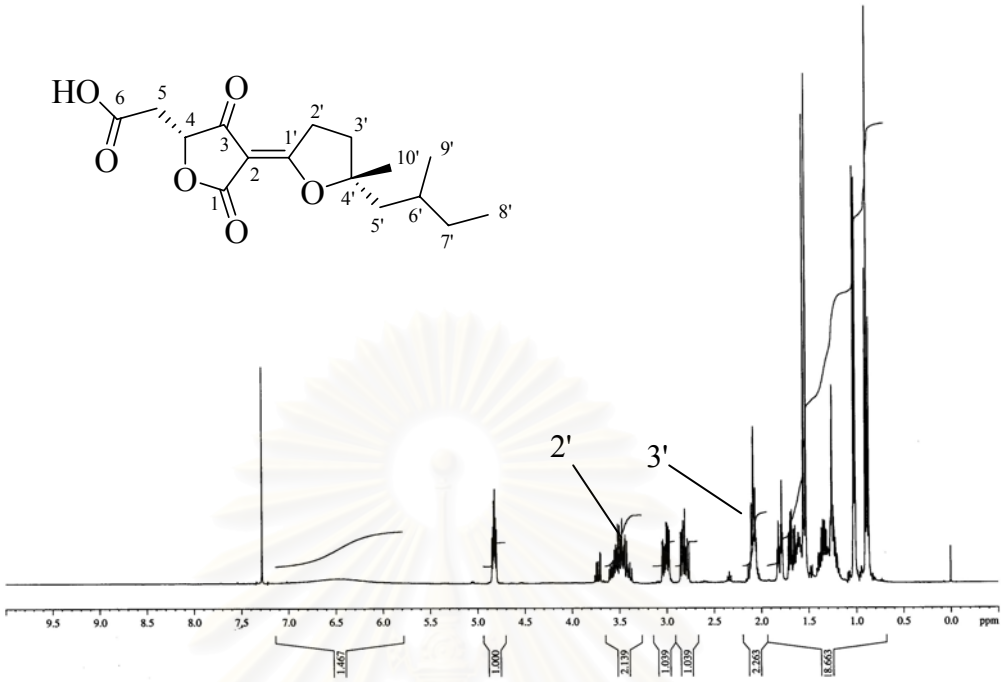

Figure A62: ^{1}H NMR ($CDCl_3$) spectrum of **compound 7**

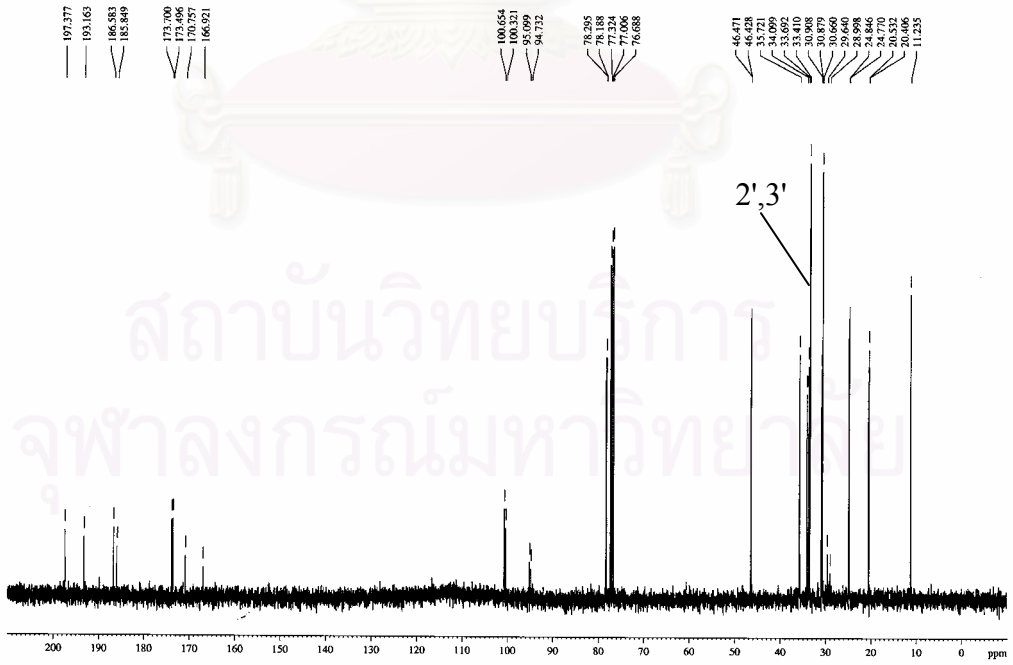

Figure A63: ^{13}C NMR ($CDCl_3$) spectrum of **compound 7**

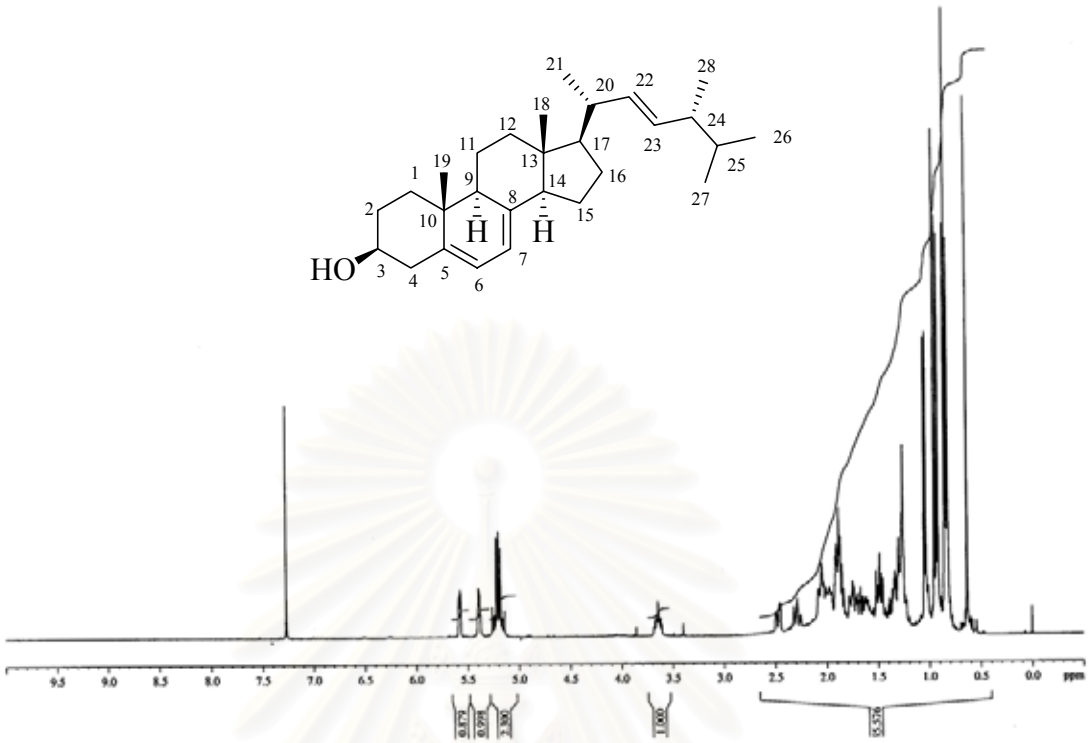

Figure A64: ^{1}H NMR ($CDCl_3$) spectrum of ergosterol

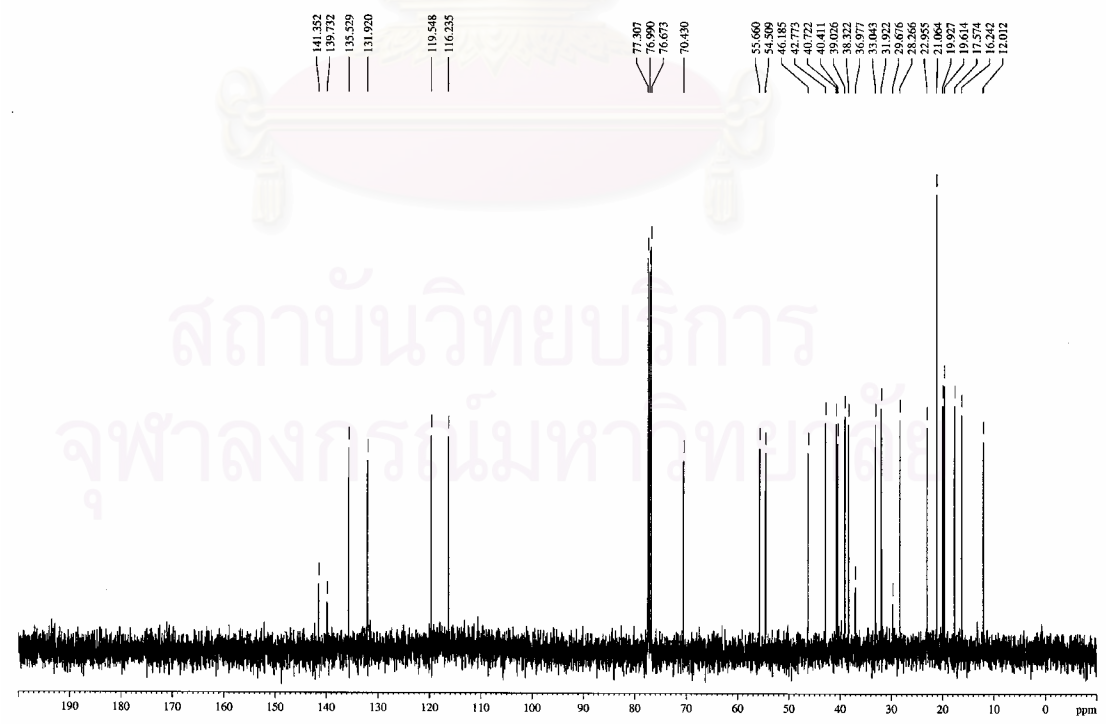

Figure A65: ^{13}C NMR ($CDCl_3$) spectrum of ergosterol

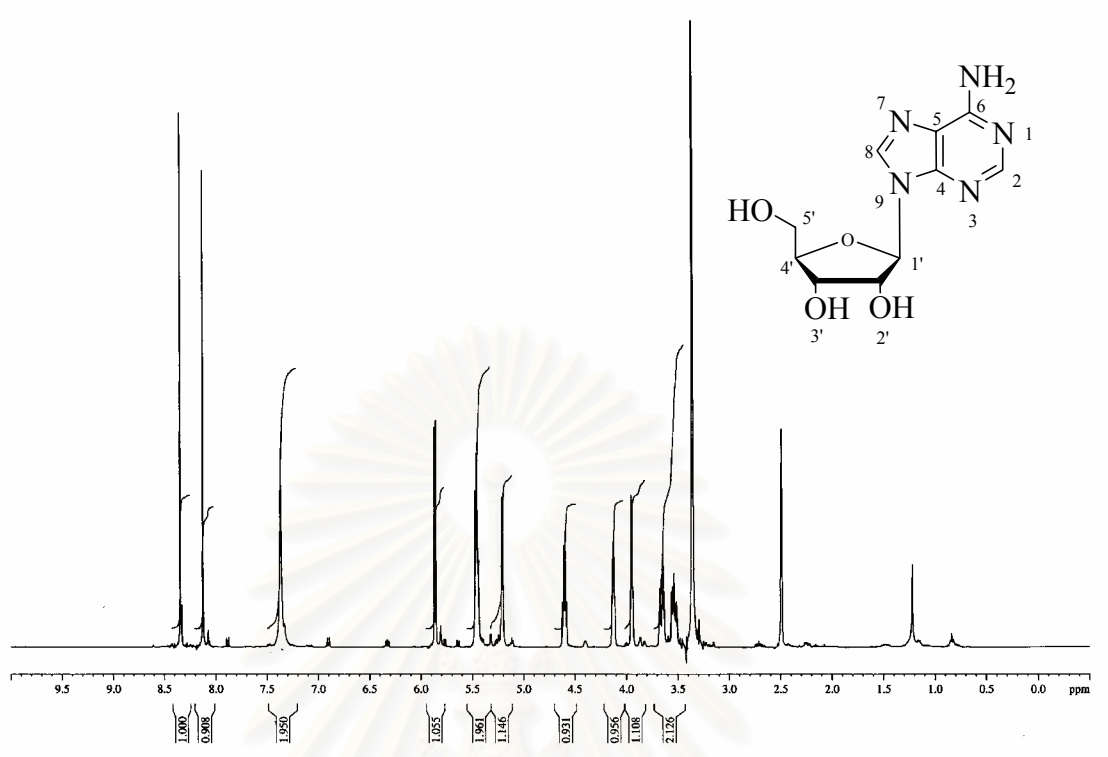

Figure A66: ^{1}H NMR (DMSO-d_6) spectrum of adenosine

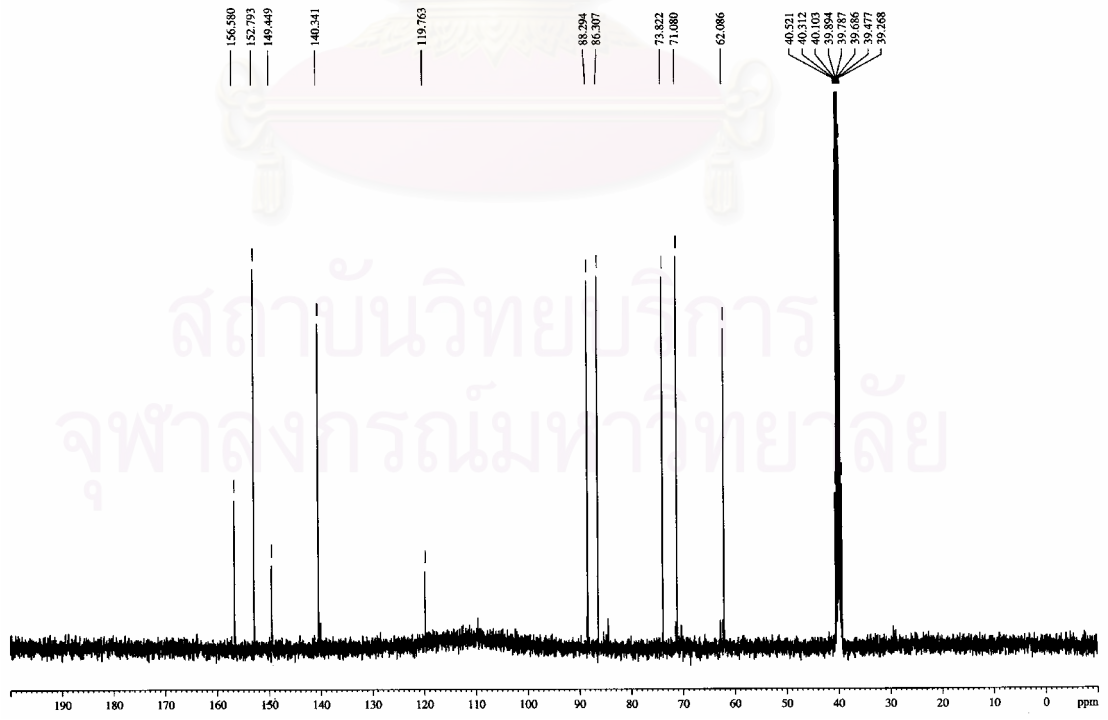

Figure A67: ^{13}C NMR (DMSO-d_6) spectrum of adenosine

BIOGRAPHY

NAME	Mr. Chairut Kasettrathat
DATE OF BIRTH	24 November 1981
PLACE OF BIRTH	Chonburi, Thailand
INSTITUTIONS ATTENDED	Srinakharinwirot University, 2000-2003: Bachelor of Education (Science-chemistry)